VOL. 6 NO. 2 AUGUST 1963

Journal of

ELECTROANALYTICAL CHEMISTRY

International Journal Dealing with all Aspects
of Electroanalytical Chemistry,
Including Fundamental Electrochemistry

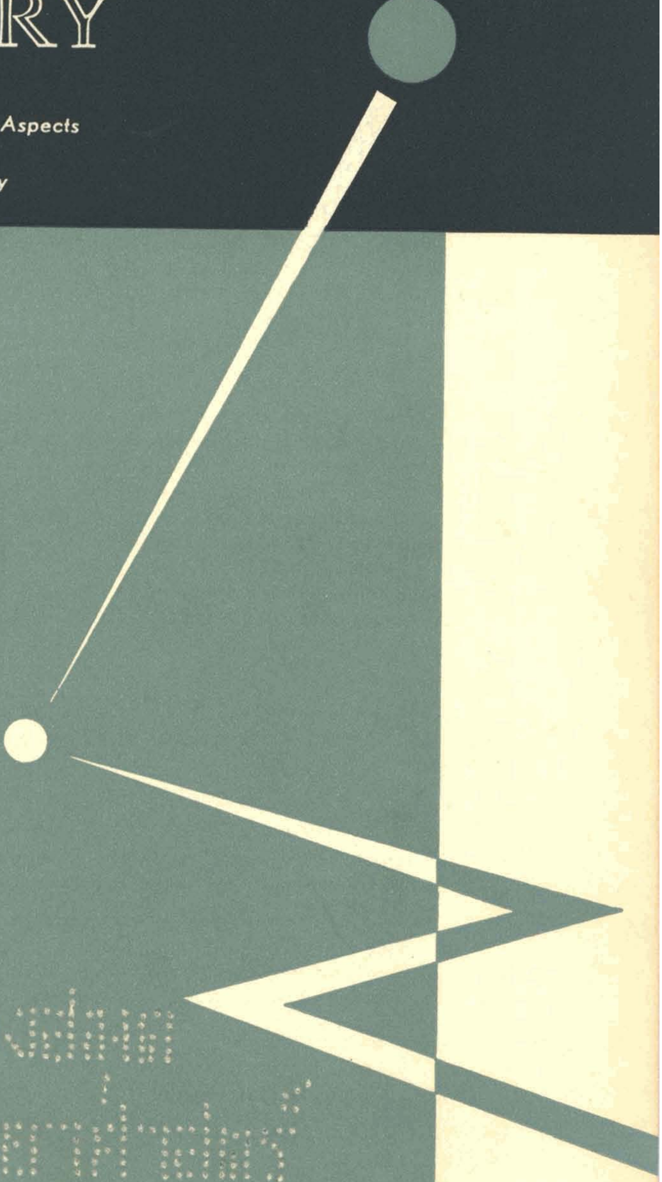

ELSEVIER

GENERAL INFORMATION

See also Suggestions and Instructions to Authors which will be sent free, on request to the Publishers.

Types of contributions

(a) Original research work not previously published in other periodicals.
(b) Reviews on recent developments in various fields.
(c) Short communications.
(d) Bibliographical notes and book reviews.

Languages

Papers will be published in English, French or German.

Submission of papers

Papers should be sent to one of the following Editors:

Professor J. O'M. Bockris, John Harrison Laboratory of Chemistry,
University of Pennsylvania, Philadelphia 4, Pa., U.S.A.
Dr. R. Parsons, Department of Chemistry,
The University, Bristol 8, England.
Professor C. N. Reilley, Department of Chemistry,
University of North Carolina, Chapel Hill, N.C., U.S.A.

Authors should preferably submit two copies in double-spaced typing on pages of uniform size. Legends for figures should be typed on a separate page. The figures should be in a form suitable for reproduction, drawn in Indian ink on drawing paper or tracing paper, with lettering etc. in thin pencil. The sheets of drawing or tracing paper should preferably be of the same dimensions as those on which the article is typed. Photographs should be submitted as clear black and white prints on glossy paper.
All references should be given at the end of the paper. They should be numbered and the numbers should appear in the text at the appropriate places.
A summary of 50 to 200 words should be included.

Reprints

Twenty-five reprints will be supplied free of charge. Additional reprints can be ordered at quoted prices. They must be ordered on order forms which are sent together with the proofs.

Publication

The *Journal of Electroanalytical Chemistry* appears monthly and has six issues per volume and two volumes per year, each of approx. 500 pages.

Subscription price (post free): £ 10.15.0 or $ 30.00 or Dfl. 108.00 per year; £ 5.7.6 or $ 15.00 or Dfl. 54.00 per volume.
Additional cost for copies by air mail available on request.
For advertising rates apply to the publishers.

Subscriptions

Subscriptions should be sent to:

ELSEVIER PUBLISHING COMPANY, P.O. Box 211, Spuistraat 110-112, Amsterdam-C.,
The Netherlands.

Elsevier Monographs

...expert knowledge in compact form...

ZONE ELECTROPHORESIS IN BLOCKS AND COLUMNS

by H. BLOEMENDAL
Senior Research Fellow in Biochemistry at The Netherlands Cancer Institute, Amsterdam, The Netherlands

Zone electrophoresis in porous media or in density gradients has a number of advantages over moving boundary electrophoresis. Several stabilizing materials are used, e.g. paper, granular or hydrolyzed starch, agar, gelatin, glass wool or beads, foam rubber, polyvinyl chloride resin, asbestos and, recently, polyacrylamide gels. In this monograph the reports of a number of workers are presented regarding the various possibilities opened up by improved methods, with a discussion of their merits and limitations. The current literature is reviewed, and advice based on the author's own experience given, enabling the reader to make an informed choice of the analytical or preparative techniques suited to his purposes.

CONTENTS

Introduction
1. Block electrophoresis
2. Gel electrophoresis
3. Continuous electrophoresis
4. Column electrophoresis
5. Column electrophoresis in density gradients
Bibliography. Subject index

5 × 7½"
viii + 219 pages
13 tables
75 illustrations
444 references
1963
40s.

ELSEVIER PUBLISHING COMPANY
AMSTERDAM LONDON NEW YORK

207 E

PAPER ELECTROPHORESIS

A Review of Methods and Results

by **LUIZ P. RIBEIRO**
EMILIO MITIDIERI
OTTILIA R. AFFONSO

of the Biochemical Laboratory, Instituto Oswaldo Cruz,
Rio de Janeiro, Brazil

This book is a completely revised and enlarged translation of the very successful Portuguese edition of 1958.
The contents fall naturally into three sections:

a) Theoretical principles, techniques and apparatus
b) The determinations of proteins and the clinical applications
c) Studies of non-macromolecular substances such as vitamins, hormones, nucleic acid fragments, sugars, inorganic ions etc.

Major emphasis has been placed on paper electrophoresis although many related methods are critically reviewed. New techniques are described in detail and the many illustrations demonstrate the principles and applications discussed in the text. There is a comprehensive list of more than 3200 references.
The book should prove of great practical and theoretical value to all scientists concerned with natural processes.

6 x 9" viii + 463 pages 130 figures 42 tables 3226 refs. £ 3.15.0

CONTENTS:

Introduction
Theoretical Considerations
Methods and Apparatus
Protein Determination
Human Serum Proteins
Animal Serum Proteins
Other Studies of Proteins
Proteins in Other Biological Fluids
Haemoglobins
Lipoproteins and Related Subjects
Glycoproteins and Mucoproteins
Enzymes and Related Substances
Hormones and Related Substances
Vitamins and Related Compounds
Carbohydrates and Polyalcohols
Nucleic Acids and Their Constituents
Amino Acids and Peptides
Inorganic Substances
Immunochemistry and Related Studies
Other Applications

ELSEVIER PUBLISHING COMPANY
AMSTERDAM LONDON NEW YORK

213 E

SUMMARIES OF PAPERS PUBLISHED IN JOURNAL OF ELECTROANALYTICAL CHEMISTRY

Vol. 6, No. 2, August 1963

THE THEORY OF CATALYTIC HYDROGEN WAVES IN ORGANIC POLAROGRAPHY

(Review article)

S. G. MAIRANOVSKII, *J. Electroanal. Chem.*, 6 (1963) 77–118

VOLTAGE SWEEP CHRONOAMPEROMETRIC STUDY OF THE BEHAVIOUR OF $[Fe(CN)_6]^{4-}$ AND Fe^{2+} IONS ON THE PASSIVATED HANGING MERCURY DROP ELECTRODE

The electrode reactions of $[Fe(CN)_6]^{4-}$, $[Fe(CN)_6]^{3-}$ and Fe^{2+} ions were studied on the mercury electrode passivated by mercurous chloride or bromide, using the voltage sweep chronoamperometric technique. It was found that the layers formed did not hinder, under certain conditions, the oxidation of ferrocyanide and the reduction of ferricyanide ions. The reactions taking place depended on the acidity of the solution and on the potential at which the deposits of the corresponding mercurous salts were formed. Fe^{2+} ions gave similar oxidations curves but only at much higher concentrations and in solutions containing considerable amounts of H^+ and Cl^- ions. The results have been compared with those obtained using the platinum micro-electrode.

W. KEMULA, Z. KUBLIK AND J. TARASZEWSKA,
J. Electroanal. Chem., 6 (1963) 119–130

POTENTIOMETRIC ACID-BASE TITRATIONS IN MOLTEN SALTS

THE NEUTRALIZATION OF SODIUM METAVANADATE AND SODIUM METAPHOSPHATE IN CHLORIDE AND NITRATE MELTS

The two acids $NaVO_3$ and $NaPO_3$ were titrated potentiometrically in molten LiCl–KCl eutectic (450°) and in KNO_3 (350°). In the chloride melt $NaVO_3$ neutralizes according to:

$$VO_3^- + O^{2-} = VO_4^{3-}$$

while $NaPO_3$ reacts as:

$$2\ PO_3^- + O^{2-} = P_2O_7^{4-}$$

and

$$P_2O_7^{4-} + O^{2-} = 2\ PO_4^{3-}$$

$Na_4P_2O_7$ in the chloride melt is a very weak acid which does not show an inflection at the equivalence point.

In the nitrate melt at 350° both $NaVO_3$ and $NaPO_3$ change to the pyro- and then to the ortho-salts. $NaVO_3$ is the stronger of the two acids; it takes its primary oxide ion from the nitrate base electrolyte and changes to pyrovanadate.

The positions of metaphosphate, pyrovanadate and pyrophosphate on the newly developed acidity–basicity scale in molten KNO_3 have been established. $Na_4V_2O_7$ is stronger than $Na_4P_2O_7$. Relative instability constants for these two anions have been calculated.

A. M. SHAMS EL DIN, A. A. EL HOSARY AND A. A. A. GERGES,
J. Electroanal. Chem., 6 (1963) 131–140

PREFERRED ORIENTATIONS IN NICKEL ELECTRO-DEPOSITS

I. THE MECHANISM OF DEVELOPMENT OF TEXTURES IN NICKEL ELECTRO-DEPOSITS

This paper presents a mechanism for (a) the preferential formation of electro-deposit facets of a particular type and (b) the alignment of these facets normal to the substrate, and then shows that the result of these two growth processes is the development of a preferred orientation in thick electro-deposits. The discussion is confined to the growth of nickel electro-deposits from *unadulterated baths*.

Facets are formed because of differences in growth velocities. Both *crystallographic* and *electrochemical* factors produce these differences. The crystallographic factors are considered in terms of the Bravais *law* of crystal growth. It is suggested that different lattice planes have different *free growth* metallic overpotentials. The electrochemical disturbance to *free growth*, stems from the hydrogen evolution reaction. Beeck's experimental studies on hydrogen adsorption on nickel are used to argue that the intermediately-produced hydrogen atoms are adsorbed more easily on lattice planes which during *free growth* have faster growth velocities. If hydrogen atom adsorption increases metallic overpotential, then facets of different types are formed with different surface coverages.

The {hkl} facets so formed are aligned normal to the substrate because the deposits tend to adopt an outward mode of growth which requires that the slowest-growing {hkl} facets (and therefore the zone-axis $\langle uvw \rangle$ of the {hkl} *Wilman facets*) stand perpendicular to the substrate surface.

All deposit-crystals being subject to similar growth influences, get identically oriented, *i.e.*, a preferred orientation develops with the texture-axis $\langle uvw \rangle$ being the zone-axis of the *Wilman facets*. The random orientation stage — which precedes the texture stage — exercises a *substrate* influence and therefore permits only a gradual development of texture.

Two important consequences follow from the theory proposed in this paper:

(1) texture changes are induced by changes in surface coverage with hydrogen atoms, and by factors such as temperature which affect this coverage;

(2) deposits having different textures should have different hydrogen contents. The experimental data of Yang supports the latter conclusion.

A. K. N. Reddy, *J. Electroanal. Chem.* 6 (1963) 141–152

PREFERRED ORIENTATIONS IN NICKEL ELECTRO-DEPOSITS

II. A CONSIDERATION OF THE EFFECT OF DEPOSITION CONDITIONS ON THE TEXTURES DEVELOPED

The theory of texture development in nickel electro-deposits, proposed in Part I of this paper, is used here to explain the trends of texture changes which result from variation in nickel deposition conditions.

Only the commonly-reported <210>, <100> and <110> orientations are considered. The occurrence of systematic texture changes (with increase of temperature and current density and with addition of oxidizing agents) is indicated in the experimental data of previous workers.

It is suggested that an increase in bath temperature leads to a decrease in the average surface concentration of adsorbed hydrogen atoms, and thus to changes to textures towards *free growth, i.e.*, <210> → <100> → <110>. This conclusion is completely in agreement with experiments conducted at a pH less then 5.

The slight *free growth* trend observed with an increase of current density is tentatively ascribed to differences in the slopes of the *free growth* η–i curve for different single-crystal faces of nickel.

The addition of oxidizing agents — it is argued — reduces surface coverage and hence produces texture changes towards *free growth*.

Some limitations of the present work are indicated.

A. K. N. Reddy and S. R. Rajagopalan,
J. Electroanal. Chem., 6 (1963) 153–158

PREFERRED ORIENTATION OF NICKEL ELECTRO-DEPOSITS

III. GENERALIZATION OF THE THEORY

This paper discusses the lines along which the proposed theory of texture development (for nickel electro-deposits) can be extended to include (a) lateral growths, (b) deposits of other metals and (c) deposits from *adulterated* baths.

It suggested that when deposits adopt the lateral mode of growth, the slowest-growing {hkl} facets are formed — in the ideal case — parallel to the substrate. The normal to these facets becomes the texture-axis. In practice, the {hkl} facets may deviate from parallelism and the texture-axis then develops a scatter from its ideal position.

The theory can be generalized to cover other metals by using the fact that surface coverage with hydrogen atoms depends on the heat of hydrogen adsorption which varies from metal to metal. Hence, the textures of Pb, Ag and Cu should correspond more to *free growth* orientations, whereas those of Fe and Co should be coverage-dependent like Ni.

The many ways in which addition agents can influence textures are indicated. Addition agents can influence, for instance, the hydrogen evolution reaction, the nucleation rate and the mode of growth. Their differential adsorption on different facets and their surface activity are also discussed.

A. K. N. REDDY AND S. R. RAJAGOPALAN,
J. Electroanal. Chem., 6 (1963) 159–163

ELECTRO-OXIDATION FOLLOWED BY LIGHT EMMISSION

(Short Communication)

T. KUWANA, *J. Electroanal. Chem.*, 6 (1963) 164–167

REVIEW

THE THEORY OF CATALYTIC HYDROGEN WAVES IN ORGANIC POLAROGRAPHY

S. G. MAIRANOVSKII

N.D. Zelinskii Institute of Organic Chemistry, Academy of Science, Moscow (U.S.S.R.)

(Received April 17th, 1963)

CONTENTS

1. INTRODUCTION

A very interesting phenomenon—catalytic waves of hydrogen evolution—is frequently encountered in practical polarography. These waves are due to the presence in the solution of certain catalytic substances which, while being themselves unaffected by the electrode process, contribute to the evolution of molecular hydrogen on the cathode with simultaneous consumption of hydrogen ions in the solution. Catalytic hydrogen waves are observed at less negative potentials than the usual waves of hydrogen discharge in the same solution; thus the catalysts diminish, as it were, the hydrogen overvoltage, accelerating (*catalyzing*) the hydrogen ion discharge. Hence the term *catalytic waves*.

On account of their complexity, catalytic waves must be considered as a special and very interesting branch of polarography. At present the catalytic process has been established as consisting of a sequence of steps; under certain conditions the kinetics of each of these steps can determine the rate of the overall process.

Some of the steps of the catalytic cycle are essentially influenced by: (a) the adsorption of substances on a dropping electrode; (b) the structure of the electric double-layer; (c) the stirring occurring under the conditions of the polarographic maximum of the second kind, etc. Therefore, by observing polarographic catalytic hydrogen waves, it is often possible to study in a relatively simple way processes and phenomena which are barely accessible (or perhaps entirely inaccessible) if approached by other methods. For example, it is possible to find the rate constants of fast protolytic reaction; to investigate adsorption phenomena at a very small coverages of the electrode surface by adsorbed particles; to determine the rate of the bi-molecular interaction of free radicals and to study quantitatively the influence of the structure of organic compounds (the catalysts) on their reactivity.

Apart from their considerable theoretical significance, catalytic hydrogen waves are of great practical interest. They can be used for analytical purposes and it is possible with the help of conventional polarographic equipment to attain sensitivities up to 10^{-7} M, *i.e.* to increase the sensitivity of the method by 2–3 orders, compared to *classic* polarography. The use of catalytic hydrogen waves in biology and medicine is of special interest; it has been found possible to develop on their basis some diagnostic techniques in particular the widely known Brdička's serologic polarographic test for cancer.

HERLES AND VANČURA were the first to observe, in 1930, an unusual wave during the polarographic analysis of blood serum solutions, using sodium, potassium and magnesium salts as supporting electrolytes. A brief description, however, of their experiments was not published until 1932[1]. HEYROVSKY AND BABIČKA, also in 1930, repeated the experiments and observed similar waves in the presence of proteins, using ammonia buffers as supporting electrolytes. They showed that these waves are caused by catalytic hydrogen evolution and not by protein reduction[2].

Later BRDIČKA[3] found that the catalytic effect of proteins and of some other sulfur-containing compounds increased greatly on the addition of cobaltous or cobaltic salts to an ammonia buffer solution.

At about the same time PECH[4] established that catalytic hydrogen evolution may be caused by organic compounds containing no sulfur, *e.g.* by alkaloids. Later catalytic hydrogen evolution caused by (1) proteins in ammonia buffer solutions in the presence of cobalt salts and (2) in solutions of alkaloids or of other nitrogen-containing substances was the object of numerous studies, (see the literature survey[5–10], the valuable experimental data are in the works of Kirkpatrick[11], Stromberg[12,13], Knobloch[14,15], Kůta and Drabek[16], Stackelberg *et al.*[17,18,19], Nürnberg[20], Lamprecht *et al.*[21], Březina *et al.*[22,23] and others).

Some characteristics of catalytic hydrogen waves

Catalytic waves are very different in character from the usual diffusion-limited polarographic waves. The limiting catalytic currents do not obey the Ilcovič equation; they have either a very high or a very low temperature coefficient and do not depend as a rule on the height of the mercury column above the dropping electrode. Sometimes, in contrast to diffusion currents, they even increase with a decrease in the height of the mercury column. Catalytic hydrogen waves always differ in shape from diffusion-limited waves and there is a complicated relationship between limiting catalytic currents and the half-wave potentials of the catalytic waves on one hand, and the concentration of the catalyst and the composition of the solution being analyzed polarographically, on the other.

Dependence of the limiting catalytic current on the catalyst concentration and solution composition

It has been established in numerous works dealing with the effects of the catalyst concentration ($c_{\text{cat.}}$) and of the solution composition on the height of catalytic hydrogen waves, that with a rising $c_{\text{cat.}}$ the limiting catalytic current at first increases in proportion to $c_{\text{cat.}}$. The increase in the height of the wave then slows down and finally at a very high $c_{\text{cat.}}$ the limiting catalytic current is no longer dependent on $c_{\text{cat.}}$ but tends to approach a certain limiting value. This phenomenon was first observed by BRDIČKA[24] in the case of catalytic hydrogen waves caused by egg albumin in both unbuffered KCl solutions and in buffer solutions of various composition and pH. BRDIČKA found that the height of the catalytic wave and the limit to which it can grow with increasing catalyst concentration, rises with an increase in the buffer capacity of the solution and a decrease in its pH.

BRDIČKA showed[25], using as examples the catalytic waves in protein solutions containing cobalt salts, that the dependence of the limiting current of the catalytic wave on the catalyst concentration (other factors being constant) obeys an expression similar in form to the Langmuir adsorption isotherm. With a rise in the concentration of cobalt ions the current increases in accordance with the empirical formula $i_{\text{lim.}} = K[Co^{2+}]^{0,74}$.

Of especial importance is the concept, developed by BRDIČKA of the regeneration of the catalyst after its participation in the electrode process. This later formed the basis of other theories concerning catalytic hydrogen waves. According to BRDIČKA, this regeneration consists of the addition of hydrogen ions to the product of the electrochemical discharge of the catalyst, by the action of the acids (proton donors) in the solution.

The growth of the catalytic wave with rising concentrations of proteins and cobalt salts was also observed by STROMBERG[12], who was the first to consider this phenomenon as affected by the kinetics of the reactions occurring at the electrode. On this basis, he deduced a relation for the limiting current of the catalytic wave. Having studied the catalytic waves caused by cystine in the presence of cobalt salts, KLUMPAR[26] proposed a new empirical formula relating the limiting catalytic current with the concentrations of cystine and cobalt salts in the solution. In ammonia buffer solutions with rising concentrations of a non-sulfur-containing catalyst (dimethylglyoxime) and of a cobalt salt, an increase in the height of the catalytic wave in accordance with a curve concaved towards the abcissa was observed by STROMBERG AND ZELIANSKAIA[13].

The effect of various factors on the catalytic hydrogen evolution caused by nitrogen-containing compounds (in particular by pyridine derivatives) in buffer solutions in the absence of cobalt salts, was first studied in some detail by KNOBLOCH[14]. He showed that the limiting current of the catalytic hydrogen wave increases with a decrease in pH of the solution and a rise in its buffer capacity. With a rising catalyst concentration, the current increases in accordance with a curve similar in form to the Langmuir adsorption isotherm. This led KNOBLOCH to suppose[14] that the current is determined by the amount of the catalyst in the adsorbed state and that the limit to the increase in the current with a rising catalyst concentration depends on the complete coverage of the electrode surface with catalyst particles. The influence of pH and of buffer capacity were explained by him as being due to the protolytic regeneration of the catalytically active cationic form of the catalyst, which, in his opinion, brings about a decrease in hydrogen overvoltage in accordance with HEYROVSKY's scheme; *i.e.* at the expense of an increase in the rate of H_2^+ formation from H atoms and protons of the cationic form of the catalyst. Thus KNOBLOCH was the first to ascribe the electrochemical activity solely to the acid–cationic form of nitrogen-containing catalysts.

The effect of the catalyst and proton donor concentrations on the catalytic waves was studied in detail for the case of the first wave on the polarograms of quinine in solutions containing practically only one kind of proton donor (hydrochloric acid), in the presence of 1 N LiCl as supporting electrolyte[27,28]. Some of the results of these experiments are shown in Figs. 1 and 2. As in the case of other catalytic hydrogen waves, the catalytic current in quinine solutions rises with increase in the concentration of the catalyst, in accordance with a curve similar to the Langmuir adsorption isotherm (see Fig. 1). The limits to which the wave heights tend to approach and above all the quinine concentration at which $i_{\text{lim.}}$ approaches the limit, prove to be[28] dependent on the concentration of the hydrochloric acid in the solution; the smaller the HCl concentration, the lower the limit to which the height of the catalytic wave tends to approach and the smaller is the quinine concentration required for the wave height to approach the limiting value (Fig. 1).

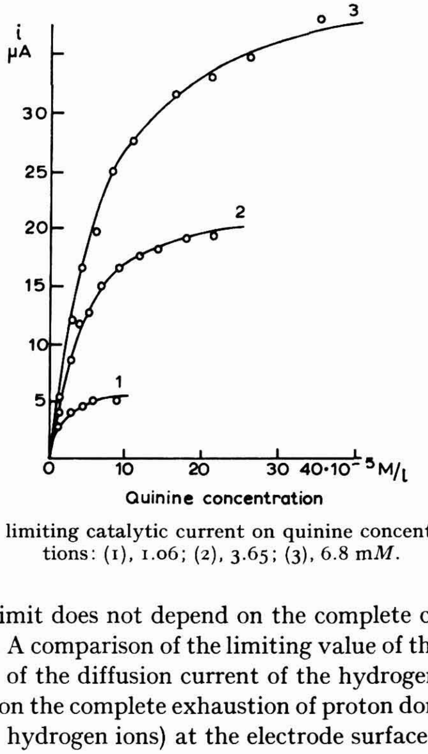

Fig. 1. Dependence of the limiting catalytic current on quinine concentration at HCl concentrations: (1), 1.06; (2), 3.65; (3), 6.8 mM.

It follows that this limit does not depend on the complete coverage of the surface with adsorbed catalyst. A comparison of the limiting value of the height of the catalytic wave with the value of the diffusion current of the hydrogen ion discharge shows that this limit depends on the complete exhaustion of proton donors, (in the case under consideration these are hydrogen ions) at the electrode surface[27,28]. If the concentration of hydrogen ions does not greatly exceed that of the catalyst, the limiting catalytic current rises linearly with increase in their concentration (Fig. 2).

In the presence of an excess of proton donors, an unusual relationship between the height of the catalytic wave and the catalyst concentration in the solution, is observed at very low catalyst concentrations; the increase in height of the wave with increase in catalyst concentration is greater then linear (see Fig. 3 reproduced from[29]). This relationship seems to occur rather frequently. Thus, for instance, the polarograms in KIRKPATRICK's work[11], show that the rise in heights of the catalytic waves caused by atropine and pylocarpine in buffered solutions becomes increasingly larger as the concentration of these alkaloids is increased. KIRKPATRICK, himself[11] paid no attention to this phenomenon and even made no mention of it in his paper.

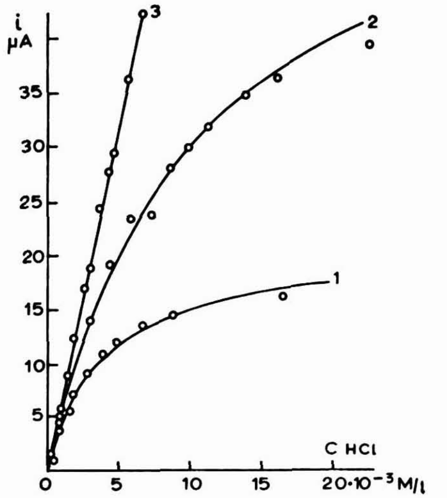

Fig. 2. Dependence of the height of the catalytic waves caused by quinine on HCl concentration, in 1 N LiCl. Quinine concentrations: (1), $3.8 \cdot 10^{-5}$ M; (2), $7.9 \cdot 10^{-5}$ M. Curve 3 is the diffusion current of the hydrogen ion discharge.

On the basis of the experimental data and making use of the concepts of Brdička, Knobloch and Stromberg, the author of the present survey has suggested[27,30] an hypothesis for catalytic hydrogen evolution, which accounts for all the phenomena observed in the experiments. Equations correctly representing the regularities observed, were deduced by using this hypothesis and introducing (1) the well known concepts of Brdička and Wiesner regarding the kinetic limitation of currents;

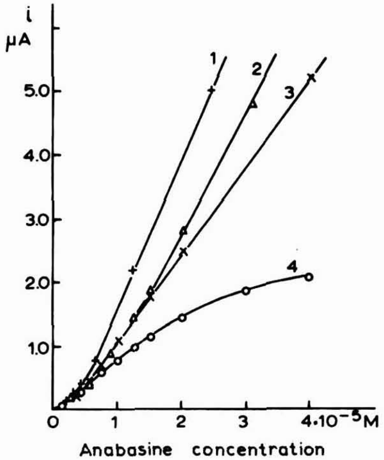

Fig. 3. Dependence of the limiting catalytic hydrogen current on anabasine concentration in acetate buffer solutions with ionic strength = 0.5: (1), pH = 4.46, $\Sigma C_{ac.} = 0.2$ M; (2), pH = 5.0, $\Sigma C_{ac.} = 0.1$ M; (3), pH = 5.0, $\Sigma C_{ac.} = 0.2$ M; (4), pH = 6.0, $\Sigma C_{ac.} = 0.1$ M.

(2) the theoretical postulates of FRUMKIN regarding the effect of the electric double-layer structure upon the electrode processes and the nature of the adsorption of organic substances on the electrode and (3) DELAHAY's and FIKE's data on adsorption kinetics.

Mechanism of catalytic hydrogen evolution in solutions of organic bases

For an organic substance to become catalytically active, it is necessary that it should be able to exist in two forms: the acid form BH^+ and the basic form B (in the Brönsted sense), which are in protolytic equilibrium with each other:

$$B + DH^+ \underset{\varrho\sigma}{\overset{\varrho}{\rightleftarrows}} BH^+ + D \tag{I}$$

Here DH^+ denotes the acids (proton donors) present in the solution and D, their conjugated bases.

The ability of some organic compounds to bring about catalytic hydrogen evolution seems to be due to their having an unshared pair of electrons (on the atoms of nitrogen, sulfur, oxygen, phosphorus, arsenic, etc.), to which a proton can be added. This results in the formation of -onium compounds capable of participating in an electrochemical reaction on the cathode. It is the chemical nature of the -onium ion which is responsible for the electrochemical activity of -onium compounds rather than the fact that they have a possitive charge, facilitating both the approach of the particle to the cathode and its discharge[31]. If the electron transfer to a protonated -onium form were due only to its positive charge, a discharge of an uncharged non-protonated form of the catalyst would also be expected, although at a more negative potential (by 200–300 mV). This is observed, for instance, in the case of the electrochemical reduction of charged and uncharged aniline and phenol derivatives[32–34], and of weak acids and their anions[35–43] but a discharge of a non-protonated form of a catalyst has never been observed and this permits us to draw the above conclusion.

The catalytic activity of substances is not connected with the mobility of hydrogen ions; thorough investigations[18] have shown that organic compounds with a very mobile hydrogen possess no catalytic activity.

As a result of the electron transfer to the protonated form of the catalyst:

$$BH^+ + \bar{e}^- \underset{\leftarrow\cdots}{\overset{\mathrm{el}}{\rightarrow}} BH \tag{II}$$

an unstable uncharged particle in the nature of a free radical is formed.

In the case of the discharge of tetra-substituted ammonium[44–46] and phosphonium salts[47] or tri-substituted sulfonium cations[48], the unstable products formed are either dimerized, as for instance, in the case of the discharge of N-alkylpyridinium salts[49–52], or the carbon-hetero-atom bond is broken, giving the corresponding tri-substituted amines, phosphines or di-substituted sulfides and hydrocarbon radicals. These, in their turn, can be reduced on the cathode or can react with the solvent as well as being dimerized or disproportionated.

When the discharge of a protonated -onium cation occurs, as in the case of catalytic hydrogen evolution, it seems to be more probable from a thermodynamic standpoint for the BH particles formed (see the scheme of Process II), no to detach the hydrocarbon radical or a hydrogen atom, but to enter into a bi-molecular interaction

$$2\,BH \xrightarrow{k_d} 2\,B + H_2 \qquad \text{(III)}$$

involving the regeneration of the catalyst in its basic form and the evolution of a hydrogen molecule. Because the bi-molecular character of this reaction, its rate is considerably reduced by a decrease in the catalyst concentration, and in some cases this may even limit the rate of the overall process. This was the case in the experiments the results of which are shown in Fig. 3. It is the reaction of the second order with respect to the catalyst, limiting the wave height under these conditions, that is responsible for a faster increase in the limiting catalytic current[11,27,29] in comparison to the increase in the catalyst concentration, which is sometimes observed.

In some cases, in particular in an anabasinium ion discharge[53], the bi-molecular interaction of radicals according to (III) involves the formation of intermediate products (relatively stable HB–BH dimers) which decompose rather slowly into two B particles and a hydrogen molecule. With increasing temperature, the stability of HB–BH dimers of dihydrodianabasine is greatly reduced, so that their formation (to be more precise, the kinetics of their decomposition) no longer has any effect upon the overall rate of process (III)[53].

The basic form of the catalyst B, formed according to (III), is again protonated according to (I), discharged (II), regenerated once more, etc., and each cycle of reactions (I–III) results in a catalyzed electrochemical transformation of two protons from DH^+ into molecular hydrogen. Each particle of the catalyst can *treat* in this way a considerable amount of particles (proton donors).

The strength of the catalytic current of hydrogen evolution depends on the rate of processes (I–III). With a limiting current, when the rate of the electrochemical step (II) becomes high enough and all the BH^+ particles located at the electrode surface are discharged on it, the height of the catalytic wave is determined by the rate of BH^+ formation in the layer near the electrode. In most cases, this process is determined mainly by protonation of the basic form of the catalyst, the rate constant of which, designated by ϱ in reaction (I), is the sum of the individual rate constants of the catalyst interaction with all the proton donors in the solution:

$$\varrho = k_1[DH^+]_1 + k_2[DH^+]_2 + \ldots + k_n[DH^+]_n \qquad (1)$$

The constant σ, of the equilibrium between the basic and the acid form of the catalyst is an important characteristic of the catalytic system. As in the case of other protolytic reactions, the value of σ is determined only by the constant of the acid dissociation of the protonated form of the catalyst and by the pH of the solution

$$\sigma = \frac{[B]}{[BH^+]} = \frac{K_A}{[H^+]} \qquad (2)$$

and, in contrast to the value of ϱ, depends neither on the nature nor on the concentration of the buffer components of the solution.

Let us consider now the relationship between the limiting catalytic current and the composition of the solution which is obtained using the hypothesis of catalytic waves suggested by the author.

Let us first consider the case when the process is limited only by the protonation rate (I), *i.e.* when the regeneration rate of the catalyst according to (III) is high enough. For the sake of simplicity, let us assume that there is only one proton donor in the solution (as for instance, in the case of the catalytic system, quinine–hydrochloric acid, in which the proton donor action of water *i.e.* the hydronium ions, may be neglected compared to the proton donor action of hydrochloric acid), then $\varrho = k_{H^+}[H^+]$.

Furthermore, let us assume, as is usually the case in practice, that the protolytic equilibrium in the solution is shifted in the direction of the basic form of the catalyst, *i.e.* $\sigma > 1$, and that because of a fast and complete regeneration of the catalyst, a steady state is established in a very short time after the formation of the drop. In this state the equilibrium concentrations of BH^+ and B already obtain at a relatively small distance from the electrode[54] and the value of the limiting catalytic current can be expressed by the equation:

$$i_{\text{lim.}} = k_{H^+}[H^+]_S[B]_S SFA \tag{3}$$

where S is the mean surface area of the dropping electrode, F, the Faraday constant and A, a factor of proportionality. For a non-adsorbed catalyst A is equal to the thickness of the reaction layer μ. In the case of the so-called surface waves, which will be discussed below, A is the factor of the transition from the bulk- to the surface concentrations, with an allowance made for the catalyst adsorption. The subscript S shows that the concentrations of the substances are taken at the electrode surface.

In the catalytic cycle, the transfer of one electron requires the consumption of one hydrogen ion and therefore, on the basis of the Ilcovič equation, it is possible to write for the hydrogen ion concentration at the electrode surface:

$$[H^+]_S = [H^+]_o - i_{\text{lim.}}/\varkappa_{H^+} \tag{4}$$

where $[H^+]_o$ is the concentration of the hydrogen ions in the bulk of the solution and $\varkappa_{H^+}$ the constant of the Ilcovič equation for hydrogen ions ($\varkappa_{H^+} = i_d/[H^+]_o$).

The quantity $[B]_S$ is proportional to the catalyst concentration in the solution, $c_{\text{cat.}}$. In the case of a non-adsorbed catalyst when $\sigma \gg 1$, $[B]_S = c_{\text{cat.}}$. By replacing $[B]_S$ by $c_{\text{cat.}}$ and substituting the value of $[H^+]_S$, from eqns. (4) and (3) we find:

$$i_{\text{lim.}} = \frac{k_{H^+}SFA\,c_{\text{cat.}}}{1 + k_{H^+}SFA\,c_{\text{cat.}}}\varkappa_{H^+}[H^+]_o \tag{5}$$

It follows from eqn (5) that, in accordance with experiment (see Fig. 1), the dependence of the limiting catalytic current on the catalyst concentration is similar in shape to the Langmuir adsorption isotherm. With a rising $c_{\text{cat.}}$ the height of the catalytic wave tends to approach a limit equal to $\varkappa_{H^+}[H^+]_o$, *i.e.* the diffusion current of the hydrogen ions in this particular solution, as can be readily proved.

According to eqn. (5), with a rising hydrogen ion concentration and a constant catalyst concentration, the catalytic current must increase in proportion to $[H^+]_o$. For not very high values of $[H^+]_o/c_{\text{cat.}}$, the height of the catalytic wave actually changes in proportion to $[H^+]_o$ (see Fig. 2), but with a very large excess of hydrogen ions, the limiting current increases somewhat more slowly than the concentration of hydrochloric acid. This is apparently due to the fact that with a considerable rise in protonation rate, the overall rate of the process becomes affected by the kinetics of another of its steps—the bi-molecular regeneration (III).

The effect of the kinetics of reaction (III) on the height of the catalytic wave becomes particularly apparent at very low catalyst concentrations. In the limiting case, when the overall process is determined by the rate of the bi-molecular interaction and assuming reaction (III) to proceed only in the bulk reaction layer μ_d, on the basis of the BRDIČKA–WIESNER method[55,56], we can write for the height of the catalytic wave:

$$i_{\mathrm{lim.}} = SFk_d\mu_d[\mathrm{BH}]_S{}^2 \tag{6}$$

where k_d is the rate constant of the bi-molecular reaction (III). In the case of a bi-molecular reaction, the reaction layer thickness μ_d is equal to[57]

$$\mu_d = \sqrt{D/k_d[\mathrm{BH}]_S} \tag{7}$$

so that

$$i_{\mathrm{lim.}} = SFk_d{}^{1/2}D^{1/2}[\mathrm{BH}]_S{}^{3/2} \tag{8}$$

where D is the coefficient of the catalyst diffusion.

When the limiting catalytic current is determined by the rate of the bi-molecular interaction (III), $[\mathrm{BH}]_S$ is proportional to $c_{\mathrm{cat.}}$ and therefore, according to eqn. (8), $i_{\mathrm{lim.}}$ must change in proportion to the catalyst concentration to the power of 3/2, which has been observed in the experiment at very low $c_{\mathrm{cat.}}$ (see Fig. 3). With a rise in $c_{\mathrm{cat.}}$ the rate of process (III) rapidly increases and ceases to be the only limiting step; in this case the limiting catalytic current no longer obeys eqn. (8).

It is impossible to obtain by means of the Brdička–Wiesner method the overall dependence of the limiting catalytic current on the catalyst concentration, if the latter changes over a very wide range. The method has been helpful, however, in solving[58] some depolarization problems for some particular cases of catalytic hydrogen waves. In the general form, the depolarization problem for *bulk* or *volume* chemical reactions (I) and (III) (*i.e.* the catalyst is not adsorbed) and for the reversible electrochemical step (II) was solved by KOUTECKY[54] by means of the so-called *exact* method developed by him.

Some of the experimental data considered above and the conclusions are aimed at illustrating the hypothesis suggested above for the occurrence of catalytic waves and have been concerned only with some simple specific cases. As a rule, catalytic hydrogen evolution is a much more complicated process, in which the adsorbed catalyst particles participate; it is essentially affected by the structure of the electric double-layer at the electrode surface and consequently, by the solution composition. Nevertheless, all available experimental data on the catalytic hydrogen evolution and on the influence of various factors on the evolution, can be completely accounted for by the hypothesis put forward.

2. BULK (VOLUME) CATALYTIC HYDROGEN WAVES WITH A REVERSIBLE ELECTROCHEMICAL STEP IN BUFFER SOLUTIONS

Reversible catalytic hydrogen waves

Catalytic hydrogen evolution with a reversible electrochemical step (II) was first observed in pyridine solutions[30,60].

The assumption that the electrochemical step in the discharge of pyridinium ions was reversible was made by analogy with the discharge of the N-alkylpyridinium cations, the reversible character of which has been demonstrated in a number of papers[51,52,61]. Later, the assumption about the reversibility of the discharge of pyridinium ions in the case of catalytic hydrogen evolution was confirmed by much experimental data. The reversibility of the catalytic waves in pyridine solutions was recently proved by measurements of the double-layer capacity[62].

A reversible electron transfer appears to take place also in the case of electrochemical processes in which other substances with -onium structures (*e.g.* the tetra-alkylammonium salts) participate[63]. In particular, the very high pseudo-capacity observed by GRAHAME[64] in the case of the electro-reduction of tetra-methylammonium ions is an indication of the reversible character of the discharge of these ions.

Bulk character of the catalytic waves in pyridine solutions

Catalytic waves can be limited by the rate of the preceding chemical reaction (I), occurring both in the bulk of the solution near the electrode surface and actually on the electrode surface, with the adsorbed substances participating. Accordingly the waves may be subdivided[34,65,66] into *bulk* or *volume*, *surface* and *mixed* waves. In the last case the reaction proceeds at comparable rates both on the electrode surface and in the *bulk* reaction layer. For the *surface* component of the kinetic current to be comparable in magnitude to the *bulk* component, it suffices in many cases that the adsorption of the electrochemically inactive form of the catalyst B should correspond only to tenths of 1% of the coverage of the electrode surface with the adsorbed substance. On account of the appreciable surface activity of many substances, resulting in catalytic hydrogen evolution, most of the catalytic waves are of a pronounced *surface* character.

One of the, apparently, very few exceptions is the wave in pyridine solutions, which under certain conditions depends only on the bulk chemical reactions. The bulk character of the waves in pyridine solutions is accounted for by a relatively slow adsorption of pyridine at the potential at which the catalytic wave occurs (about -1.8 V *vs.* S.C.E.). Consideration of *i–t* curves shows that a completely bulk catalytic wave caused by pyridine can be obtained[67,68,69] only in the presence of high concentrations of the supporting electrolyte (for potassium salts 0.2 M[67,105]), when the adsorption of pyridine is markedly lowered. This occurs only if electrodes with a very short dropping time are used, such as those fitted with a spatula for a forced detachment of drops. If the dropping time is very short (less than 0.5 sec) there is not enough time for an amount of pyridine to become adsorbed on the electrode surface[69], large enough to produce a surface wave, and no appreciable amounts of polymeric, catalytically active byproducts formed by the electrochemical reduction of pyridine in buffer solutions[68] can accumulate.

Equations for reversible bulk catalytic hydrogen waves in buffer solutions

On the basis of the reaction layer concept, let us consider a common case when the limiting current of the catalytic waves is determined by the rate of the preceding protonation (I) alone and not affected by the kinetics of the subsequent bi-molecular reaction (III). For the preceding bulk reaction (I) the reaction layer thickness is equal to

$$\mu = \sqrt{D/\varrho\sigma} \tag{9}$$

The height of the catalytic wave is determined by the amount of BH^+ particles formed in a unit of time within the layer with the thickness μ:

$$i_{\text{lim.}} = SF\mu[\text{B}]_S\varrho \tag{10}$$

Assuming, as is usually the case, that $\sigma \gg 1$, *i.e.* that the catalyst in the solution exists mainly in the basic (non-protonated) form and that due to complete regeneration of the catalyst, a steady state is established at the electrode in a very short time, the quantity $[\text{B}]_S$ may be taken as equal to the total, analytical concentration of the catalyst in the solution ($c_{\text{cat.}}$). Taking into account eqn. (9), we may write for the height of the catalytic wave

$$i_{\text{lim.}} = SFc_{\text{cat.}}\varrho^{1/2}D^{1/2}/\sigma^{1/2} \tag{11}$$

If we write the Ilcovič equation for a hypothetical diffusion current which would be present in the case of the usual diffusion-limited catalyst discharge at $n = 1$, as

$$i_d = 1.235\, SFc_{\text{cat.}}D^{1/2}t^{-1/2} \tag{12}$$

(where t is the dropping time), the ratio of the limiting catalytic current to the diffusion current will be in the form of a simple expression[58]:

$$\frac{i_{\text{lim.}}}{i_d} = 0.81\sqrt{\frac{\varrho t}{\sigma}} \tag{13}$$

On the basis of eqn. (13), from the experimental values of $i_{\text{lim.}}$, we can readily calculate the overall constant of the protonization rate ϱ determined by eqn. (1). It should be noted that an equation practically coinciding with eqn. (13) has also been obtained by an exact solution of a depolarization problem for the conditions stated (eqn. (49) in[54]).

If the value of the limiting current of the catalytic wave is markedly affected by the kinetics of the subsequent reaction, an exact solution[54] gives for the value of ϱ the relation:

$$\varrho = \frac{(i_{\text{lim.}}/i_d)^2\sigma}{0.81^2 t\left[1 - \left(\frac{3}{2}\cdot\frac{(i_{\text{lim.}}/i_d)^2}{0.81^2 k_d c_{\text{cat.}} t}\right)^{1/3}\right]^2} \tag{14}$$

It will be seen that with an increase in the rate of the bi-molecular interaction of the electrode products, *i.e.* with the rise in $c_{\text{cat.}}$ or an increase in k_d, eqn. (14) is transformed into eqn. (13). Another equation, similar to eqn. (14) can also be deduced on the basis of the reaction layer concept (eqn. (30) in[58]). It differs from eqn. (14) only in the absence of the numerical coefficient 3/2 before the second term in square brackets.

In the case when the bi-molecular interaction (III) is the step determining the limiting catalytic current, an exact solution of the depolarization problem gives an expression for the limiting current (eqn. (50) in[54]), differing from eqn. (8) only in the presence of a numerical factor equal to $\sqrt{2/3}$. Thus with catalytic waves of this type, both the exact and the approximate methods for the solution of the depolarization problem lead to practically identical results.

When the preceding protonation is the limiting step and $\sigma \gg 1$, the equation for the shape of a reversible bulk catalytic hydrogen wave can be obtained by substituting the values of $[BH^+]_S$ and $[BH]_S$, *i.e.* the surface concentrations of the redox system (II) components, into the Nernst equation[30,58].

$$E = \varepsilon_0 - \frac{RT}{F} \ln \frac{i^{2/3}}{i_{\text{lim.}} - i} \tag{15}$$

where the characteristic potential ε_0, which is not dependent on the catalyst concentration and corresponds to a point on the wave where $i^{2/3} = i_{\text{lim.}} - i$, is given by

$$\varepsilon_0 = E_0 - \frac{RT}{3F} \ln \left(\frac{SFD^{1/2} \varrho^{3/2} \sigma^{3/2}}{k_d} \right) \tag{16}$$

E_0 is the redox-potential of system (II).

An exact solution of the depolarisation problem[54] gives for the half-wave potential in the case under consideration:

$$E_{1/2} = E_0 + \frac{RT}{3F} \ln \frac{c_{\text{cat.}} k_d}{3\sigma^2 \varrho} \tag{17}$$

A similar expression for $E_{1/2}$[30,58] can also be obtained from eqn. (15) by assuming $i = 1/2\, i_{\text{lim.}}$ and taking into account eqns. (11) and (16); it differs from eqns. (17) only in that we have in the denominator under the sign of the logarithm, the quantity 2 in place of 3.

Experimental verification of the equations for reversible bulk waves in buffer media

The most distinct catalytic waves occurring in the presence of pyridine and its homologues are observed[29,30,67,70] in borate and veronal buffer solutions at a pH within the range 7.5–10. Under these conditions, in accordance with theory, the limiting catalytic current is proportional to the area of the dropping electrode and does not depend on the height of the mercury column above it. In the solution under consideration the protonation of the catalyst is the limiting step of the waves; therefore, with an increase in the buffer capacity of the solution (the pH and the ionic strength of the solution remaining constant) and from theoretical considerations, the protonation rate ϱ always rises and, consequently, so does the limiting catalytic current (see Fig. 4). With an increase in pH of the solution, when $\sigma = K_A/[H^+]$ rises, as shown by numerous experimental data[30,59,70,71], a lowering of the catalytic waves is observed (see eqn. (11) or (13)).

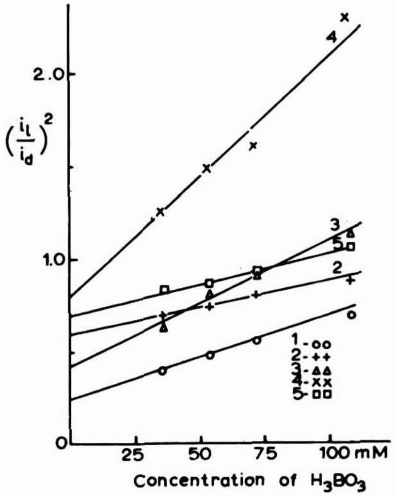

Fig. 4. Dependence of $(i_{\text{lim.}}/i_d)^2$ on the concentration of undissociated H_3BO_3 in a borate buffer pH = 8.40 (ionic strength = 0.5 M) for the catalytic hydrogen waves caused by ~0.5 mM solutions of: (1), pyridine; (2), α-picoline; (3), β-picoline; (4), γ-picoline; (5), α,α′-lutidine.

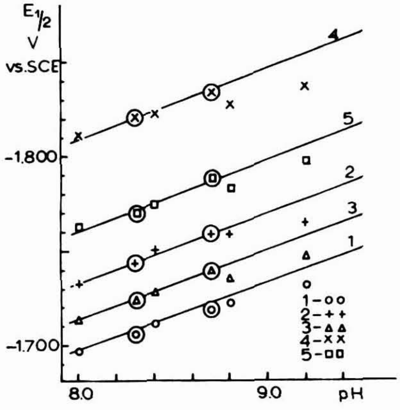

Fig. 5. Dependence of $E_{1/2}$ of the catalytic waves on pH of the solution at a catalyst concentration ~ 0.5 mM and $\varrho \approx 1500$ sec^{-1}. Catalyst: (1), pyridine; (2), α-picoline; (3), β-picoline; (4), γ-picoline; (5), α,α′-lutidine. Plain signs, borate buffer solutions; surrounded with circles, veronal solutions.

Equation (15) demonstrates that the bulk catalytic hydrogen waves with a reversible electrochemical step are assymetrical. As shown by experiment[30], their plots in the $E - \log i^{2/3}/(i_{\text{lim.}} - i)$ coordinates is a straight line with the reciprocal value of the slope of about 59 mV. In accordance with theory, the values of $E_{1/2}$ (see eqn. (17)) become about 20 mV more positive with a ten-fold increase in $c_{\text{cat.}}$[30].

When the protonation of the catalyst is the limiting step of the process, the value of $E_{1/2}$ of the reversible bulk wave becomes more negative with an increase in pH of the solution (*i.e.* with an increase in σ) and, in accordance with theory (see eqn. (17)), at a not too high pH $\Delta E_{1/2}/\Delta\text{pH} \approx -40$ mV (Fig. 5). Figure 5 shows that at pH > 8.8, the change in $E_{1/2}$ with an increase in σ becomes smaller; this is due to the influence of the double-layer structure, which becomes apparent when the thickness of the reaction region diminishes. This question will be considered in more detail in subsequent sections.

The effect of the buffer capacity of the solution on the value of $E_{1/2}$ of the reversible wave is most important for the verification of the validity of the suggested hypothesis of catalytic waves. For most processes limited by the preceding protonation, a shift in $E_{1/2}$ in the direction of less cathodic potentials, is to be expected with an increase in the buffer capacity. This is observed, for instance, in the case of the reduction of nitro-compounds in an acid medium[72]. Similarly, from the theory of catalytic waves, of KNOBLOCH[14] and STACKELBERG AND NÜRNBERG[19], $E_{1/2}$ would be expected to become less negative with an increase in buffer capacity. Equation (17) shows, however, that with an increase in ϱ due to the rising buffer capacity of the solution, $E_{1/2}$ should become more negative. This conclusion is completely confirmed by experiment. Figure 5 shows the dependence of $E_{1/2}$ of the waves caused by pyridine[59], on changes in ϱ, which in turn, are due to changes in concentration of the buffer components of variaous solutions (their pH and ionic strength remaining constant). $E_{1/2}$ of the reversible catalytic waves becomes about 20 mV more negative for a ten-fold increase in ϱ. This is in quantitative agreement with eqn. (17).

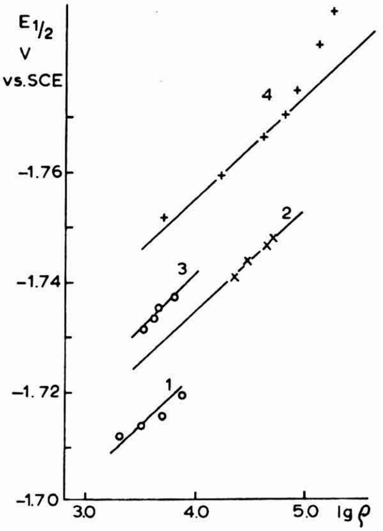

Fig. 6. Dependence of $E_{1/2}$ of the catalytic wave in pyridine solutions on the observed values of ϱ: (1), veronal buffer, pH = 8.3, (3), borate buffer, pH = 9.0; (2) and (4), ammonia solutions, pH = 9.0 and 9.5, respectively.

It is not possible to obtain a sufficiently distinct limitation of the catalytic current by the bi-molecular reaction with pyridine as a catalyst[29]. This is due to the fact that with a decrease in pH of the buffer solution to below pH 7.0, the formation of a catalytically active polymer from pyridine[68] becomes particularly pronounced and this hinders the experiments. Moreover, a decrease in the pyridine concentration results in a shift of the wave in the direction of negative potentials and, as the wave is superimposed upon by the discharge current of the supporting electrolyte, especially at pH < 7.0, it becomes very difficult to determine with sufficient accuracy the values of $i_{\text{lim.}}$ and $E_{1/2}$ of the catalytic wave. Nevertheless, we were able to observe the catalytic wave caused by pyridine down to pH 6.0 (acetate buffer) and to show that under these conditions the current is to an appreciable extent limited by the bi-molecular interaction[29,71]. We should even estimate approximately the rate constant of the bi-molecular reaction (II), which at 25° proved to be in the order of $5 \cdot 10^8$ l/mol. sec.

A somewhat clearer picture of the limitation of the reversible catalytic wave by the rate of the bi-molecular regeneration was observed in the case of the waves caused by 2.6-lutidine[29].

Determination of the rate constants of catalyst protonation; effect of the double-layer structure on the protonation occurring in the "bulk" reaction region

From values of the limiting current of bulk catalytic waves it is possible by means of eqn. (14) to find the ϱ-constants of the catalyst protonation rate in a particular solution. The value of the hypothetical diffusion current i_d of the catalyst is either calculated by means of the Ilcovič equation (assuming $n = 1$), or taken as equal to the discharge diffusion current of a substance with a similar structure.

In the case of the waves caused by pyridine, the value of $k_d = 5 \cdot 10^8$ l/mol.sec was used in the calculations[59,71], the discrepancy in the values of ϱ, determined from eqns. (13) and (14) varing within 5–20%, depending on the value of $c_{\text{cat.}}$. It should be noted that the value of $k_d = 5 \cdot 10^8$ for pyridine is not very accurate, but it can be readily understood that, as the expression in the round brackets in the denominator in eqn. (14) is close to unity, even considerable variations in the value of k_d have almost no effect on the values of ϱ.

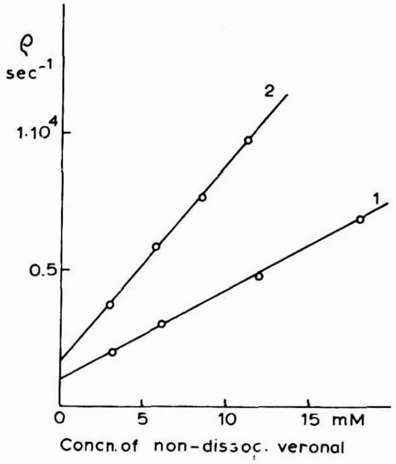

Fig. 7. Dependence of ϱ on the concentration of undissociated veronal in solutions. (1), pH = 8.30; (2), pH = 8.70.

The quantities ϱ are the overall rate constants of the catalyst interaction with all the proton donors in the solution. The specific rate constants of catalyst protonation by the action of individual acids present in the solution, can be found from the dependence of ϱ on the concentration of one proton donor, with the concentrations of the other proton donors remaining constant. Figure 7 shows, as an example, the dependence of ϱ on the concentration of un-dissociated veronal (one of the buffer components of the solution) with pH and the ionic strength of the solution remaining constant. The quantity ϱ increases linearly with veronal concentration. The slope of the straight lines (ϱ/concentration of the acid component) gives directly the value of a specific constant of the catalyst protonation rate under the action of a given proton donor.

The specific constants of the catalyst protonation rate determined directly from the dependence of ϱ on the concentration of the undissociated acid prove to be dependent on pH, their values rising with an increase in the latter. An apparent rise in the rate constants is explained by the growing influence of the electric double-layer structure observed with an increase in pH of the solution[59].

The structure of the electric double-layer affects the distribution of ions and the velocity of their motion in the region near the electrode[73-76]. GRABOWSKI AND BARTEL[77] were the first to take into consideration the effect of the double-layer structure on the preceding reaction of protonation; this problem was later considered in a more general form by a number of other investigators[78-80].

If the thickness of the reaction layer greatly exceeds the extent of the diffuse part of the double-layer, the effect of the latter on the mean concentration of ions within the reaction layer may be neglected[79]. As the thickness of the reaction region diminishes, an ever greater part of it will be taken up by the diffuse part of the double-layer and its effect will increase. In the case of bulk catalytic currents, the thickness of the reaction region diminishes with an increase in pH of the solution (*i.e.* with a rise in σ, (see eqn. (9)) and therefore, the effect of the double-layer structure becomes more and more apparent. As shown in[34,66,81], the action of the electrostatic field of the electrode in buffer solutions results in a considerable increase in pH in the region near the electrode, compared to the pH in the bulk of the solution; it is the lower pH in the region near the electrode which is responsible for an apparent rise in the rate constants of protonation with a decrease in the thickness of the reaction region.

A change in pH of the solution (the ionic strength being constant) involves a change in the thickness of the reaction region μ only, whereas the effective extent of the diffuse part of the double-layer remains unchanged. The relationship between the extents of these layers may also be varied by changing the thickness of the diffuse part of the double-layer, while keeping μ constant. This is effected by changing the ionic strength of the solution, the pH and buffer capacity remaining constant. With an increase in ionic strength, the thickness of the diffuse part of the double-layer diminishes, the difference between the pH in the region near the electrode and that in the bulk of the solution becomes smaller, and consequently, the mean value of pH in the reaction layer rises somewhat and the limiting catalytic current decreases. Calculations show that the decrease in the height of the catalytic wave of pyridine observed with an increase in the ionic strength of the solution[34], is quantitatively described by the change in the effect of the double-layer structure[82].

In order to find the true values of the rate constants of catalyst protonation undistorted by the effect of the electrode field, it is necessary to extrapolate the values found directly from experiment to the range of very large μ, *i.e.* to low pH values, where the rate constants are not affected by the double-layer structure. Experience shows that the ***apparent*** values of the specific constants of protonation found in the experiment $k'_A = \Delta\varrho/\Delta[DH^+]_A$ (from the plots of the type shown in Fig. 7), change linearly with the reciprocal of the hydrogen ion concentration[30,70,71]. By plotting the values of k_A' *vs.* $1/[H^+]$ and extrapolating them to $1/[H^+] \to 0$, it is possible to find the true values of the protonation rate constants k_A. Figure 8 shows a similar extrapolation[59] for the rate constants of pyridine protonation with undissociated boric acid (straight line 1) and veronal (2) at 25°, with an ionic strength of the solution of 0.5. The true values of the rate constants for pyridine determined from the intersection of the straight lines with the ordinate axis proved to be equal to, $k_{H_3BO_3} = 9.0 \cdot 10^3$ and $k_{ver.} = 1.2 \cdot 10^5$ l/mol.sec[59,71].

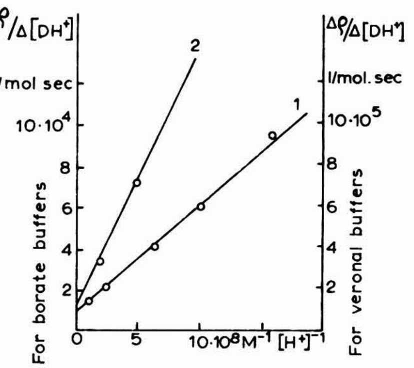

Fig. 8. Dependence on $1/[H^+]$ of the observed specific rate constans of pyridine interaction with: (1), H_3BO_3; (2), veronal.

The intersection points of the straight lines of the type shown in Fig. 7, with the ordinate axis, correspond to the *apparent* values of ϱ_0' the sum of the rate constants of protonation under the action of water and hydrogen ions. In order to find the values of ϱ_0 undistorted by the effect of the double-layer, it is necessary to divide ϱ_0' by the ratio k_A'/k_A for the solution in question. Using the relation between the corrected values of ϱ_0 and $[H^+]$ the rate constant of pyridine protonation by hydrogen ions was estimated as $k_{H^+} \approx 2.5 \cdot 10^{10}$ and by water as $k_{H_2O} \approx 7$ l/mol.sec[59].

The stronger the acid (proton donor) the larger the value of the rate constants of pyridine protonation. As in the case of other protolytic reactions, the specific constants of pyridine protonation, k_A, are related to the constants of acid dissociation K_A by the Brönsted relationship (see [83]):

$$k_A = pG\left(\frac{q}{p} K_A\right)^{\alpha} \qquad (18)$$

where G and α are constants and p and q the so-called statistical factors which take account of the number of protons that can be detached from various atoms of a particular acid or that can be added to various atoms of its conjugate base, respectively. In the case of pyridine protonation at 25°, with the ionic strength of the solution = 0.5, the value of α proved to be equal to 0.58[71].

Effect of temperature on bulk catalytic waves in buffer solutions

The height of bulk catalytic hydrogen waves increases with rising temperature. The specific rate constants of pyridine protonation were found from the dependence of the limiting currents on the concentration of the acid components at different temperatures corrected for the double-layer effect[71].

It is of interest to note that the temperature has almost no influence upon the relative change in the apparent protonation rate constants produced by the double-layer effect, with an increase in pH of the solution, *i.e.* upon the quantity $\Delta k_A'/\Delta(1/[H^+])k_A$. This is due to the fact that the difference between the value of the pH at the electrode surface and that in the bulk of the solution (which is responsible for the apparent change in the constants of the protonation rate) changes in proportion to the quantity $\exp(-\psi_1 F/RT)$[34,66], which in turn is almost independent of the temperature, since the value of ψ_1 (if it is not too small) changes almost linearly with the absolute temperature[73]. In the case of solutions with higher ionic strength (1.0 instead of 0.5), because of the smaller thickness of the diffuse part of the double-layer, the apparent increase in the protonation rate constants markedly diminishes with a rise in pH of the solution[71].

The values of the activation energies of the interaction of pyridine: with boric acid, 5.1 cal/mol; with veronal, 6.4 cal/mol; with hydroxonium ions, ~2.4 cal/mol and with water, ~6 cal/mol[71] were calculated from the dependence of the specific constants of protonation on the reciprocal of the temperature.

It is of interest to note that the straight lines corresponding to the Brönsted equation (18) for pyridine protonation, plotted for various temperatures, do not change their slope within experimental error, but are only shifted somewhat parallel to themselves[71].

Effect of stirring of the solution on catalytic hydrogen waves under conditions of the polarographic maximum of the second kind

The mixing of the solution caused by the tangential motions of the surface of a mercury dropping electrode with rapidly flowing mercury, results in a disturbance of the diffusion layer and consequently, in an increase in the observed polarographic diffusion current. This phenomenon, studied in detail by FRUMKIN *et al.*[73] has been called the polarographic maximum of the second kind[84,85].

The investigation of the influence of stirring under the conditions of the maximum of the second kind, upon bulk catalytic waves in pyridine solutions, showed in a number of cases that stirring results in an increase in the catalytic current[86]. The stirring effect depends on the thickness of the reaction layer μ. It attains the maximum value, almost twice as large as the corresponding value for the diffusion current, at $\mu \approx 100$ Å. Processes which are limited, by the reaction occurring in a very thin layer (<20 Å), or on the electrode surface (with the participation of the adsorbed substances), are not affected by stirring. This seems to be due to the fact that at very small μ the whole reaction layer is located within the stationary (with respect to the electrode) boundary layer of the solution.

Under the conditions of stirring the protolytic equilibrium between the catalyst forms seems to be restored more rapidly, and this results in a decrease in the effective μ and in an apparent increase in ϱ. As a result of the increase in ϱ upon stirring, in accordance with eqn. (17), $E_{1/2}$ of the waves in a pyridine solution are shifted in the direction of more negative potentials[86].

3. REVERSIBLE BULK CATALYTIC HYDROGEN WAVES IN UNBUFFERED SOLUTIONS

Deduction of equations[60]

In an unbuffered solution in neutral or alkaline media practically the only proton donor (DH^+) is water, and its conjugated base D is the hydroxyl ion. Therefore:

$$\varrho = k_1[H_2O] \qquad \varrho\sigma = k_2[OH^-]_S \tag{19}$$

It follows from the scheme of the process that each catalytic cycle (reactions (I–III)) involves the formation of an OH^- ion. By using the Ilcovič equation for calculating the rate of removal of OH^- from the electrode, and considering that in neutral or weakly alkaline solutions during the electrolysis $[OH^-]_S \gg [OH^-]_o$ we find that

$$[OH^-]_S = \frac{i}{\varkappa_{OH^-}} \tag{20}$$

where $\varkappa_{OH^-}$ is the constant of the Ilcovič equation for OH^-. The thickness of the reaction layer of the protolytic reaction (I) is determined in this case by the rate of the binding of the active form of the catalyst BH^+ by the hydroxyl ions; therefore, if μ is small enough for the concentration of OH^- within its range to be considered constant, μ will be equal to

$$\mu = (D/k_2[OH^-]_S)^{1/2} = (D\varkappa_{OH^-}/k_2 i)^{1/2} \tag{21}$$

For the limiting currents from eqns. (10) and (21), (taking into consideration eqn. (19) and also that $[B]_S = c_{\text{cat.}}$), we find:

$$i_{\text{lim.}} = (Qc_{\text{cat.}})^{2/3} \tag{22}$$

where

$$Q = k_1 SFD^{1/2}\varkappa_{OH^-}^{1/2}[H_2O]/k_2{}^{1/2} \tag{23}$$

It follows from eqn. (22) that in unbuffered solutions the height of the bulk catalytic wave changes in proportion to the catalyst concentration raised to the power of 2/3.

The equation for the wave shape can be obtained by substituting the values of $[BH^+]_S$ and $[BH]_S$ into the Nernst equation[60]

$$E = \varepsilon_0'' - \frac{RT}{F}\ln\frac{i^{5/3}}{i_{\text{lim.}}{}^{3/2} - i^{3/2}} \tag{24}$$

and if the current strength in eqn. (24) is expressed in μA,

$$\varepsilon_0'' = E_0 + \frac{RT}{F}\ln\frac{k_d{}^{1/3}\varkappa_{OH^-}^{1/2}}{k_2{}^{1/2}(SF)^{1/3}D^{1/6}} + 59\text{ mV} \tag{25}$$

Experimental verification of equations

Figure 9 shows[67] the dependence of the heights of the catalytic waves in a 0.5 N KCl solution on the concentration of pyridine and its homologues, raised to the power of 2/3. We can see from the figure that eqn. (22) is fulfilled with sufficient accuracy. The constants of the protonation rates for pyridine and its homologues under the action of water (see Table 1), were found from the slope of the $i_{\text{lim.}} - c_{\text{cat}}^{2/3}$ curves, *i.e.* from the values of Q using eqn. (23).

Figure 10 shows the dependence of the function of the current log $i^{5/3}/(i_{\mathrm{lim.}}^{3/2} - i^{3/2})$ on the potential for the catalytic waves at the catalyst concentration $c_{\mathrm{cat.}} = 24$ mM (for the waves in pyridine solutions the data corresponding to various $c_{\mathrm{cat.}}$ are presented). The upper part of the polarograms (at higher values of the current than those at which a very small but finite value of the buffer capacity of KCl solution due to the traces of dissolved CO_2 or other impurites, has been already exhausted) is satisfactorily described by eqn. (24), by means of which the straight lines on Fig. 10 are plotted. The function of the current found from eqn. (24) for the waves in the presence of the same catalyst, irrespective of its concentration, must be located on one straight line. The values for several concentrations of pyridine presented in Fig. 10 show that with a rise in the concentration, the straight lines are somewhat shifted in the direction of negative potentials. This is probably due to a certain rise in pH in the

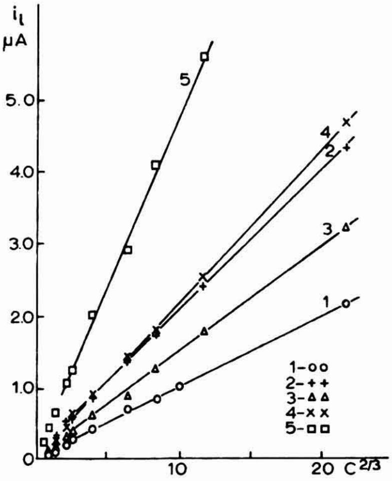

Fig. 9. Dependence of the limiting catalytic currents on the catalyst concentration raised to the power of 2/3 for the waves in unbuffered solutions of: (1), pyridine; (2), α-picoline; (3), β-picoline; (4), γ-picoline; (5), α,α′-lutidine.

TABLE 1

PROPERTIES OF PYRIDINE AND ITS METHYL DERIVATIVES

Catalyst	*Pyridine*	*α-Picoline*	*β-Picoline*	*γ-Picoline*	*α.α′-Lutidine*
pK_A 2(5° 0.5 M KCl)	5.50	6.15	5.90	6.19	6.83
k_d [l/mol.sec]	$5.0 \cdot 10^8$	$3.8 \cdot 10^7$	$1.4 \cdot 10^8$	$\sim 3 \cdot 10^5$	$1.5 \cdot 10^6$
E_0 (V *vs.* S.C.E.)	−1.632	−1.670	−1.655	−1.673	−1.710
$k_{H_3BO_3}$ (l/ml.sec)	$7 \cdot 10^3$	$1.5–2 \cdot 10^3$	$7–10 \cdot 10^3$	$1–2 \cdot 10^4$	~ 100
$k_{\mathrm{ver.}}$ [l/mol.sec]	$1.3 \cdot 10^5$	$4 \cdot 10^4$	$1–2 \cdot 10^5$	$3–6 \cdot 10^5$	$\sim 8 \cdot 10^3$
N-methyl iodides in 0.5 M KCl					
$E_{1/2}$ ($\sim$0.5 mM solns.)	−1.522	−1.620	−1.560	−1.671	−1.698
D [cm²/sec · 10⁵]	1.05	1.05	0.95	1.00	1.10

bulk of the solution with an increase in the catalyst concentration, which was not taken into account in the deductions of eqn. (24).

4. SURFACE CATALYTIC HYDROGEN WAVES

Main characteristics

In the case of catalytic waves of a completely surface character, the catalyst participates in the protonation reaction on the electrode surface in the adsorbed state[65,87,88].

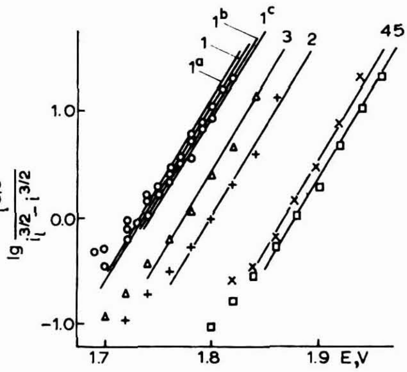

Fig. 10. Dependence of log $i^{5/3}/(i_{\mathrm{lim.}}^{3/2} - i^{3/2})$ on E of the catalytic hydrogen waves with 0.5 *M* KCl supporting electrolyte in 24 m*M* solutions of: (1), pyridine; (2), α-picoline; (3), β-picoline; (4), γ-picoline; (5), α,α′-lutidine. Pyridine concentrations: (1a), 16; (1b), 40; (1c), 100 m*M*.

The strength of the surface catalytic current is proportional to the amount of adsorbed catalyst. Therefore, on the basis of the general hypothesis for the occurrence of the catalytic wave, limited by protonation kinetics, we may write:

$$i = SF(\varrho_{\mathrm{surf.}}\Gamma - \varrho_{\mathrm{surf.}}\Gamma' \cdot \sigma_{\mathrm{surf.}}) \qquad (26)$$

and for the limiting current

$$i_{\mathrm{lim.}} = SF\varrho_{\mathrm{surf.}}\Gamma \qquad (27)$$

where Γ and Γ' are the adsorbed amounts of the basic (B) and the acid (BH^+) forms of the catalyst, respectively. As shown by experiment, surface catalytic currents have an irreversible electrochemical step[89]. Therefore, on the basis of the slow discharge theory[73], we may write for the current:

$$i = Sk_{\mathrm{el}}\Gamma' \mathrm{e}^{-\alpha FE/RT} \qquad (28)$$

If the catalyst adsorption did not change with the electrode potential and were equal to the value Γ^0, which it has at the potential of maximum adsorption E_m, using eqns. (26), (27) and (28) we could write for the wave to be observed in that case:

$$E = E_{1/2} - \frac{RT}{\alpha F} \ln \frac{i^0}{i^0_{\mathrm{lim.}} - i^0} \qquad (29)$$

the superscript *zero* indicating that the values correspond to the adsorption state at E_m.

Let the catalyst adsorption obey the Langmuir isotherm

$$\Gamma_{\mathrm{e}} = \Gamma_{\infty} \frac{\beta c_{\mathrm{cat.}}}{1 + \beta c_{\mathrm{cat.}}} \qquad (30)$$

where Γ_e and Γ_∞ are the equilibrium and the maximum amounts of the adsorbed substance, respectively and β the adsorption index. The adsorption equilibrium is usually not established during the life of the drop[90]. Therefore, at the moment of time t which has elapsed since the beginning of formation of the drop:

$$\Gamma = y\Gamma_e \tag{31}$$

Complete establishment of the equilibrium y depends on the time of adsorption, the rate of the transport of the substance to the electrode and on the value of β[90,91]. Long before the establishment of the equilibrium, *i.e.* when $y \ll 1$, the value of y increases approximately in proportion to the square root of the adsorption time[91]:

$$y \approx kt^{1/2} \tag{32}$$

On the basis of the results of an accurate calculation of the kinetics of a diffusion-limited adsorption towards a dropping electrode[90], it is possible to show, as has been done in Fig. 11, that with $c_{\text{cat.}}$ and t constant, the value of y (at $y \leqslant 0.55$) rises with an increase in β in accordance with the equation[87]:

$$y = 1 + \beta c_{\text{cat.}} \tag{33}$$

According to FRUMKIN[92], the adsorption of substances on the electrode decreases with the removal of the potential from that of maximum adsorption, in agreement with the equation:

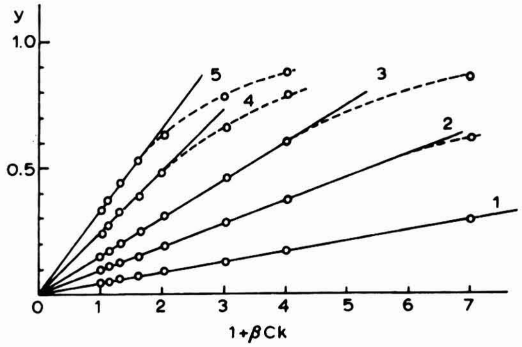

Fig. 11. Dependence of y on $1 + \beta c_{\text{cat.}}$ at different adsorption times at a dropping electrode, plotted from the data of DELAHAY AND FIKE[90]: (1), 0.2; (2), 0.5; (3), 1.0; (4), 2.0; (5), 4.0 sec.

$$\beta = \beta^0\, e^{-\frac{\frac{1}{2}(C - C')}{RT\Gamma_\infty}\varphi^2} = \beta^0\, e^{-a\varphi^2} \tag{34}$$

where φ is the potential measured, as referred to E_m (*i.e.* $\varphi = E - E_m$) and C and C' the capacities of the electrode double-layer in the absence of a surface active substance and with a complete coverage of the electrode surface with a monolayer of surface active substance, respectively.

The overall adsorption of the catalyst depends on the adsorption of its basic and acid forms, which are in protolytic equilibrium with each other. The data of GOUY AND BUTLER for organic bases in neutral and acid solutions[93,94,95] suggest that the surface activity of the basic form on mercury is much higher than that of the acid form. Moreover, the adsorption of the cation form on the cathode changes much less with the potential than that of the basic form, which is uncharged[93]. Therefore, the change in the overall catalyst adsorption (especially when the equilibrium (I) is shifted to the left) is determined mainly by the change in the adsorption of its basic form, although the amount of the adsorbed substances depends on the proportions of the two forms, *i.e.* on the pH of the solution as well.

Because of a decrease in the adsorption of the catalyst with a rise in cathodic potential, the catalytic current actually observed is smaller than the current i^0 and $i/i^0 = \Gamma/\Gamma^0$, or taking into account eqns. (30) and (31)

$$\frac{i}{i^0} = \frac{y\beta}{1 + \beta c_{\mathrm{cat.}}} : \frac{y^0\beta^0}{1 + \beta^0 c_{\mathrm{cat.}}} \qquad (35)$$

Taking into account eqns. (33) and (34), we shall have for $y \leqslant 0.55$ (the latter inequality is almost always observed on the dropping electrode under the usual conditions):

$$\frac{i}{i^0} = \frac{\beta}{\beta^0} = \mathrm{e}^{-a\varphi^2} \qquad (36)$$

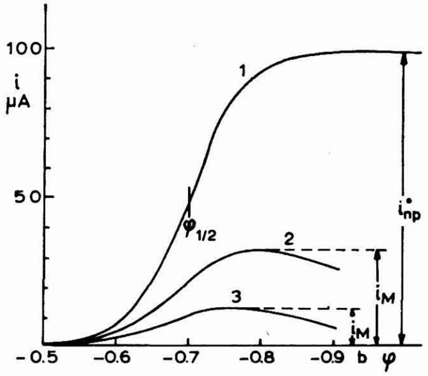

Fig. 12. Scheme explaining the formation of a hump-like shape of the surface catalytic wave. (1), curve plotted with no allowance made for the change in asdorptivity with the potential, in accordance with eqn. (29): (2) and (3), waves obtained with the change in adsorptivity with the potential allowed for (a = 1.63 and a = 3.27 V^{-2} in eqn. (36), respectively).

The characteristic *hump-like* shape of the surface catalytic hydrogen waves observed[87] is described by a combination of eqns. (29) and (36). Figure 12 shows schematically the formation of the descending part of the surface waves. As is evident from Fig. 12, the maximum height of the wave observed, i_m, does not represent its limiting current. In most cases i_m is practically proportional to $i^0_{\mathrm{lim.}}$ and for the purposes of analysis it is therefore permissible to use instead of $i^0_{\mathrm{lim.}}$ of the catalytic waves, the quantity i_m, which can be directly measured.

Experimental verification of surface waves equations

The validity of the equations deduced was proved[87], using as examples the surface catalytic waves caused by anabasine and quinine.

As with all currents limited by the kinetics of the preceding protonation, the surface catalytic wave grows with a rise in the buffer capacity. The dependence of the catalytic current in anabasine solutions on the concentration of undissociated acetic acid was used to estimate[87] the value of the rate constant of the adsorbed anabasine protonation under action of CH_3COOH as $2.9 \cdot 10^5$ l/mol. sec at a potential -1.84 V *vs.* S.C.E.

It should be borne in mind that the electric field of the electrode brings about polarization of the particles, which possibly affects[77] the values of the rate constants of *surface* reactions.

In a number of cases *surface* waves possess a very interesting characteristic; they have an unusual dependence on h, the height of the mercury column above the dropping electrode. If the limiting diffusion currents and the adsorption *pre-waves* decrease with a diminishing h and the *bulk* kinetic and catalytic currents do not depend on h the waves limited by the preceding *surface* reactions often increase with the lowering of h[34]. This phenomenon is observed in those cases where the adsorption equilibrium has not yet been established, and an increase in dropping time, *i.e.* the adsorption time, results in a closer approach to the establishment of the adsorption equilibrium and, consequently in a rise in Γ.

The dependence of the surface component of the kinetic current density on the time, often obeys eqn. (32). This was demonstrated for the case of the second wave on the polarograms of maleic acid[96]. A rise in catalytic waves with a lowering of the height of the mercury reservoir was observed by VOJIŘ[97,98] and ASAHI[99].

A similar effect was observed by many investigators[100,101] in the case of currents caused by the cobalt complexes of amino-acids and proteins. When determining the i–t curves during the life of one drop, STACKELBERG AND FASSBENDER[17] found that the catalytic current rose in accordance with the law $i \approx t^\nu$, the value of ν being greater than unity in the presence of catalysts with large molecular weights. Figure 2 in[17], indicates that ν in some cases attained the values $\sim 7/6$, which corresponds to the total effect of the increase in the electrode area (2/3) and to a rise in the amount of the catalyst adsorbed (1/2), according to eqn. (32).

As in the case of surface kinetic waves[96], surface catalytic currents often undergo almost no change with rising temperature[53] as an increase in the rate constant of catalyst protonation is compensated for by a decrease in its adsorption on the electrode surface[34].

It is well known that the addition of surface active substances (S.A.S.) to the polarographic solution often appreciably lowers the catalytic wave[15]. This is accounted for by the fact that foreign S.A.S. displace the catalyst from the electrode surface. The magnitude of the suppressing action of S.A.S. evidently depends on the relationship between the concentrations of S.A.S. and the catalyst, and their adsorption.

If the desorption of S.A.S. occurs before that of the catalyst and if the desorption potential of S.A.S. is located in the region of catalytic hydrogen evolution, a marked increase in the catalytic current is observed on the polarograms during the desorption of S.A.S.[102,103]. This may be considered as the occurrence of a new wave. This phenomenon somewhat resembles the formation of the pseudo-waves of reduction, which is observed in the case of S.A.S. desorption, when adsorbed S.A.S. either hinders the course of the electrode process[104] or suppresses the tangential motions of mercury.

Mixed "bulk-surface" catalytic waves

It is evident that all catalytic currents observed in practice must be considered as the sum of the surface and the bulk components, and only in very rare cases may we speak of practically completely surface or completely bulk waves. The appearance of the surface component could be observed[67,69] even in the case of pyridine.

The surface component of the current increases with a decrease in the ionic strength of the solution[105], especially upon transition to solutions containing only non-adsorbing cations[106,107], *e.g.* lithium ions[108].

Generally, the bulk and the surface components of the current give only one total wave on polarograms, although in some cases two separate waves might be expected. When, in the region near the electrode, there is a considerable increase in the concentration of the irreversibly discharging particles during their adsorption, it is sometimes possible to observe[109,110] on the polarograms, the appearance of an additional wave of the discharge of strongly adsorbed particles. This is followed at more negative potentials by the discharge of the non-adsorbed particles, (to be more precise, by the poorly adsorbed ones or by those less advantageously oriented from an energy point of view). Thus, in the case of surface currents, the effect of a marked increase in the catalyst concentration in the region near the electrode should cause a shift in the surface catalytic wave in the direction of less cathodic potentials, compared to the bulk wave. On the other hand, the adsorption of an electrochemically active particle (*i.e.* its orientation on the electrode surface), may affect the rate constant of the electrochemical step proper. Thus, for instance, in the case of the polarographic analysis of indolenium salts[111], the discharge of which is somewhat similar to the electron transfer to a particle of protonated catalyst, the irreversibility of the wave, judging by its slope, increases with a rise in pH. This appears to be due to an increase in the adsorption of the depolarizer upon its transition to its basic uncharged form.

Thus, adsorption may greatly change the rate of the electrode process and shift the potentials of the wave in the direction of the anode or of the cathode.

Bulk waves of solutions of pyridine and its homologues possess a reversible electrochemical step, whereas no reversible electrochemical processes have ever been observed in the case of surface catalytic waves. In this connection, it is of especial interest to note that when large amounts of a strongly adsorbed substance were added to a quinine solution, a reversible catalytic wave of hydrogen evolution was apparently obtained[89]. The total height of the wave decreased in this case to about a thirtieth of its previous value and the potential of the half-wave became somewhat more positive (compared to $E_{1/2}$ of the surface wave of the same height). This points to the fact that the bulk component of the catalytic wave in the quinine solution is reversible and may be observed at less negative potentials than the surface wave. The foregoing favours the possibility that the total catalytic wave may become divided under certain favourable conditions into bulk and surface steps. This division of the wave could in fact be observed in the case of the catalytic currents in quinine solutions[65].

The appearance of the two *humps* on the catalytic waves in a solution of the leucoform of malachite green and β-naphtho-quinoline observed by STACKELBERG *et al.*[18], may be supposed to be due also to the separation of the surface and the bulk components of the currents.

Effect of the double-layer structure on surface catalytic waves

In the case of surface catalytic hydrogen waves, a change in the double-layer structure affects the adsorption of the catalyst, the value of the pH in the layer near the electrode and to a certain extent the dissociation constant of the catalyst, which is in the adsorbed state. Figure 13 shows the effect of the addition of sodium chloride upon the catalytic wave caused by quinine, when the pH, the buffer capacity of the solution and the catalyst concentration are kept constant[81]. With an increase in the overall concentration of sodium ions in the solution from 0.04 *M* to 0.08 *M*, the maximum height of the catalytic wave decreases to about one-third of its previous value (Fig. 13); the potential of the maximum becomes more positive because of an increase in the double-layer capacity and the consequent increase in the value of *a* in eqn. (36). The curves in Fig. 13 are plotted from eqns. (29) and (36), the points corresponding to the experimental values.

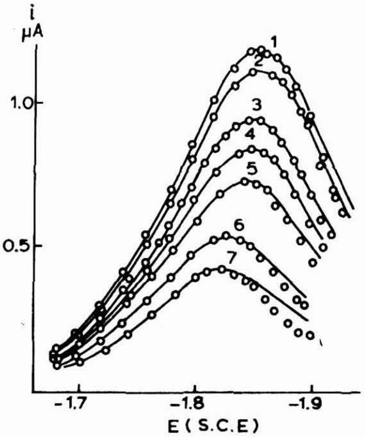

Fig. 13. Catalytic waves of quinine ($c_{\text{quin}} = 3 \cdot 10^{-6}$ *M*) in borate buffer solution, pH = 9.5 at different concentrations of Na^+: (1), 0.040; (2), 0.045; (3), 0.050; (4), 0.055; (5), 0.060; (6), 0.070; (7), 0.080 *M*.

A change in the nature of the cation of the supporting electrolyte has a much greater effect upon surface waves than an increase in the concentration of the supporting electrolyte. The catalytic wave decreases sharply upon transition from solutions containing Li^+ to those containing Cs^+. In the series from Li^+ to Cs^+ the *super-equivalent* adsorption of these cations on a mercury electrode increases[106,107], the absolute value of the ψ_1-potential diminishes, the double-layer capacity rises and consequently, so does the quantity *a* in FRUMKIN's equation. As a result of all these factors, $i^0_{\text{lim.}}$ decreases and the slope of the surface catalytic waves becomes steeper[81] on transition to solutions containing cations of larger radii.

In the case of surface waves with a preceding protonation (and in this case only[87,66]), the difference between the pH in the bulk of the solution and that in the layer near the electrode is a simple function of the ψ_1-potential. Therefore, it was possible to determine almost quantitatively the effect of a change in the concentration of potassium and sodium ions in the solution upon surface catalytic currents[81].

The effect of the double-layer structure can also be used in explaining[112] the very interesting observations of PUNGOR AND FARSANG[113-116]. These authors found, in particular, that the gradual addition of a tetra-ethylammonium salt to a solution being analyzed polarographically, gives first a rise in the catalytic wave of quinine, and then a decrease. PUNGOR AND FARSANG worked with phosphate buffer solutions where HPO_4^{2-} and $H_2PO_4^-$ anions are the main proton donors; therefore, at a small concentration of the surface active cation of tetra-ethylammonium, the negative ψ_1-potential decreases and thus the approach of the proton donors (phosphate anions) to the electrode is facilitated. When the concentration of tetra-ethylammonium rises, the displacement by the latter of quinine from the electrode begins to have effect, resulting in a decrease in the catalytic current. A similar phenomenon was also observed upon the addition of surface active cations to the solution, in the case of the kinetic surface wave caused by the recombination of acid anions[88,117,118].

Effect of organic solvents

The addition of organic solvents to solutions of catalytically active systems results in a decrease in catalytic currents[15,16,119–122].

The action of organic solvents results in (1): a decrease in the dissociation constants of the acids (proton donors) and hence a rise in pH of the solution[123,124]; (2) a decrease in the dissociation constants of the catalyst[119–123] and consequently, in a still larger rise in σ compared to the change in pH; and, finally, which is of special importance in the case of surface currents, (3) a considerable diminution in the adsorption of the catalyst.

5. CATALYTIC WAVES CAUSED BY SULFUR-CONTAINING COMPOUNDS

Mechanism of the process

Many organic compounds containing a sulphydryl group possess a marked ability for producing catalytic hydrogen waves. A characteristic feature of sulfur-containing catalysts is the sharp increase in their catalytic activity upon the addition of cobalt or nickel salts to the solution. This was first observed by BRDIČKA[3]. In spite of the large amount of research devoted to the study of catalytic waves in solutions of sulfur-containing compounds (see literature surveys[5,8,9,10], and new experimental data[18,21–23,101–103,125–132]), some features of the mechanism of the process have not yet been elucidated.

BRDIČKA advanced a hypothesis[9,25] to explain the catalytic action of substances containing sulphydryl groups (thiols). He suggested that the hydrogen in the —SH group on account of its high mobility, becomes readily detached in the course of the electrochemical reaction

$$RSH + e^- \rightarrow RS^- + H \qquad (IV)$$

and the RS^- anions formed are rapidly protonated at the expense of the proton donors of the solution, regenerating the electrochemically active form RSH. A point in favour of this scheme is the fact, established by BRDIČKA[9,133], that the catalytic activity of thiols is suppressed when a salt of mono-iodoacetic acid is introduced into the solution and its residue combines with sulfur instead of a mobile hydrogen atom.

While investigating the reduction of sulfones on a dropping electrode, MAIRANOVSKII AND NEUMAN[134] found that the reduction product (probably p,p′-dichlordiphenylsulfide) of p,p′-dichlordiphenylsulfone (with a transfer of 4 electrons), also causes a catalytic wave, although it contains no —SH group. On this account, the authors supposed that the mechanism of the occurrence of the catalytic wave under the action of sulfur-containing catalysts is the same as in the case of nitrogen-containing bases, *i.e.* it is the sulfonium ion formed during the protonation of sulfide, which is discharged. The catalytic evolution of hydrogen under the action of compounds containing a sulfide sulfur has been observed a number of times. It occurs, for instance, in a solution of ethylene-bis-thioglycollic acid[18] ($HOOC.CH_2.S.CH_2.S—CH_2COOH$) as well as in the case of sulfides formed during the electro-reduction (with $n = 2$) of tri-substituted sulfonium ions[48]. A mechanism involving the discharge of a sulfonium cation has been shown by FRUMKIN AND ANDREEVA[31] to be more likely, taking into account the effect of the double-layer structure at the electrode surface. This effect can also account for the suppression of the catalytic activity of the catalyst during its interaction with iodoacetate; the product formed assumes a negative charge, which hinders this reactions on the cathode.

The fact that the catalytic activity of cysteine continues to be appreciable when the hydrogen of its-SH group is substituted by a mercuribenzoate residue[21]

$$RSH + ClHgC_6H_4COOH \rightarrow RSHgC_6H_4COOH$$

also favours the sulfonium scheme for the occurrence of catalytic waves.

Available experimental data are, however, insufficient for favouring any particular scheme for the discharge process of hydrogen catalyzed by substances containing sulfydryl groups.

As already mentioned, the presence of cobalt ions in the solution is a very important factor in the marked increase in the catalytic activity of sulfur-containing substances. The Co^{2+} reduction wave precedes the catalytic hydrogen evolution; therefore, in the case of the adsorption of an organic catalyst, some investigators[9,12] supposed catalytically active centres to be formed on metallic cobalt deposited on a mercury surface. BŘEZINA[135] proved this concept to be wrong by demonstrating that preliminary electrolysis of the solution on a stationary mercury electrode at a potential at which Co^{2+} is discharged, but at which no catalytic hydrogen evolution occurs (*i.e.* there is an accumulation of metallic cobalt on the electrode), has no effect on the catalytic wave subsequently determined. Thus a complex of a cobalt ion with an organic molecule must serve as a catalyst.

The fact that catalytic waves are almost always observed in Co^{2+} solutions and are often absent in solutions containing Co^{3+} permits us to suppose that the catalytically active complexes[125] contain mainly cobaltous ions, although sometimes cobaltic ion complexes are more catalytically active than cobaltous ion complexes[23].

The effect of the concentration of sulfur-containing compounds on the $E_{1/2}$ of the Co^{2+} reduction wave observed by many investigators is an indication of the formation of Co^{2+} complexes with these compounds.

It may be supposed that Co^{2+} can form several complexes of varying composition with the same thiol[9], some of which are so stable that they hardly participate in an electrochemical reaction which gives a deposit of cobalt, but mainly cause catalytic hydrogen evolution. Stable Co^{2+} complex which are not discharged on the cathode are formed, for instance, by ethylenediaminetetra-acetic acid[137]. Partial formation of a *non-discharging* (*i.e.* involving no deposition of metallic cobalt during the electrode reaction) Co^{2+} complex with cysteine is to some extent confirmed by a decrease in the height of the Co^{2+} discharge wave with an increase in the cysteine concentration in the solution, as observed by SUNAHARA[128].

Yet, a discharge of the metal ion from the complex with thiol occurs simultaneously with catalytic hydrogen evolution[132,136]. The effect of this discharge becomes appreciable at relatively low concentrations of the complexing agent ion in the solution. As the result of a deficiency of these ions in the layer near the electrode, aggravated by their partial discharge from the complex, the catalytic current may become dependent on the diffusion of these ions from the bulk of the solution, and the observed catalytic wave may assume certain characteristics of the diffusion current. This seems to be responsible for the effects observed in a cysteine solution containing a small concentration of Ni^{2+} ions[137,22]. Discharge of Ni^{2+} from the catalytically active complexes proceeds rather slowly, so that there is time for the complex to participate more than once in the catalytic process before Ni^{2+} is discharged from it. This accounts for the fact that the catalytic current is much higher than the diffusion current of Ni^{2+} ions[137].

A rise in the catalytic activity of thiols when they form complexes with Co^{2+} seems to be the result of an increase in the mobility of thiolic hydrogen[9], and what is most important, a rise in the catalyst charge by two units, which considering the effect of the double-layer structure should considerably facilitate the electron transfer to these particles.

It is of interest to note that Co^{2+} and Ni^{2+} increase the catalytic activity not only of sulfur-containing compounds, but also of those of pyridine[139]. The catalytic activity of pyridine is appreciably higher in the presence of Co^{2+} than of Ni^{2+} at the same concentration. It is especially high when both Ni^{2+} and Co^{2+} are present in the solution. The catalytic hydrogen wave caused by pyridine complexes with Co^{2+} or Ni^{2+} is of a pronounced surface character. With a rise in the temperature, the height of the catalytic wave rapidly decreases, and disappears entirely at a temperature above 35°, in 0.1 *N* pyridine solution and 0.1 *N* pyridinium chloride solution containing a $5 \cdot 10^{-4}$ *M* Co^{2+} and Ni^{2+} [139].

Sulfur-containing organic compounds possess a high surface activity at the mercury-solution interface. In particular, the suppression of a maximum on the cobalt wave observed upon the addition of these compounds to the polarographic solution, as well as the lowering of other maxima on the waves, due to tangential motions[140] are an indication of this. The complexes of sulfur-containing substances with cobaltous (or cobaltic) ions seem to possess high adsorptivity. Therefore, the catalytic waves caused by them are of a completely surface character and their properties (particularly their shape) are described by the equations of surface waves[87].

The majority of compounds which are of biological interest contain not only a catalytically active sulfur, but also nitrogen (in the form of amino groups) which is also capable of catalyzing hydrogen evolution. The catalytic effect observed in solutions of these compounds is determined by the combined action of all active groups in the molecule. SUNAHARA[129] showed that in the case of waves caused by cystine and its derivatives, in which either the amino groups or the carboxyls are blocked, that the blocking of amino groups (N,N-diacetylcystine) results in total loss of the catalytic activity of cystine, whereas the esterification of carboxyls (diethyl ester of cystine) has almost no effect on the catalytic wave. Therefore, it may be supposed that in catalysts containing both amino- and sulphydryl groups, catalytic activity is mainly due to amino groups, whereas adsorptivity of the catalyst is determined principally by —SH groups[22]. This probably accounts for the parallelism, observed by IVANOV[140], between the ability of the catalysts to suppress the polarographic maximum, (*i.e.* their adsorptivity), and the height of the catalytic wave caused by them, at identical weight concentrations. The adsorptivity of the catalysts which (other conditions being equal) determines the limiting catalytic current, rises with an increase in the size of their molecules or in the number of the —SH groups contained in them. However, the number of amino groups per unit weight of catalysts having similar structures is almost independent of the size of the catalyst molecules. This probably accounts for the approximately proportional rise in catalytic activity, observed by ITO[141], with increase in the number of cysteine residues contained in the catalysts (proteins).

With an increase in catalyst concentration in the solution, the height of the catalytic wave caused by sulfur-containing compounds rises in accordance with a curve similar in shape to the Langmuir adsorption isotherm. Although the catalyst is adsorbed on the electrode surface, this similarity, as shown by KLUMPAR[26], is purely formal. The lag in the build up of the limiting catalytic current, compared to the direct proportionality observed with an increase in catalyst concentration, is not due to the coverage of a considerable part of the dropping electrode surface by the catalyst, but to the exhaustion of the buffer capacity of the solution in the region near the electrode (see the introduction to this survey), or to the exhaustion of the concentration of the complexing ions (Co^{2+}, Ni^{2+}) near the electrode.

It is of interest to note that the frequently observed decrease in the limiting currents (the *hump-like* shape) of the catalytic waves in protein solutions may disappear if the concentration of protein is considerably increased, the concentrations of buffer solution and of cobalt ions being kept constant (see Figs. 3 and 4, pp. 115 and 117 in[3] and [137]). This means that the protein concentration no longer determines the rate of formation of a catalytically active complex and the desorption of protein brings about no decrease in the catalytic current with an increase in the cathodic potential.

The effect of pH on the catalytic waves caused by the complexes of cobalt or nickel ions with sulfur-containing compounds is much more complicated than in the case of simple nitrogen-containing catalysts. In the case of catalysis by complexes the maximum wave height is observed at a certain pH of the solution[22]. At very high pH values the wave diminishes because of a decrease in the protolytic reaction rate. In spite of an increase in the protonation rate the wave diminishes with a decrease in pH below the optimum value since the formation of a catalytically active complex is hindered by the protonation of the functional groups of the organic molecule which participate in the formation of the complex[22].

The *surface* character of catalytic waves in a solution containing cobalt complexes of amino acids or proteins is responsible for an unusual change in the dependence of the height of the peak of the catalytic wave on the i–E oscillopolarograms, upon the rate of application of the polarizing voltage $\partial E/\partial t$, described by VALENTA AND WITWICKI[142]. For bulk catalytic waves the peak current should not depend on $\partial E/\partial t$, as is the case with a hydrogen peroxide reduction catalyzed by iron ions[142]. In the case of protein catalytic waves, a rather large rise in the peak current with an increase in $\partial E/\partial t$ is at first observed; then this rise slows down and at high enough rates of change in potential the peak current attains the limit. The change in the peak current with $\partial E/\partial t$ is caused by catalyst desorption with a shift in the potential in the direction of the cathode. With an increase in the rate of the application of potential, an ever greater part of the desorbed catalyst is unable to leave the reaction layer near the electrode surface, remains there and continues to participate in the catalytic process. This accounts for the rise in the peak height with an increase in $\partial E/\partial t$ observed on the i–E oscillopolarograms.

Nature of the doubling of protein waves

In contrast to the waves caused by many amino-acids, the catalytic waves observed in protein solutions containing cobalt ions often have a characteristic *two-humped* shape.

In order to determine the nature of this doubling of catalytic waves, the effect of the electrode dropping time on the height of the separate steps of this wave (with a relative excess of Co^{2+} ions) was studied[100]. A special dropping electrode fitted with a spatula for forced detachment of the drops, which could be adjusted by means of a micro-screw, was used in the experiments. Thus at a practically constant rate of mercury flow (m = 0.69 mg/sec) the dropping time t varied over a wide range.

Figure 14 shows the dependence of the logarithm of the height of the steps on log t. This dependence is of a rectilinear character for all the steps.

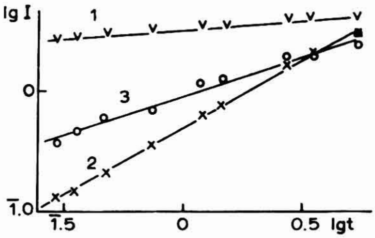

Fig. 14. Dependence of the heights of separate steps of the protein wave on the dropping time. (1) cobalt wave; (2), the first protein step; (3), the second step.

In the case of a cobalt diffusion wave (straight line 1, Fig. 14) the slope of the straight line log i_d — log t is close to 0.18, as should be expected[143]. The slope of the straight line for the first protein step (straight line 2) is close to 7/6 and this step rises in proportion to $t^{7/6}$. Evidently, the rise in the current proportional to $t^{7/6}$ is due to an increase in the surface concentration of the adsorbed catalyst when the process of catalyst adsorption (occurring long before the establishment of the adsorption equilibrium) is limited by the diffusion, the catalyst being either poorly adsorbed or its concentration in the solution very small. The slope of the straight line 3 (Fig. 14) corresponding to the height of the second protein wave equal to 2/3, points either to the surface character of the wave with an established (or almost established) adsorption equilibrium of the catalyst, or to a process occurring in the bulk of the solution. In both cases the current is proportional only to the electrode surface area. The hypothesis about the bulk nature of the second wave is at variance with the experimental data. Thus, if by analogy with the quinine waves[65], we suppose the second wave to be caused by the same catalyst as the first, but acting in the bulk of the solution, the effect of higher fatty acids interacting chemically with the catalyst[144] would lower both waves to the same degree. In practice, it is only the second wave which diminishes in this case[144]. Thus both waves seem to be of a surface nature.

The difference in character of the adsorption processes corresponding to the first and to the second protein steps indicates that the catalytically active centres which cause them do not belong to the same protein molecule. In other words, this points to the presence in the solution of at least two catalysts of different properties[100].

Numerous facts point in favour of a lesser adsorptivity of the catalyst of the first protein step. Thus under the action of surface active gelatine, the height of the first step diminishes and that of the second step remains almost unchanged (see, for instance, Fig. 4 in the work of Marha[144]). A smaller temperature coefficient of the first wave [145] can also be taken as an indication of lesser adsorptivity if it is assumed that the activation energies of the chemical processes determining the heights of both waves are similar in their values. In some cases, however[23], the second wave diminishes with rising temperature to a greater degree than the first.

The existence of two kinds of catalyst cannot be ascribed to the presence in the solution of various protein molecules, as the double wave is observed also in the case of individual proteins in solutions of cobalt salts.

The appearance of two waves is probably due to the formation of several types of Co^{2+} complexes with a protein molecule which differ in their composition or structure[146] and in their catalytic properties. In the opinion of IVANOV and RAKHLEEVA[147], the first step is due to the complex of cobalt ions with protein in the globular state and the second to the same protein, but in a non-globular state.

The concentration of Co^{2+} ions in the solution has a varying effect on the heights of the protein waves; *i.e.* it affects the formation of the corresponding catalytic complexes in a different ways. As follows from BRDIČKA's work[25], the height of the second maximum rises linearly with the $CoCl_2$ concentration, whereas the increase in the first maximum slows down and its height tends to approach a limit[100].

It is of interest to note that when ethylenediamine-tetra-acetic acid (EDTA) is added to the solution, the second wave diminishes first (see Fig. 4 in[138]). This can be readily explained by the fact that EDTA binds the Co^{2+} ions and diminishes their concentration in the solution; the dependence of the wave heights on the concentration of the Co^{2+} ions remaining in the solution is about the same as that in[25].

BŘEZINA[135] observed that the catalytic wave disappeared in the case of binding of cobalt ions by a complexing agent. If the solution contains a complexing agent which binds cobalt more firmly than the catalyst causing the second wave, but less firmly than the catalyst causing the first wave, only the first protein wave should remain on the polarograms. This phenomenon was actually observed by ITO[141] while working with a tris-(ethylenediamine)–cobaltic chloride solution.

The influence of various chemical factors which change the heights of protein waves, such as the effect of higher fatty acids[144] or formaldehyde[148], can be explained either by the blocking of the catalytically active centres, or by the binding of the groups participating in the formation of the complexes, or by a change in the adsorptivity of one of the catalysts.

6. DEPENDENCE OF CATALYTIC HYDROGEN WAVES ON THE STRUCTURE OF ORGANIC CATALYSTS

General

KNOBLOCH[14] was the first to notice that the decrease in the hydrogen overvoltage on a dropping mercury electrode in the presence of a number of heterocyclic catalysts is greater the higher the acidity of the catalyst. The data obtained by STACKELBERG *et al.*[18] for various classes of organic substances (catalysts) also show that in many cases catalytic hydrogen evolution is facilitated by a decrease in pK_A for a series of catalysts of similar structure. This can be readily explained qualitatively by means of the hypothesis for the occurrence of the catalytic wave, described in this paper. The discharge of an electrochemically active acid form of the catalyst proceeds (in accordance with the SHIKATA-TACHI rule[149]) more easily the more electronegative the residue bound with the reducing group; the introduction of a negative group into the acid molecule is known to lower its pK_A.

On the contrary the height of the catalytic wave is usually greater in the case of a catalyst with a higher pK_A[14,150]. Roughly speaking, this is due to the fact that, other conditions being equal, an increase in pK_A of the catalyst results in the protolytic equilibrium between its forms (process I of the general scheme) being shifted in the direction of its electrochemically active (acid) form.

Reversible bulk catalytic waves in buffer solutions

The dependence between the catalyst structure and the character of the catalytic wave can best be studied quantitatively with reversible bulk catalytic waves, when adsorption which complicates the problem is absent. For this purpose, the bulk catalytic waves caused by pyridine, picolines and α,α'-lutidine were studied[70].

Figure 4 shows the dependence of $(i_{\text{lim.}}/i_d)^2$ on the concentration of undissociated boric acid in the solution, with the pH constant at 8.40. It follows from Fig. 4, that $(i_{\text{lim.}}/i_d)^2$ changes linearly with $[H_3BO_3]$, the slope of the straight lines obtained, which is determined by the protonation rate, depending on the nature of the catalyst. The values of ϱ calculated from eqn. (14) (see below for the determination of the values of k_d necessary for the calculation of ϱ from eqn. (14)) were plotted against the concentration of the acid component of the buffer at a constant pH. As in the case of pyridine, the values of the specific constant of the protonation rate of a catalyst k_A' with a given proton donor were found from the slope of the straight lines obtained. As with pyridine, k_A' increases with a rise in pH of the solution also in the case of other catalysts, on account of the enhancing effect of the electric double-layer structure. A plot of k_A' against $1/[H^+]$ and extrapolation to $1/[H^+] \rightarrow 0$ gives the real values of k_A. The slope of the extrapolation straight lines for the waves of the homologues is almost the same as for pyridine: $\Delta k_A'/k_A \,.\, \Delta(1/[H^+]) = 6\text{–}10 \cdot 10^{-9}$ M. The values of the rate constants obtained are listed in Table 1. In the case of lutidine at high pH, the values of k_A' increase somewhat faster than $1/[H^+]$. This appears to be due to a certain adsorptivity of α,α'-lutidine, which with a rise in pH (*i.e.* with a decrease in the reaction layer thickness) brings into play the surface component of the current. Since, with lowering of pH, the discharge current of the supporting electrolyte is superimposed upon the catalytic waves, especially in γ-picoline solutions, the errors in the determination of $i_{\text{lim.}}$ become greater and consequently, the accuracy of the determination of the values of k_A decreases considerably.

For a series of catalysts of similar structure, the constants of the protonation rates k_A, with the same acid, must rise with an increase in pK_A of the catalyst in accordance with the Brönsted relationship.

In the case of protonation by the action of H_3BO_3 and veronal, $k_{H_3BO_3}$ and $k_{\text{ver.}}$ for α-methyl derivatives (see Table 1) are much lower than they should be from the Brönsted relationship, because of steric hindrance[151]. Steric factors may therefore exert a considerably influence on the heights of catalytic waves.

With an increase in the buffer capacity at a constant pH, $E_{1/2}$ of the bulk catalytic waves of the compounds studied become more negative; in accordance with eqn. (17) $\Delta E_{1/2}/\Delta \log \varrho \approx -20$ mV. $E_{1/2}$ also become more negative with a rise in pH. In Fig. 5 are presented the values of $E_{1/2}$ of the waves in ~0.5 mM solutions of the substances studied, referred to the same $\varrho \approx 1500$ sec^{-1}, at different pH values.

By means of eqn. (17) it is possible to find the values of normal redox potentials E_0 for reactions (II). By substituting into eqn. (17) the values of k_d for pyridine and α,α'-lutidine found in[29,71], we obtained for E_0 of the discharge of their ions the values -1.626 and -1.715 V S.C.E. respectively. The values of E_0 are related to pK_A by the formula

$$E_0 = \text{constant} - \frac{2.3\ RT}{F}\ pK_A \tag{37}$$

From eqn. (37) by using the experimental values for pyridine and α,α'-lutidine, the values -1.302 and -1.312 V, respectively, were obtained for the constant. Taking into account the low accuracy of the determination of k_d[29,71], the discrepancy in the values of the constant should be considered as insignificant and the values of k_d taken as being of the correct order of magnitude. The values of k_d of the picolines were found from eqns. (17) and (37) at a value for the constant of -1.307 V, (Table I). These were used in calculating ϱ by means of eqn. (14). Equations (17) and (37) show the relationship between $E_{1/2}$ of the catalytic waves and pK_A of the catalysts.

Large negative values for $E_{1/2}$ of the catalytic wave in a solution of γ-picoline (Fig. 5) and also for $E_{1/2}$ of the reduction wave of its *N*-methyl derivative (Table 1) are to be noticed. This fact is accounted for in the case of γ-picoline derivatives, by the relatively low values of the rate constant k_d of the bi-molecular interaction of radicals in accordance with scheme III (see eqn. (17)). Lower values of k_d in the case of γ-derivatives show that the radicals formed upon the discharge of pyridine derivatives interact with the formation of dipyridyls (rapidly decomposing in the case of catalytic waves) mainly in the γ-, rather than in the α-position. A direct evaluation of k_d for γ-picoline, as for pyridine and α,α'-lutidine, proved to be impossible on account of the very negative potentials at which the catalytic wave in γ-picoline solutions is observed.

Bulk waves in unbuffered media

The rate constants of the protolytic interaction of pyridine homologues with water were determined[67] from the dependence of the limiting currents of polarographic catalytic waves occurring in unbuffered solutions, upon the concentration of the catalysts (see Fig. 9). The values of the rate constants of protonation with water (k_1) and those of deprotonation under the action of OH^- (k_2) for the substances investigated, in 0.5 *M* KCl solution at 25°, are listed in Table 2.

Table 2 shows that the values of k_1 rise with an increase in pK_A of the catalysts, as it should be in accordance with the Brönsted equation, which for this particular case (the protonation of bases with similar structure by the same acid) is of the form:

$$\log k_1 = \log G + \beta pK_A \tag{38}$$

The values of k_1 of the catalysts (except α-picoline) obey the Brönsted equation within $\pm 5\%$; for α-picoline the accuracy is within 12%. The coefficients of the Brönsted equation for the reaction in question are: $\log G = -2.15$, $\beta = 0.5$.

It was shown by BROWN *et al.*[151,152] that as a result of steric hindrance the rate constants of chemical interaction (with the atom of nitrogen) in the case of pyridine derivatives having a CH_3 group in the α-position, are much smaller than would be expected from the law of linear dependence of the change in the free energies[153]. For the same α-substituted pyridine derivative, the steric effect is greater the larger the sizes of the molecules in the reagent which is interacting with nitrogen in the pyridine ring[152].

As has been already mentioned, steric hindrance also becomes apparent in the case of protonation of pyridine homologues by the action of boric acid and veronal. In the case of protonation of α-methyl derivatives of pyridine with water, however, no steric hindrance is observed; this is due, evidently to the small size of water molecules. Protonation under the action of hydroxonium ions also proceeds without steric hindrance[152].

The values of k_1 found for pyridine and the picolines appear to be the true constants of the bulk reactions; they are practically unaffected by the influence of the electrode field. In unbuffered solutions both components of the direct reaction (I) are uncharged. Consequently, we may conclude that the latter is unaffected by the electric double-layer structure. The effects of the field on the concentrations of BH^+ and OH^- ions are opposite in sign and practically of the same magnitude, so that the product of the concentrations of these ions determining the rate of the reverse reaction (I) is also almost independent of the double-layer structure.

Let us consider now the effect of the nature of the catalyst upon the potentials at which catalytic waves are observed in unbuffered solutions.

TABLE 2

SOME CONSTANTS FOR PYRIDINE, PICOLINES AND α,α′-LUTIDINE IN 0.5 *M* KCl SOLUTION AT 25°

No.	*Substance*	pK_A	k_1 *[l/mol.sec]*	$k_2/10^{10}$ *[l/mol.sec]*	ε'' *at °*$C_{cat.}$ *= 24 m M (V vs. S.C.E.)*	E_0 *(V vs. S.C.E)*
1.	Pyridine	5.50	5.5	9.8	−1.733	−1.614
2.	α-Picoline	6.15	10.1	4.0	−1.800	−1.675
3.	β-Picoline	5.90	8.0	5.5	−1.775	−1.656
4.	γ-Picoline	6.19	12.5	4.5	−1.869	−1.699
5.	α,α′-lutidine	6.83	26	2.1	−1.875	−1.732

It follows from Fig. 10 that with a rise in pK_A of the catalyst, as in the case of buffered solutions, the wave is shifted in the direction of negative potentials. For comparison, it is convenient to use the values of the characteristic potentials ε_0'', which are listed in Table 2. Equation (25) shows that the values of ε_0'' depend mainly on those of E_0 of the redox system, which in turn (see eqn. (37)) are linearly shifted in the direction of negative potentials with a rise in pK_A of the substance being discharged.

From experimental values of ε_0'' and the rate constants, it is possible by means of eqn. (25) to estimate the values of E_0. Table 2 lists the values of E_0 thus found; the values of k_d the rate constants of the bi-molecular interaction used in the calculation were the same as those used for buffered solutions (see Table 1).

The values of the potentials for the pH-dependent electrode processes in unbuffered solutions cannot be very stable; therefore, the values of E_0 found from experiments in unbuffered solutions are evidently less accurate than those obtained in buffered solutions. Nevertheless, the values of E_0 for α- and β-picolines determined in unbuffered solutions practically coincide with those listed in Table 1. The discrepancy for pyridine is +18 mV, but for γ-picoline and lutidine in an unbuffered medium, E_0 is shifted by *ca.* 25 mV in the direction of negative potentials, apparently on account of the higher pH in the bulk of the solution in the presence of stronger bases.

Irreversible surface waves

The dependence of irreversible surface catalytic waves on the catalyst structure is complicated by the effect of its adsorption, which while enhancing the catalytic current may shift the wave towards less cathodic potentials.

In the case of a number of catalysts with approximately identical adsorptivity, the values of the potentials ($E_{1/2}$ or the potentials of the *half-maximum*, which are much more readily determined in the experiment) depend on pK_A of the catalysts in accordance with one of the modified Hammet equations[153,154]; with a rise in pK_A the wave must become more negative. As already stated, the limiting current increases with a rise in pK_A of the catalyst and there are numerous examples illustrating this fact in the papers already mentioned[14,18,150].

ZUMAN AND KUIK[155] showed that the introduction of substituents into the 5-th position of pyrimidine increases the catalytic activity in Co^{2+} solutions in the sequence $-OH < -NH_2 < -SH$. The increase in the activity is explained by the authors, as due to the change in acid properties of the substances and their ability to form a complex with Co^{2+}.

LAMPRECHT *et al.*[21] studied the ability of a large number of sulfur-containing substances to produce catalytic hydrogen evolution. They established that the character of the catalytic wave is dependent on the kind of complex the molecule of the sulfur-containing substance forms with Co^{2+}. Thus if in addition to $-SH$ (or $-SS-$) groups, the carboxyls located in their vicinity also participate in the formation of the complex, a catalytic wave occurs directly after the discharge of cobalt and has a characteristic hump-like shape (for instance, in cysteine and Co^{2+} solutions). If the complex with Co^{2+} is formed by sulfur and the $-NH_2$ or $-NH-$ group present in the molecule, the wave caused by this complex is somewhat lower and in place of the characteristic descending part, a flat section of the limiting current is observed. During polarographic investigations of organic molecules in ammonia–cobalt solutions, in the absence of active groups other than $-SH$ or $-SS-$, only a rise in the current without a clearly defined flat section of the limiting current, is observed before the discharge of the supporting electrolyte.

The observations of STEVANČEVIČ[156], who studied the catalytic activity of quinoxaline-2,3-dithiol in solutions of Co^{2+} and Ni^{2+} are of interest. It follows from the data given that the catalytic wave in a solution of a nickel salt is much lower than in cobalt solutions, and located at less negative potentials. If the adsorptivities of quinoxaline-dithiol complexes with Ni and Co ions are to be considered to be approximately identical, the difference in the catalytic waves observed can apparently be explained by a higher value of pK_A of the complex with Co^{2+} than that of the complex with Ni^{2+}. From the dependence of the heights of the catalytic waves on the concentrations of quinoxaline-dithiol and Co^{2+} and Ni^{2+} ions, STEVANČEVIČ established the fact that there are two molecules of quinoxaline-dithiol per one atom of metal in the complex[156].

TOROPOVA AND ELIZAROVA[157] showed that not only the complexes of sulfur-containing compounds with Co^{2+} and Ni^{2+}, but alo those with Fe^{2+} possess catalytic activity. They also found that an addition to a polarographically analyzed solution, of metal ions that form a more stable complex with thiols than nickel, results in a decrease in the height of the catalytic hydrogen wave[157–159]. An original method for the determination of small concentrations of a number of metal ions is based on the displacement of nickel from a catalytically active complex[159].

It is of interest to note that the dependence of the catalytic wave on pK_A of the catalyst may be used for an approximate estimation of pK_A of catalytically active substances[160].

In the case of catalysts with different surface activities, the height of the catalytic wave increases upon transition to substances with greater adsorptivity[140,141]. Surface waves are very sensitive to subtle changes in the catalyst structure. ZUMAN[161], for instance, found the second wave on the polarograms of erythro-phenyl-cysteine in an ammoniacal solution of $CoCl_2$, to be almost twice as high as that of the treo-isomer.

Catalytically active organic substances

As has been already noted, the catalytic activity of organic catalysts is due to the presence of an unshared pair of electrons in their nitrogen, sulfur, phosphorus, oxygen or arsenic atoms, and to the ability of the catalysts to accept a proton with the formation of -onium compounds. Therefore, catalytic waves are observed in solutions of amines (but not of tetra-substituted amines), thiols and sulfides, phosphines[98] and arsines[162-165]. Recently KNOBLOCH[15,166] studied in detail the catalytic hydrogen waves caused by oxonium compounds—the derivatives of chromone. A catalytic hydrogen evolution in the presence of oxonium catalysts (the products of an electrochemical reduction of unsaturated diketones with carbomethoxyl groups) was observed by RYVOLOVÁ[167], ZHDANOV and POLIEVKTOV[168] described the catalytic waves caused by diphenyl-cyclopropenone in acid solutions.

7. SOME OTHER THEORIES OF CATALYTIC HYDROGEN WAVES

A number of other theories and schemes have been developed, to explain the nature and mechanism of catalytic hydrogen waves. Let us consider them briefly. One of the first theories was advanced by BRDIČKA to explain the mechanism of catalytic waves in a solution of sulfur-containing substances. According to BRDIČKA, hydrogen is detached from the $-SH$ group and the subsequent protonation of the RS^- anion under the action of acids, occurs near the electrode. This theory has been briefly discussed in Section V. BRDIČKA's conception is well known and as it is described in most textbooks on polarography, there is no need to consider it further. It should be noted however that BRDIČKA's theory is inapplicable to catalytic waves caused by nitrogen-containing bases. STROMBERG[12] was the first to note the kinetic limitations of catalytic waves in solutions of catalysts containing cobalt salts and he deduced relevant equations for the dependence of the limiting current on the composition of the solution, *i.e.* on the concentration of the components whose rate of interaction determines the catalytic wave. In his calculations STROMBERG proceeded from the scheme of the process suggested by BRDIČKA, considering the atoms of discharged cobalt to be the catalytically active centres.

KIRKPATRICK[11], who studied the catalytic evolution of hydrogen under the action of a large number of different alkaloids, assumed that the catalytic action was due to the alkaloid accepting the electron from the electrode and transferring it to the hydrogen ion in the solution. According to KIRKPATRICK, the catalytic activity of the alkaloid is greater the larger its *electronic capacity*, *i.e.* its ability to accept electrons from the cathode.

KNOBLOCH[14] extended BRDIČKA's scheme to the catalytic waves caused by heterocyclic and aromatic amines. Like BRDIČKA, KNOBLOCH believed that the catalyst accelerated the formation of H_2 from the hydrogen atoms evolved at the cathode and thus decreased the hydrogen overvoltage (in accordance with HEYROVSKY's theory of hydrogen overvoltage[169]). In a more recent work[15] KNOBLOCH has already used the theory of catalytic waves suggested by STACKELBERG *et al.*[17-19].

According to STACKELBERG[17-19], the catalyst acts only when it is in an adsorbed state on the electrode, and his theory is closest to the hypothesis developed by the author of this work. After the catalyst has accepted the proton, it changes into an electrochemically active cationic form, which is irreversible discharged at the electrode, evolving hydrogen and regenerating the catalyst in its basic form. The last step of the process, the regeneration of the catalyst and the formation of molecular hydrogen, is not considered in Stackelberg's theory. Thus if we disregard the last step, Stackelberg's scheme corresponds to the particular case of irreversible surface waves in MAIRANOVSKII's theory. STACKELBERG's ideas do not embrace all the observed facts, since, as was shown in preceding sections, there are catalytic processes in which the protonation reaction occurs in the region near the electrode (*i.e.* without the adsorption of the catalyst—an indispensable requirement of STACKELBERG's theory) and the electron transfer to the protonated article of the catalyst may proceed at such a high rate that the electrochemical step assumes a reversible character.

The concept of STACKELBERG *et al.*, which supposes that the catalyst can be protonated only by hydroxonium ions, and that other acids present in the solution can act only after the dissociation of these acids and the formation of hydroxonium ions, seems to be erroneous:

$$HA \rightarrow H^+ + A^- \tag{V}$$

$$B + H^+ \rightarrow BH^+ \tag{VI}$$

On the basis of these concepts, STACKELBERG *et al.*[170-172] attempted to determine the dissociation rate constants of the acids HA from the values of the catalytic currents in the solutions of acids HA (and also by means of RÜETSCHI's method[173], from kinetical currents limited by the protonation rate). In reality, the processes studied by them were limited mainly by the kinetics of a direct interaction of HA with B[36,37,88,174-176]. Let us consider this question in more detail.

The acid HA can react with all the bases present in the solution, B and H_2O included (since the dissociation of the acid represents its protolytic interaction with the solvent acting as a base). In accordance with the Brönsted relationship, the rate constant of the interaction of HA with a strong base B must be much higher than that with a very weak base H_2O. Taking into account the fact that the concentration of H_2O is much higher than that of B, we may consider the rates of interaction of HA with B and H_2O to be similar in order of magnitude. The particles of BH^+ formed according to the reaction (B + HA) participate in an electrochemical reaction, while the hydroxonium ions may react both with B and with other bases in the solution, including A^- (according to the reverse reaction V), tending to restore the concentration of HA, which is an equilibrium one at a given pH. In the case of weak acids not completely dissociated in the solution, the anions A^- are very strong bases (usually stronger than B) and their concentration in the solution, especially in the layer near the electrode, is much greater than that of B; therefore, the hydroxonium ions, which may be formed according to (V), will interact mainly with A^- and only slightly with B. Thus BH^+ are mainly formed by the reaction of HA with B.

The mechanism of catalyst protonation (V–VI) suggested by STACKELBERG is invalid also in the case of poorly buffered or unbuffered solutions, when the concentration of H^+ in the layer near the electrode may become very low and conditions favourable for process (V) would seem to be established. In this case, however, the concentration of the strongest base (the hydroxyl ions) in the region near the electrode becomes high enough and an interaction of HA with OH^- occurs in place of process (V). The rate of dissociation of H_2O into ions $2\ H_2O \rightarrow H_3O^+ + OH^-$ ($k = 2 \cdot 10^{-5}\ \mathrm{sec}^{-1}$ [177]) cannot ensure the value of the catalytic current observed in unbuffered solutions, which was shown to correspond to the rate of catalyst protonation by the action of water (for pyridine, *e.g.* $k_1 = 5.5$ l/mol. sec).

It should be noted, by the way, that if catalyst protonation by undissociated acids of the type of HA should pass through a step of their dissociation, steric hindrance in the protonation by undissociated boric acid and veronal[67] of α-picoline and α,α'-lutidine would not be observed, since steric hindrance is absent in the case of protonation of these compounds by water and hydroxonium ions[152].

To conclude this brief survey of the theories of catalytic waves, we should consider an ingenious explanation for the readier discharge of catalyst cations, compared to the evolution of hydrogen ions, suggested by FRUMKIN[31,178]. Frumkin confines his considerations to the conditions when the slowest step of the catalytic process is the electrochemical reaction proper, and the catalyst exists both in the solution and in the adsorbed state, mainly as an electrochemically active cation BH^+ (*i.e.* $\sigma \ll 1$). Considering the discharges of BH^+ and H_3O^+ to be of the same kind, (*i.e.* the transfer coefficient α is identical for both reactions) for the rate constants of electron transfer to BH^+ and H_2O^+, FRUMKIN uses the Brönsted equation, which relates the values of the rate constants of the electrode processes with the dissociation constants of the acids being discharged. He shows that for the BH^+ discharge to proceed faster than that of H_3O^+ in the same solution, it is necessary for BH^+ to be a cation and possess an appreciable specific adsorptivity. Only in this case is the effect of the electric double-layer structure manifested in such a way that it facilitates the discharge of BH^+ to a much greater degree than that of H_3O^+. In this theory, however, the adsorbed hydrogen atom rather than the BH radical, is assumed to be the product of the electrochemical reaction. This is the reason why this theory cannot account, in particular, for the occurrence of reversible catalytic waves and it is also inapplicable in the cases when $\sigma \gg 1$, *i.e.* when the catalyst is present mainly in its basic (non-protonated) form.

REFERENCES

1 F. HERLES AND A. VANČURA, *Bull. Intern. Acad. Sci. Bohême*, N 42 (1932) 1.
2 J. HEYROVSKÝ AND J. BABIČKA, *Collection Czech. Chem. Commun.*, 2 (1930) 370; *Chem. News*, 141 (1930) 369.
3 R. BRDIČKA, *Collection Czech. Chem. Commun.*, 5 (1933) 112, 148.
4 J. PECH, *ibid.*, 6 (1934) 190.
5 R. BRDIČKA, *Z. Phys. Chem.*, Sonderheft, Juli 1958, S. 165.
6 I. M. KOLTHOFF AND J. J. LINGANE, *Polarography*, Gostekhkhimizdat, Moscow, 1948.
7 T. A. KRIUKOVA, S. I. SINIAKOVA AND T. V. AREFIEVA, *The Polarographic Method (Polarograficheski metod)*, Gostekhkhimizdat, Moscow, 1959.
8 I. D. IVANOV, *The Polarography of Proteins (Polarografia belkov)*, Izd. Akad. Nauk SSSR, Moscow, 1961.
9 R. BRDIČKA, *Research, London*, 1 (1947) 25.
10 M. BŘEZINA AND P. ZUMAN, *Polarography in Medicine, etc.*, Interscience Publishers, Inc., New York, 1958.

11 H. F. W. Kirkpatrick, *Quart. Journ. Pharm. Pharmacol.*, 18 (1945) 245; 18 (1945) 338; 19 (1946) 8; 19 (1946) 127, 526; 20 (1947) 87.
12 A. G. Stromberg, *Zh. Fiz. Khim.*, 20 (1946) 409.
13 A. G. Stromberg and A. I. Zelianskaia, *Zh. Obshch. Khim.*, 15 (1945) 303.
14 E. Knobloch, *Collection Czech. Chem. Commun.*, 12 (1947) 407.
15 E. Knobloch, *ibid.*, 25 (1960) 3330.
16 J. Kůta and I. Drabek, *ibid.*, 20 (1955) 902.
17 M. von Stackelberg and H. Fassbender, *Z. Elektrochem.*, 62 (1958) 834.
18 M. von Stackelberg, W. Hans and W. Jensch, *ibid.*, 62 (1958) 839.
19 M. von Stackelberg and H. W. Nürnberg, *Rev. Polarog. (Kyoto)*, 6 (1958) 27.
20 H. W. Nürnberg, *Advances in Polarography*, Pergamon Press, London, 1960, p. 694.
21 W. Lamprecht, S. Gudbjarnason and H. Katzlmeier, *Z. Anal. Chem.*, 181 (1961) 201.
22 M. Březina and V. Gultjaj, *Collection Czech. Chem. Commun.*, 28 (1963) 181.
23 B. Alexandrov, M. Březina and V. Kalous, *ibid.*, 28 (1963) 210.
24 R. Brdička, *Bull. Intern. Acad. Sci. Bohême*, 1 (1936).
25 R. Brdička, *Collection Czech. Chem. Commun.*, 11 (1939) 614.
26 J. Klumpar, *ibid.*, 13 (1948) 11.
27 S. G. Mairanovskii, *Izv. Akad. Nauk SSSR, Otd. Khim. Nauk*, No. 4 (1953) 615.
28 S. G. Mairanovskii, *ibid.*, No. 5 (1953) 805.
29 S. G. Mairanovskii, J. Koutecky and V. Hanuš, *Zh. Fiz. Khim.*, 37 (1963) 18.
30 S. G. Mairanovskii, *Dokl. Akad. Nauk SSSR*, 114 (1957) 1272.
31 A. N. Frumkin and E. P. Andreeva, *ibid.*, 90 (1953) 417.
32 E. Fornasari, G. Giacometti and G. Rigatti, *Advances in Polarography*, Pergamon Press, London, 1960, p. 895.
33 G. Rigatti, *ibid.*, p. 904.
34 S. G. Mairanovskii, *J. Electroanal. Chem.*, 4 (1962) 166.
35 R. Brdička and K. Wiesner, *Collection Czech. Chem. Commun.*, 12 (1947) 138.
36 R. Brdička, *ibid.*, 12 (1947) 212.
37 E. G. Clair and K. Wiesner, *Nature*, 165 (1950) 202.
38 V. Hanuš and R. Brdička, *Khimia*, 1 (1951) 28; *Chem. Listy*, 44 (1950) 291.
39 J. Volke and V. Volková, *Chem. Listy*, 49 (1955) 490.
40 Y. Nagata and I. Tachi, *Bull. Chem. Soc. Japan*, 27 (1954) 290.
41 J. Volke and V. Volková, *Collection Czech. Chem. Commun.*, 22 (1957) 1777.
42 A. Ryvolová and V. Hanuš, *ibid.*, 21 (1956) 853.
43 E. Gergely and T. Iredale, *J. Chem. Soc.*, 1953, 3226.
44 M. Finkelstein, R. C. Petersen and S. D. Ross, *J. Am. Chem. Soc.*, 81 (1959) 2361.
45 S. D. Ross, M. Finkelstein and R. C. Petersen, *ibid.*, 82 (1960) 1582.
46 L. Robert, R. Goldstein and J. Polonovski, *Mikrochim. Acta*, No. 2 (1959) 318.
47 E. L. Colichman, *Anal. Chem.*, 26 (1954) 1204.
48 E. L. Colichman and D. L. Love, *J. Org. Chem.*, 18 (1953) 40.
49 B. Emmert, *Ber.*, 42 (1909) 1507.
50 P. Tompkins (cit. from S. Wawzonek, *Anal. Chem.*, 21 (1949) 64.
51 S. G. Mairanovskii, *Dokl. Akad. Nauk SSSR*, 110 (1956) 593.
52 S. G. Mairanovskii, Trudi 4 Vsesoiuznogo soveshchania po electrokhimii v 1956g., Izd. Akad. Nauk SSSR, 1959, p. 223.
53 S. G. Mairanovskii, N. V. Barashkova and F. D. Alashev, *Zh. Fiz. Khim.*, 35 (1961) 435.
54 J. Koutecky, V. Hanuš and S. G. Mairanovskii, *ibid.*, 34 (1960) 651.
55 R. Brdička and K. Wiesner, *Naturwissenschaften*, 31 (1943) 247.
56 K. Wiesner, *Z. Elektrochem.*, 49 (1943) 164.
57 V. Hanuš, *Chem. Zvesti*, 8 No. 10 (1954) 702.
58 V. Hanuš, S. G. Mairanovskii and J. Koutecky, *Zh. Fiz. Khim.*, 36 (1962) 2010.
59 S. G. Mairanovskii, J. Koutecky and V. Hanuš, *ibid.*, 36, No. 12 (1962) 2621.
60 S. G. Mairanovskii, *ibid.*, 33 (1959) 691.
61 E. Colichman and P. O'Donovan, *J. Am. Chem. Soc.*, 76 (1954) 3588.
62 G. A. Tedoradze and S. G. Mairanovskii, *Izv. Akad. Nauk SSSR, Otd. Khim. Nauk*, No. 3 (1963) 577.
63 B. C. Southworth, R. Osteryoung, K. D. Fleisher and F. C. Nachod, *Anal. Chem.*, No. 2 (1961) 208.
64 D. C. Grahame, *J. Am. Chem. Soc.*, 63 (1941) 1207.
65 S. G. Mairanovskii, *Dokl. Akad. Nauk SSSR*, 132 (1960) 1352.
66 S. G. Mairanovskii, *ibid.*, 142, No. 5 (1962) 1120.
67 S. G. Mairanovskii, *Izv. Akad. Nauk SSSR, Otd. Khim. Nauk*, No. 5 (1962) 784.
68 G. A. Tedoradze, S. G. Mairanovskii and L. D. Kliukina, *ibid.*, No. 7 (1961) 1352.
69 L. D. Kliukina and S. G. Mairanovskii, *ibid.*, No. 7 (1963).
70 S. G. Mairanovskii, *Dokl. Akad. Nauk SSSR*, 142 No. 6 (1962) 1327.

71 S. G. Mairanovskii and L. I. Lishcheta, *Izv. Akad. Nauk SSSR, Otd. Khim. Nauk*, No. 2 (1962) 227.
72 S. G. Mairanovskii, V. M. Belikov, Ts. B. Korchemnaia and S. S. Novikov, *ibid.*, No. 3 (1962) 523.
73 A. N. Frumkin, V. S. Bagotskii, Z. A. Jofa and B. N. Kabanov, *The Kinetics of Electrode Processes (Kinetika electrodnikh protsessov)*, Izd. MGU, Moscow, 1952.
74 A. Frumkin, *Z. Phys. Chem.*, (A), 164, (1933) 121.
75 A. N. Frumkin, *Zh. Fiz. Khim.*, 24 (1950) 244.
76 R. Parsons, *Advances in Electrochemistry and Electrochemical Engineering*, Interscience Publishers, Inc., New York, Vol. 1. 1961.
77 Z. Grabowski and E. Bartel, *Roczniki Chem.*, 34 (1960) 611.
78 H. Matsuda, *J. Phys. Chem.*, 64 (1960) 336.
79 L. Gierst and H. Hurwitz, *Z. Elektrochem.*, 64 (1960) 36.
80 H. Hurwitz, *ibid.*, 65 (1961) 178.
81 S. G. Mairanovskii, L. D. Kliukina, A. N. Frumkin, *Dokl. Akad. Nauk SSSR*, 141 (1960) 147.
82 V. G. Levich, B. I. Haikin and S. G. Mairanovskii, *ibid.*, 145 (1962) 605.
83 A. I. Shatenstein, *Theories of Acids and Bases (Teorii kislot i osnovanii)*, Goskhimizdat, 1949, p. 183.
84 T. A. Kriukova, *Zavodsk. Lab.*, 14 (1948) 511, 639.
85 T. A. Kriukova, *Zh. Fiz. Khim.*, 21 (1947) 365.
86 S. G. Mairanovskii, *ibid.*, 36 (1962) 389.
87 S. G. Mairanovskii, *Dokl. Akad Nauk SSSR*, 133 (1960) 1962.
88 S. G. Mairanovskii and L. I. Lishcheta, *Collection Czech. Chem. Commun.*, 25 (1960) 3025
89 S. G. Mairanovskii, *Dokl. Akad. Nauk SSSR*, 120 (1958) 1294.
90 P. Delahay and C. Fike, *J. Am. Chem. Soc.*, 80 (1958) 2628.
91 P. Delahay and I. Trachtenberg, *ibid.*, 79 (1957) 2355.
92 A. N. Frumkin, *Tr. Khim. Inst. Karpova*, 5 (1926) 3.
93 J. Butler, *Proc. Roy. Soc. (London)*, A. 122 (1929) 399.
94 G. Gouy, *Ann. Chim. Phys.*, (7) 29 (1903) 145.
95 G. Gouy, *ibid.*, (8) 9 (1906) 116, 75.
96 S. G. Mairanovskii and L. I. Lishcheta, *Izv. Akad. Nauk SSSR, Otd. Khim. Nauk*, No. 11 (1962) 1984.
97 V. Vojíř, *Collection Czech. Chem. Commun.*, 18 (1953) 629.
98 V. Vojíř, *ibid.*, 26 (1961) 289.
99 A. Asahi, *Bull. Chem. Soc. Japan*, 34 (1961) 1185.
100 S. G. Mairanovskii and E. F. Mairanovskaia, *Izv. Akad. Nauk SSSR, Otd. Khim. Nauk*, (1961) 922.
101 H. Sunahara, D. N. Ward and A. C. Griffin, *J. Am. Chem. Soc.*, 83 (1960) 6017.
102 M. Shinagawa and H. Nezu, *Bull. Chem. Soc. Japan*, 33 (1960) 272.
103 M. Shinagawa, H. Imai and H. Nezu, *ibid.*, 34 (1961) 445.
104 M. A. Loshkarev, *Dokl. Akad. Nauk SSSR*, 72 (1950) 729.
105 M. K. Polievktov and S. G. Mairanovskii, Tesisi dokladov na 4 soveshchanii po organ. electrokhim, Moscow, 1962.
106 A. N. Frumkin, B. B. Damaskin and N. V. Nikolaeva-Fedorovich, *Dokl. Akad. Nauk SSSR*, 115 (1957) 751.
107 B. B. Damaskin, N. V. Nikolaeva-Fedorovich and A. N. Frumkin, *ibid.*, 121 (1958) 129.
108 S. G. Mairanovskii, M. K. Polievktov, *Izv. Akad. Nauk SSSR, Otd. Khim. Nauk* (in press).
109 A. B. Ershler, G. A. Tedoradze and S. G. Mairanovskii, *Dokl. Akad. Nauk SSSR*, 145 (1962) 1324.
110 G. A. Tedoradze, A. B. Ershler and S. G. Mairanovskii, *Izv. Akad. Nauk SSSR, Otd. Khim. Nauk*, No. 2 (1963) 235.
111 F. Ender, E. Moisar, K. Schäfer and H. J. Teuber, *Z. Elektrochem.*, 63 (1959) 349.
112 S. G. Mairanovskii, *Zh. Fiz. Khim.*, 37 No. 2, (1963) 451.
113 E. Pungor and Gy. Farsang, *Acta Chim. Acad. Sci. Hung.*, 25 (1960) 293.
114 E. Pungor and Gy. Farsang, *Ann. Univ. Sci. Budapest Rolando Eotvos Nominatae, Sect. Chim.*, 2 (1960) 299.
115 E. Pungor and Gy. Farsang, *Acta Chim. Acad. Sci. Hung.*, 27 (1961) 175.
116 E. Pungor and Gy. Farsang, *J. Electroanal. Chem.*, 2 (1961) 291.
117 V. Volková, *Advances in Polarography*, Pergamon Press, London, 1960, p. 840.
118 V. Volková, *Nature*, 185 (1960) 743.
119 N. A. Izmailov and V. D. Bezugly, *Tr. Komis. po Analit. Khim. Akad. Nauk SSSR*, IV, (VII) (1952) 29.
120 E. Coufalik and F. Šantavý, *Collection Czech. Chem. Commun.*, 19 (1954) 457.
121 G. Horn and P. Zuman, *ibid.*, 25 (1960) 3401.
122 H. Wagner and H. Berg, *J. Electroanal. Chem.*, 1 (1959/60) 61.

123 K. Schwabe, Trudi IV Vsesoiuzn. soveshch. el. khim., Izd. Akad Nauk SSSR 1959, p. 170.
124 K. Schwabe, *Z. Phys. Chem.*, 1958, Sonderheft, S. 289.
125 V. Trkal, *Collection Czech. Chem. Commun.*, 21 (1956) 945.
126 H. Sunahara, D. H. Ward and A. C. Griffin, *J. Am. Chem. Soc.*, 82 (1960) 6023.
127 H. Sunahara, *Rev. of Polarog. (Kyoto)*, 9 (1961) 165.
128 H. Sunahara, *ibid.*, 9 (1961) 222.
129 H. Sunahara, *ibid.*, 9 (1961) 233.
130 M. Březina, *Advances in Polarography*, Pergamon Press, London, 1960. p. 833.
131 V. Kalous, *ibid.*, p. 294.
132 M. Shinagawa, H. Nezu, H. Sunahara, F. Nakashima, H. Okashita and T. Yamada, *ibid.*, p. 1142.
133 R. Brdička, *Nature*, 139 (1937) 330, 1020.
134 S. G. Mairanosvkii and M. B. Neiman, *Dokl. Akad. Nauk SSSR*, 87 (1952) 805.
135 M. Březina, *Collection Czech. Chem. Commun.*, 24 (1959) 4031.
136 V. Chmelař, M. Březina and V. Kalous, *ibid.*, 28 (1963) 197.
137 A. Basiński, M. Kuik and J. Ceynova, *Roczniki Chem.*, 36 (1962) 1889.
138 V. Chmelař and J. Nosek, *Collection Czech. Chem. Commun.*, 24 (1959) 3084.
139 J. Řiha, *Electrochim. Acta*, 6 (1962) 75.
140 I. D. Ivanov, *Dokl. Akad. Nauk SSSR*, 138 (1961) 952.
141 M. Ito, *J. Electrochem. Soc. Japan*, 27 (1959) 78.
142 P. Valenta and I. Witwicki, *Collection Czech. Chem. Commun.*, 24 (1959) 4029.
143 W. Hans, W. Henne and E. Meurer, *Z. Elektrochem.*, 58 (1954) 836.
144 K. Marha, *Collection Czech. Chem. Commun.*, 22 (1957) 153.
145 O. Jírovec and K. Wenig (cit. from[10]).
146 G. Gorin, J. E. Spessard, G. A. Wessler, J. P. Oliver, *J. Am. Chem. Soc.*, 81 (1959) 3193.
147 I. D. Ivanov and E. E. Rakhleeva, *Izv. Akad. Nauk SSSR, Otd. Biol. Nauk* (1963) (in print).
148 A. Kočent, *Naturwissenschaften*, 45 (1958) 628.
149 M. Shikata and I. Tachi, *Collection Czech. Chem. Commun.*, 10 (1938) 368.
150 M. Strier and J. Cavagnol, *J. Am. Chem. Soc.*, 80 (1958) 1565.
151 H. C. Brown and R. R. Holmes, *ibid.*, 77 (1955) 1727.
152 H. C. Brown, D. Gintis and L. Domash, *ibid.*, 78 (1956) 5387.
153 V. A. Palm, *Usp. Khim.*, 30 (1961) 1069.
154 P. Zuman, *Collection Czech. Chem. Commun.*, 25 (1960) 3225.
155 P. Zuman and M. Kuik, *Naturwissenschaften* 45 (1958) 541.
156 D. B. Stevančevič, *Bull. Inst. Nucl. Sci. "Boris Kidrich", Belgrado*, 9 No. 167 (1959) 57.
157 V. F. Toropova, G. L. Elizarova, Materiali 2 soveshch. po polarogr. Kazan, 1962, p. 134.
158 V. F. Toropova and G. L. Elizarova, *ibid.*, p. 133.
159 V. F. Toropova and G. L. Velkes, *Zh. Analit. Khim.*, 27 (1962) 282.
160 E. Pungor and E. Rokosinyi-Hollós, *Acta Chim. Acad. Sci. Hung.*, 22 (1960) 69.
161 P. Zuman, *Chem. Listy*, 52 (1958) 1349.
162 N. Ia. Khlopin, *Zh. Org. Khim.*, 18 (1948) 364, 1019.
163 N. Ia. Khlopin, N. A. Rafalovich and G. P. Axenova, *Zh. Analit. Khim*, 3 (1948) 16.
164 N. Ia. Khlopin, N. A. Rafalovich and G. P. Axenova, *Zh. Org. Khim.*, 18 (1948) 1009.
165 As. Trifonov and N. Elenkova, *Izv. Khim. Inst. Bulgar. Akad. Nauk*, 4 (1956) 35.
166 E. Knobloch, *Advances in Polarography*, Pergamon Press, London, 1960, p. 875.
167 A. Ryvolová, *Chem. Listy*, 50 (1956) 1918.
168 S. I. Zhdanov and M. K. Polievktov, *Zh. Org. Khim.*, 31 (1961) 3870.
169 J. Heyrovsky, *Polarographie*, Springer Verlag, Wien, 1941.
170 H. W. Nürnberg, *Advances in Polarography*, Pergamon Press, London, 1960, p. 694.
171 H. W. Nürnberg, G. van Riesenbeck, M. von Stackelberg, *Z. Elektrochem.*, 64 (1960) 130.
172 H. W. Nürnberg, G. van Riesenbeck and M. von Stackelberg, *Collection Czech. Chem., Commun.*, 26 (1961) 126.
173 P. Rüetschi, *Z. physik. Chem.*, 5 (1955) 323.
174 W. Kemula, Z. Grabowski and E. Bartel, *Roczniki Chem.*, 33 (1959) 1125.
175 K. Wiesner, M. Wheatley and J. Los, *J. Am. Chem. Soc.*, 76 (1954) 4858.
176 P. H. Given and P. E. Peover, *Collection Czech. Chem. Commun.*, 25 (1960) 3195.
177 M. Eigen, *Discussions Faraday Soc.*, 17 (1954) 194.
178 A. Frumkin, *Advances in Electrochemistry and Electrochemical Engineering* Vol. 1, Interscience Publishers Inc., New York, 1961, p. 65.

VOLTAGE SWEEP CHRONOAMPEROMETRIC STUDY OF THE BEHAVIOUR OF $[Fe(CN)_6]^{4-}$ AND Fe^{2+} IONS ON THE ANODICALLY PASSIVATED HANGING MERCURY DROP ELECTRODE

WIKTOR KEMULA, ZENON KUBLIK AND JOANNA TARASZEWSKA

Institute of Physical Chemistry, Polish Academy of Sciences, and Department of Inorganic Chemistry, Warsaw University (Poland)

(Received April 23rd, 1963)

A mercury electrode which is polarized anodically is covered with a thin layer of the corresponding mercurous salt and becomes passive[1-4]. The dissolution of mercury is hence limited and only small currents can flow across the phase boundary. The question then arises whether these passive layers formed on the mercury surface can conduct electrical charges and enable various redox reactions in the positive potential range to take place as the oxide layers form on the platinum electrode. Literature on this subject is rather scarce and somewhat contradictory.

KEMULA, GALUS AND KUBLIK[5] were not able to record the oxidation currents of Fe^{2+} and Ce^{3+} ions at the hanging mercury drop electrode covered with a calomel layer, although they observed effects corresponding to the oxidation of metals previously introduced in the bulk of the mercury drop. KUWANA AND ADAMS[6] did not observe under similar conditions the oxidation of Co^{2+}, Fe^{2+} and U^{4+} ions, but they recorded currents corresponding to the oxidation of some organic compounds and $[Fe(CN)_6]^{4-}$ ions, if these compounds were added to the solution after the formation of the passive layer at the electrode surface. No oxidation of the above mentioned ions at the mercury electrode was noted by SCHWABE AND CHAU-DIEU AI[7].

In the present paper reactions occurring at the passive mercury electrode are discussed. As we have previously observed a mercury electrode coated with a layer of mercurous bromide behaves similarly to an electrode covered with calomel. It was impossible to obtain satisfactory results with electrodes covered with other deposits such as Hg_2SO_4, HgO, Hg_2I_2 and HgF, because either the potential range in which the passive layer existed was too narrow, or the currents flowing in the passive state were too large.

EXPERIMENTAL

Current–voltage curves were recorded using a Radiometer PO4 polarograph. The previously described hanging mercury drop electrode with a surface area of 0.018 cm² and a small stationary platinum micro-electrode with a surface area of 0.022 cm² were used. A saturated calomel electrode was applied, as external reference electrode. All solutions were deaerated with hydrogen or with nitrogen when the platinum electrode was used. The area under the recorded curves was measured by a planimeter.

RESULTS

Behaviour of $[Fe(CN)_6]^{4-}$ ions in neutral solutions

The influence of $[Fe(CN)_6]^{4-}$ ions on the course of the anodic passivation of mercury in solutions containing Cl^- ions depends largely upon the concentration ratio of the two ions. The curve obtained in 0.1 *M* KCl solution in the absence of $K_4[Fe(CN)_6]$ is shown in Fig. 1. At first, the dissolution of mercury at a potential +0.1V gives an increase of the anodic current. The current then diminishes rapidly, because anodically produced Hg_2^{2+} ions react with Cl^- ions forming the insoluble calomel layer. The formation of this layer hinders any further dissolution of mercury.

Curve 4 in Fig. 1 was recorded for a solution containing $[Fe(CN)_6]^{4-}$ ions in the absence of Cl^- ions. Comparison of Curves 1 and 4 shows, that at a given concentration ratio of Cl^- and $[Fe(CN)_6]^{4-}$ ions, ferrocyanide ions react with mercury at a more negative potential than chloride ions. Therefore, during the polarization of the mercury electrode from negative towards positive potentials in solutions containing low concentrations of $[Fe(CN)_6]^{4-}$ ions, and Cl^- ions at a concentration 10^{-1} *M*, the mercury ferrocyanide layer was formed preferentially (Curves 2 and 3). This layer is probably not as compact as the calomel layer and therefore further reactions do take place and peaks b and c are recorded. Since we observed that these peaks were higher in the presence of Cl^- ions it is possible that Cl^- ions also take part in the reactions accompanying their formation. The height of the peaks depends on the concentration of ferrocyanide ions in a rather complicated manner. With increase of $K_4[Fe(CN)_6]$ concentration, the height of peaks a and b remains constant and peak c increases.

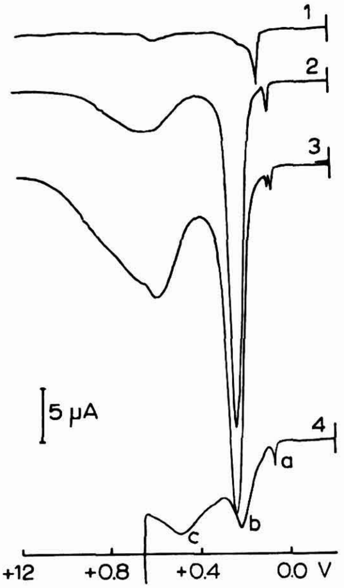

Fig. 1. Current–voltage curves for solutions containing; (1), 0.1 *M* KCl; (2), 0.1 *M* KCl and $2 \cdot 10^{-3}$ *M* $K_4[Fe(CN)_6]$; (3), 0.1 *M* KCl and $8 \cdot 10^{-3}$ *M* $K_4[Fe(CN)_6]$; (4), 0.1 *M* KNO_4 and $8 \cdot 10^{-3}$ *M* $K_4[Fe(CN)_6]$.

In solutions of Cl^- ions more concentrated than 0.5 *M*, or in solutions containing Br^- ions, ferrocyanide does not interfere with the formation of Hg_2Cl_2 or Hg_2Br_2 passive layers. It seems, that under these experimental conditions the reaction between ferrocyanide ions and mercury must be hindered, because at the potential range corresponding to this reaction we are not working with the pure mercury electrode, but with an electrode covered with a deposit of the corresponding mercurous salt.

Curves obtained under such conditions are shown in Fig. 2. The height and shape of the first peak a, corresponding to the formation of Hg_2Br_2 (or Hg_2Cl_2) does not depend now on the presence of $[Fe(CN)_6]^{4-}$ ions in the solution. Two further peaks b and c

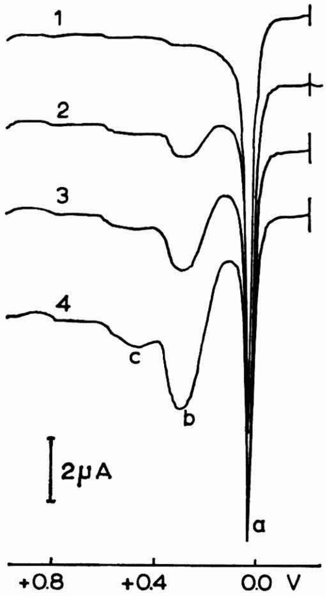

Fig. 2. Current–voltage curves for 0.1 *M* KBr solutions containing the following concentrations of $K_4[Fe(CN)_6]$: (1), 0; (2), $1 \cdot 10^{-3}$ *M*; (3), $2 \cdot 10^{-3}$ *M*; (4), $4 \cdot 10^{-3}$ *M*.

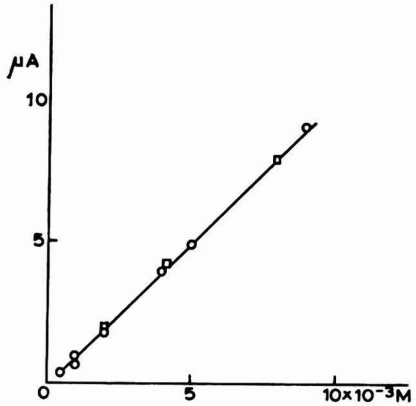

Fig. 3. The dependence of the peak current on the concentration of $[Fe(CN)_6]^{4-}$ ion.

are due to the ferrocyanide. The height of the second peak b is now proportional to the concentration of the ferrocyanide ions in the solution and this dependence is plotted in Fig. 3. No change in height or of potential value at which the second peak b occurred was observed after a change of chloride to bromide ions. Peaks b and c are also obtained when $[Fe(CN)_6]^{4-}$ ions are added to the solution after the formation of the passive layer, but their height depends considerably on the manner of formation of the layer. When $[Fe(CN)_6]^{4-}$ ions are added to the solution just after the polarization of the electrode to +0.18 V (Curve 2, Fig. 4), the recorded curve differs only slightly from the curve obtained with the solution in which $[Fe(CN)_6]^{4-}$ ions were introduced simultaneously with Cl^- or Br^- ions (Curve 3 ,Fig. 4). Peak b is only slightly smaller

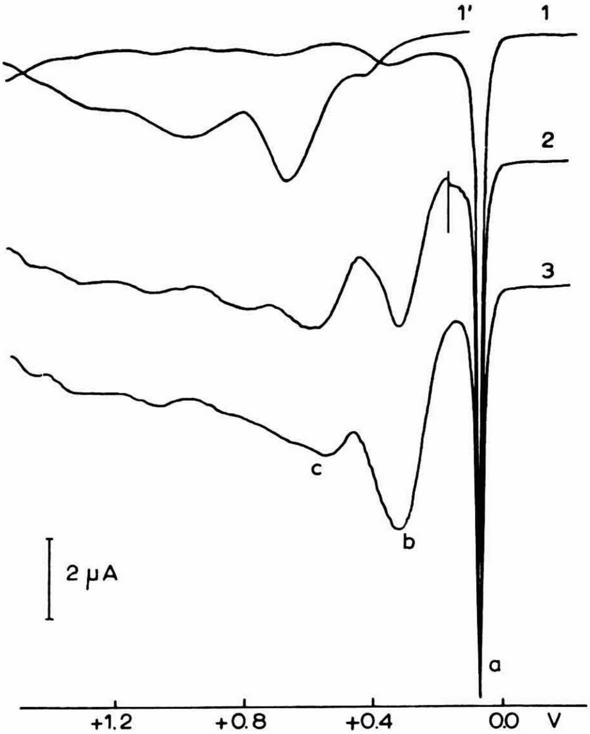

Fig. 4. Current–voltage curves for solutions containing: (Curve 1), 1 *M* KCl; (Curve 1'), 1 *M* KCl to which $5 \cdot 10^{-3}$ *M* $K_4[Fe(CN)]_6$ was added after the electrode was polarized to +1.5 V; (Curve 2), As Curve 1' but polarized to 0.18 V; (Curve 3), $K_4[Fe(CN)]_6$ solution introduced simultaneously with KCl solution.

and peak c is somewhat better defined. If the electrode is polarized for several minutes at a potential equal to +0.18 V, the course of the recorded curve changes only slightly, although it seems that the time of polarization at +0.18 V was sufficient to increase the thickness of the passive layer. On the other hand, if ferrocyanide ions are added to the solution after polarization of the mercury electrode to a more positive potential range (Curve 1', Fig. 4), peak b becomes markedly smaller and peak c greater. Simultaneously the positions of the both peaks are shifted somewhat towards a more positive potential range, probably because of the increase of the ohmic drop.

Species generated at the potential corresponding to peak b are electroactive, because after reversal of the direction of the voltage sweep the corresponding cathodic peak appears (Fig. 5, Curves 1 and 2). Probably only a small part of the anodically produced species is reduced in the cathodic sweep, because this peak is smaller than its anodic analogue. The other part of the produced species is reduced either together with mercurous bromide (or chloride) at the potential value of peak a or diffuses away from the electrode into the bulk of the solution. It follows from the coulometric data given in Table 1 that most of the produced species diffuses away from the electrode, because in the solution that does not contain $[Fe(CN)_6]^{4-}$ ions the total quantity of electricity used for oxidation differs only slightly from that used for reduction. In the presence of ferrocyanide ions the quantity of the electricity used for reduction is much smaller than for oxidation.

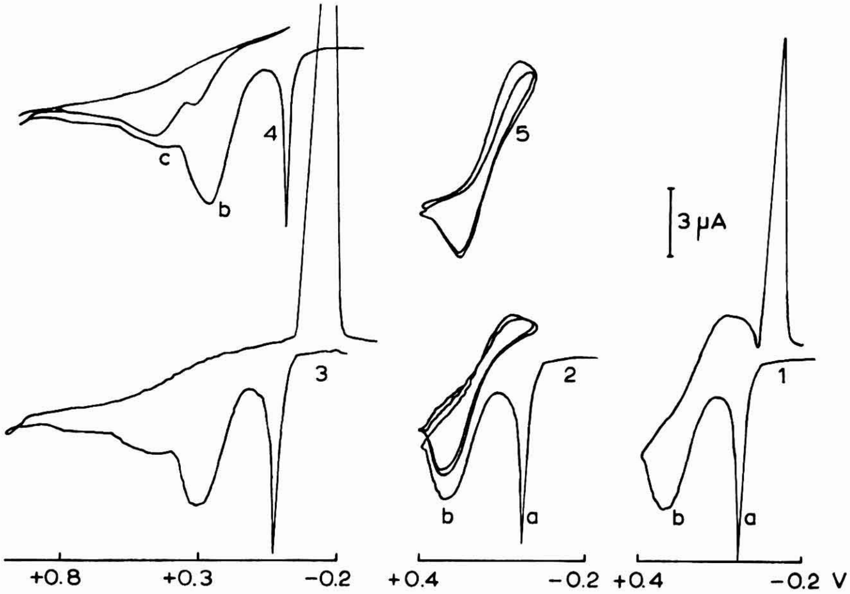

Fig. 5. Cyclic current–voltage curves recorded in various potential ranges for 0.1 *M* KBr solutions containing: (1–4), $5 \cdot 10^{-3}$ *M* $K_4[Fe(CN)_6]$; (5), $5 \cdot 10^{-3}$ *M* $K_3[Fe(CN)_6]$.

TABLE 1

Range of polarization (V)		*1 M KCl*		*1 M KCl + $K_4[Fe(CN)_6]$*	
		oxidation *(μ coulombs)*	*reduction*	*oxidation* *(μ coulombs)*	*reduction*
+0.4	−0.2	36.0	28.8	110.7	74.7
+0.6	−0.2	40.5	36.9	173.7	90.9
+0.7	−0.2	42.3	38.7	216.0	84.0

The height of the cathodic peak b depends to a large extent on the manner of polarization. A multiple cyclic polarization in a potential range which is insufficient to record peak c, changes the shape of the anodic and cathodic peak b only slightly (Curve 2, Fig. 5). On the other hand polarization of the electrode to a much more positive potential range causes considerable changes in the properties of the mercury halide film. After reversal of the course of polarization at +1.0 V (Curve 3, Fig. 5), the cathodic part of peak b practically disappears. Under these circumstances the cathodic peak of the reduction of Hg_2Cl_2 (or Hg_2Br_2) considerably increases, although the quantity of electricity used for the oxidation is markedly greater than for the reduction. The multiple cyclic polarization in the potential range (Fig. 5, Curve 4), exerts a considerable influence also on the anodic peaks. In the second cycle peak b is much smaller and in consequence of this, peak c is markedly better defined. Simultaneously there is a certain displacement of peaks b and c towards a more positive potential range probably caused by the increase of the ohmic resistance of the passive layer. In the next cycles, peak c also decreases. The almost reversible system represented in Curves 1 and 2 (Fig. 5), is due to $[Fe(CN)_6]^{4-}$ ions. A similar system appears in the same potential range, as can be seen in Curve 5 in Fig. 5, if $[Fe(CN)_6]^{3-}$ ions are added to the base solution instead of $[Fe(CN)_6]^{4-}$ ions. Under these circumstances the cathodic part of peak b is higher than the secondary anodic peak and its height increases with increase in concentration of $[Fe(CN)_6]^{3-}$ ions in the solution. This peak does not correspond to the reduction of the deposit of mercury ferricyanide because the reduction curves of deposits have a different appearance.

Considering the presented results it is difficult to give a simple interpretation of the

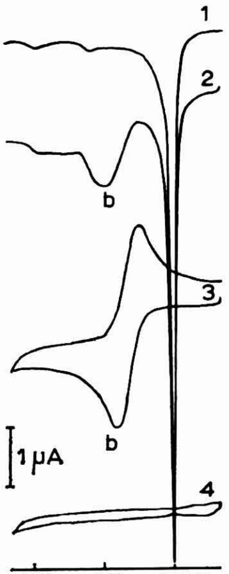

Fig. 6. Current–voltage curves for 0.1 *M* KBr solution containing: (1 and 4) No $K_4Fe(CN)_6$; (2 and 3), $1 \cdot 10^{-3}$ *M* $K_4Fe(CN)_6$. (Curves 1 and 2), hanging mercury electrode; (3 and 4), platinum microelectrode.

processes responsible for the formation of peaks b and c. However, there is evidence to show that peak b can correspond to the oxidation of $[Fe(CN)_6]^{4-}$ ions to $[Fe(CN)_6]^{3-}$ ions.

In order to test this hypothesis the *i–V* curves were also recorded using the microplatinum electrode. Comparison of the curves obtained by means of both kinds of electrodes is represented in Fig. 6. The position of peak b (Curves 2 and 3) obtained with the hanging mercury drop electrode agrees with the oxidation peak of ferrocyanide recorded on the platinum electrode and we can therefore assume that peak b is caused by the oxidation of the ferrocyanide ion at the electrode surface.

Investigations in acidic solutions

In solutions of chloride or bromide ions of moderate acidity and in the presence of $[Fe(CN)_6]^{4-}$ ions the observed effects are very similar to those obtained previously in neutral solutions. Peak b is a little smaller, but peak c is more pronounced. In strongly acidic solutions, however, the phenomena due to the presence of ferrocyanide ions are totally different. The addition of ferrocyanide ions to an hydrochloric acid solution caused the appearance of a small peak at a potential value +0.25 V and of two badly defined current increases at potentials about +0.8 V and +1.1 V (see Curves 2 and 3 in Fig. 7).

The position of any of these peaks does not agree with the position of the oxidation peak for ferrocyanide ion recorded for the same solution using the platinum electrode (Curve 4, Fig. 7). The height of the peak occurring at a potential +0.25 V is poorly reproducible and changes considerably even during the recording of consecutive curves in the same solution. The height of further peaks increases with rise in the concentration of ferrocyanide ions, as shown in Curve 3. Under these conditions both peaks are better developed.

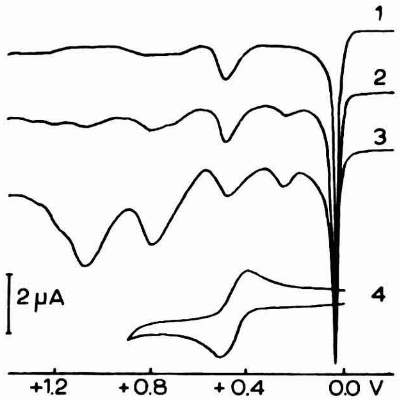

Fig. 7. Current–voltage curves for 1 *M* HCl solutions containing the following concentrations of $K_4[Fe(CN)_6]$: (1), 0; (2 and 4), $1 \cdot 10^{-3}$ *M*; (3), $6 \cdot 10^{-3}$ *M*. (Curves 1, 2, 3), hanging mercury electrode; (4), platinum microelectrode.

The ratio of current heights obtained using platinum and mercury electrodes when the differences in areas of both are taken into account was equal to 5 : 2. The analogous ratio for curves obtained in the neutral solution was about 3:2. We did not obtain any cathodic peaks using the mercury electrode after reversal of course of the polarization, which was similar to the behaviour in neutral solutions.

Behaviour of Fe^{2+} ions

The oxidation of the chloride complexes of Fe^{2+} at a platinum electrode occurs at a potential about 0.2 V more positive than the oxidation potential of $[Fe(CN)_6]^{4-}$ ions.

It was very interesting to determine if the oxidation peaks of $[Fe(CN)_6]^{4-}$ ions at a passive mercury electrode could be obtained in the presence of Fe^{2+} ions.

The presence of Fe^{2+} ions in the concentration range in which $[Fe(CN)_6]^{4-}$ ions yielded the described effects did not cause any changes in *i–V* curves either in acidic or neutral solutions of chloride or bromide ions. The oxidation peaks appeared only at concentrations greater than $1 \cdot 10^{-2}$ *M* and only in strongly acidic solutions containing a large concentration of Cl^- ions.

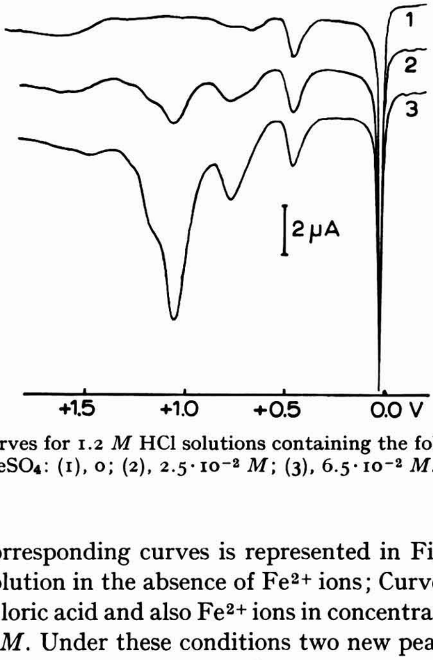

Fig. 8. Current–voltage curves for 1.2 *M* HCl solutions containing the following concentrations of $FeSO_4$: (1), 0; (2), $2.5 \cdot 10^{-2}$ *M*; (3), $6.5 \cdot 10^{-2}$ *M*.

The course of the corresponding curves is represented in Fig. 8. Curve 1 was recorded in 1.2 *M* HCl solution in the absence of Fe^{2+} ions; Curves 2 and 3 in solutions containing the hydrochloric acid and also Fe^{2+} ions in concentrations corresponding to $2.5 \cdot 10^{-2}$ and $6.5 \cdot 10^{-2}$ *M*. Under these conditions two new peaks appear the heights of which grow with increase in the concentration of Fe^{2+} ions. The position of these peaks agrees very well with the position of peaks appearing in the presence of $[Fe(CN)_6]^{4-}$ ions in acidic medium (see Fig. 7). The heights of the peaks in question depend not only on the concentration of Fe^{2+} ions but also on the concentration of hydrochloric acid. A 10-fold increase of the concentration of the acid from 0.12 *M* to 1.2 *M* caused a 2.5-fold increase in the height of these peaks.

The cyclic curves recorded in the same base solution are represented in Fig. 9. In the cathodic sections of Curve 1 and 2 there is a peak corresponding to the reduction of calomel, but no other independent peaks appear whether the course of polarization was reversed after recording of the first or the second peak. Unlike the results obtained for solutions containing ferrocyanide ions under the same conditions, peaks did not appear in the second cycle. The results obtained by measurement of the areas under the recorded curves using the planimeter are represented in Table 2.

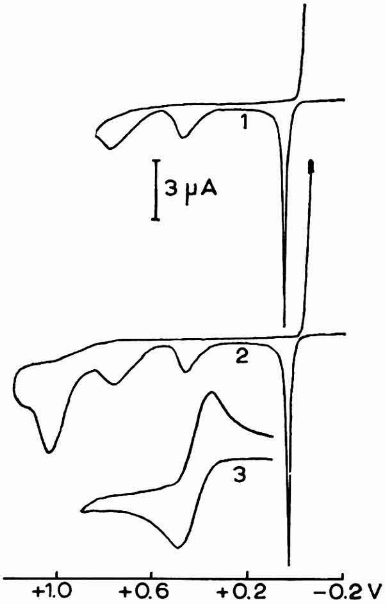

Fig. 9. Cyclic current–voltage curves for solutions containing: (Curves 1 and 2), 1.2 M HCl and $4.5 \cdot 10^{-2}$ M $FeSO_4$; (Curve 3), 1.2 M HCl and $2.5 \cdot 10^{-3}$ M $FeSO_4$. (Curves 1 and 2), hanging mercury electrode; (3), platinum microelectrode.

TABLE 2

Potential range (V)		*1.2 M HCl*		*1.2 M HCl + $4.5 \cdot 10^{-2}$ M Fe^{2}*	
		oxidation	*reduction*	*oxidation*	*reduction*
		(μ coulombs)		*(μ coulombs)*	
+0.85	−0.2	64	60	76	64
+1.2	−0.2	81	69	175	67.0

A considerable increase in electricity consumed for the oxidation of investigated species is followed by an insignificant increase in electricity consumed for reduction. These facts show that species formed at the potential corresponding to the anodic peaks are either electro-inactive or the deposit formed at the more positive potentials has different properties although this could also depend on the time of the electrolysis.

Curve 3 in Fig. 9 was recorded using the platinum electrode at the same recorder sensitivity but with about a 20-fold smaller concentration of Fe^{2+} ions in the solution. A peak corresponding to the oxidation of Fe^{2+} ions at the platinum electrode appears at a potential about 0.28 V less positive than the first peak obtained at the passive mercury electrode. From the comparison of the heights of the recorded curves it follows that the height of the current recorded using the platinum electrode is about 50-fold greater than the height of the peak occurring at the passive mercury electrode at about +0.8 V, and about 20-fold greater than the peak appearing at about +1.1 V.

DISCUSSION

From these results it follows that the passive layer formed during the anodic polarization of the mercury electrode does not always suppress other electrode reactions. Under certain conditions, at the mercury electrode covered with a mercurous bromide or chloride film, in the presence of $[Fe(CN)_6]^{4-}$ or $[Fe(CN)_6]^{3-}$ ions, reactions of their oxidation or reduction can occur and in the i–V curves the corresponding peaks can be recorded. By comparing the position, shape and height of the discussed peaks with the same characteristics of the peaks obtained for the same solution at the platinum electrode, it can be seen that in neutral or slightly acidic solutions the oxidation of ferrocyanide ions or the reduction of ferricyanide ions does occur. This reaction is specific for $[Fe(CN)_6]^{4-}$ and $[Fe(CN)_6]^{3-}$ ions. For Fe^{2+} ions in neutral or slightly acidic medium similar effects could not be observed.

The occurrence of the effects observed for the solution containing $[Fe(CN)_6]^{4-}$ or $[Fe(CN)_6]^{3-}$ ions depends to a large extent on the manner of formation of the passive layer. The corresponding peaks occurred even under conditions of multiple cyclic polarization but only in the case when the electrode was not polarized towards too positive a potential. After polarization of the electrode in a more pronounced positive potential range, the observed peaks disappeared. This difference cannot be attributed to an increase in the thickness of the film formed, during the polarization to a more positive potential, because the mercury halide layer is also increased during a prolonged polarization at a not so very positive potential, for example at +0.18 V, and in spite of this the oxidation of $[Fe(CN)_6]^{4-}$ ions can still be observed (Fig. 4). The properties of the passive layers formed, probably depend considerably on the potential of the deposition.

In the strongly acidic solutions the observed effects are different. After the addition of Fe^{2+} ions to the solution containing 1 M hydrochloric acid, two anodic peaks appear. These peaks are markedly smaller and occur at much more positive potentials than peaks obtained for the same solution at the platinum electrode. Assuming that the first peak occurring at the less positive potential corresponds to the oxidation of Fe^{2+} ions, the existence of a considerable ohmic drop must be supposed. The resistance of layers due to such an ohmic drop should be equal to about 1 $M\Omega$. In an acidic medium effects due to the presence of the ferrocyanide ions are also complicated. The anodic peaks are also markedly smaller and occur at more positive potentials than the corresponding peaks recorded at the platinum electrode, but their positions agree with the position of the peaks obtained in the solutions containing Fe^{2+} ions.

A change in the mechanism of the oxidation of $[Fe(CN)_6]^{4-}$ ion at the mercury electrode covered with mercurous halide film, after the replacement of the neutral solution by an acidic medium, was undoubtedly connected with the decomposition of potassium ferrocyanide.

According to PINTER AND KARAŠ[10], in an acidic medium and in the presence of the small quantities of Hg^{2+} ions, the decomposition of ferrocyanide ions takes place according to the reaction $[Fe(CN)_6]^{4-} \rightleftarrows Fe^{2+} + 6CN^-$. Similarly AŠPERGER AND PAV-

LOVIČ[11] state that Hg^{2+} and Hg_2^{2+} ions, even at a concentration 10^{-7} *M* and in acid solution, catalyse the decomposition of ferrocyanide ions. According to them, however, the complex ion $[Fe(CN)_5H_2O]^{3-}$ and not Fe^{2+} ion, is formed as the first step. In connection with this it is evident why the peaks due to the presence of Fe^{2+} and $[Fe(CN)_6]^4$ ions in the acidic solution occur at the same potential. In both cases the same Fe^{2+} ion not connected with CN^- ions takes part in the electrode process. The fact, that the described effects occur at much lower concentration of $[Fe(CN)_6]^{4-}$ ions than of Fe^{2+} ions, is caused by the probable presence of ferrocyanide in the passive layer. The products generated by the decomposition of ferrocyanide present in the layer can more easily attain the electrode surface than Fe^{2+} ions present in the bulk of solution. The facts given in this paper partially explain difficulties encountered during the investigation of similar problems by other authors. KEMULA, GALUS AND KUBLIK[5] did not obtain oxidation of the Fe^{2+} ions because they worked in insufficiently acid solutions. Similarly SCHWABE AND CHAU DIEU-AI[7] did not observe the oxidation of $[Fe(CN)_6]^{4-}$ ions because in their work the passive layer was probably formed at too positive a potential. Irreproducible results obtained by KUWANA AND ADAMS were due to an insufficient concentration of Cl^- ions in the solution. On the other hand it is not clear why KUWANA AND ADAMS obtained well defined peaks, when the investigated substances were added to the solution only after polarization of the electrode to a positive potential. In the present investigations such a procedure has led to a considerable weakening of the observed effects.

From our investigations it follows that in the neutral solutions peak b is due to the reversible electrode reaction

$$[Fe(CN)_6]^{4-} = [Fe(CN)_6]^{3-} + e^-$$

However, taking into account the complex structure of the passive layer, it is not clear in what manner the mass transfer takes place. It seems that the assumption concerning the electronic conductivity of layers of Hg_2Cl_2 or Hg_2Br_2 is not justified. If the passive layer were the electronic conductor, effects of the oxidation of Fe^{2+} ions should occur also in neutral solution and the height of the peaks due to the oxidation of Fe^{2+} and $[Fe(CN)_6]^{4-}$ ions in acid solution should not differ very much. A significant decrease of anodic current intensity in solutions containing chloride or bromide ions can be explained simply as the result of decrease of the effective surface of the electrode.

According to BOULT AND THIRSK[4], irregularly shaped holes approximately 100 Å in diameter exist in the anodically formed calomel layers. The residual current flowing in the passive state should be therefore proportional to the area occupied by the holes. The diffusion currents calculated on the base of the Frankanthal and Shain equation[12] for Cl^- ions in an 0.1 *M* KCl solution is equal to 303 μA. A comparison of this value with the intensity of current actually flowing enables the effective area occupied by the hypothetic holes to be calculated. This area should be equal to *ca.* $2 \cdot 10^{-5}$ cm². According to this the effect corresponding to the reduction of the $[Fe(CN)_6]^{4-}$ ions at such a small surface should be completely negligible. In reality the recorded currents are only 30% smaller than at the platinum electrode of the same size. Hence we can conclude that the permeability of the film covering the electrode is different for various kinds of ions, *i.e.* the reaction between metallic mercury and Cl^- or $[Fe(CN)_6]^{4-}$ ions, leading to the formation of the corresponding deposited salts, is hindered. The reaction of the anodic oxidation of Fe^{2+} ions is similar. On the other hand the oxidation reaction of $[Fe(CN)_6]^{4-}$ proceeds without any blocking.

Similar effects due to the selective permeability of the passive layers formed by the reduction of CrO_4^{2-} ions on a platinum electrode were observed by KOLTHOFF AND SHAMS EL DIN[12]. The film studied by these authors was found to be practicallyim permeable to aquo–ferric and ferrous iron and cuprous copper species, while the limiting currents of the reduction of Ag^+ and oxidation of Tl^+ were not suppressed.

The problem which is presented here is very complex. Further investigations are necessary and the work is being continued.

SUMMARY

The electrode reactions of $[Fe(CN)_6]^{4-}$, $[Fe(CN)_6]^{3-}$ and Fe^{2+} ions were studied on the mercury electrode passivated by mercurous chloride or bromide, using the voltage sweep chronoamperometric technique. It was found that the layers formed did not hinder, under certain conditions, the oxidation of ferrocyanide and the reduction of ferricyanide ions. The reactions taking place depended on the acidity of the solution and on the potential at which the deposits of the corresponding mercurous salts were formed. Fe^{2+} ions gave similar oxidation curves but only at much higher concentrations and in solutions containing considerable amounts of H^+ and Cl^- ions. The results have been compared with those obtained using the platinum micro-electrode.

REFERENCES

1 R. H. COUSENS, D. J. G. IVES AND R. W. PITTMAN, *J. Chem. Soc.*, (1953) 3988.
2 V. MAJER, *Collection Czech. Chem. Commun.*, 7 (1935) 215.
3 A. M. SHAMS EL DIN, S. E. KHALAFALLA AND Y. A. TANTAWY, *J. Phys. Chem.*, 62 (1958) 1307; 63 (1959) 1224.
4 E. H. BOULT AND H. R. THIRSK, *Trans. Faraday Soc.*, 50 (1954) 404.
5 W. KEMULA, Z. GALUS AND Z. KUBLIK, *Bull. Acad. Polon. Sci. Ser. Chim.*, 6 (1958) 661.
6 T. KUWANA AND R. N. ADAMS, *Anal. Chim. Acta*, 20 (1959) 51, 60.
7 K. SCHWABE AND CHAU-DIEU AI, *Electrochim. Acta*, 7 (1962) 1.
8 W. KEMULA, Z. KUBLIK AND J. TARASZEWSKA, *Bull. Acad. Polon. Sci. Ser. Sci. Chim.*, 8 (1960) 269.
9 W. KEMULA AND Z. KUBLIK, *Anal. Chim. Acta*, 18 (1958) 104; W. KEMULA, Z. KUBLIK AND S. GLODOWSKI, *J. Electroanal. Chem.*, 1 (1959) 91.
10 T. PINTER AND V. KARAŠ, *Croat. Chem. Acta*, 28 (1956) 107.
11 S. ÄSPERGER AND D. PAVLOVIČ, *J. Chem. Soc.*, (1955) 1449.
12 I. M. KOLTHOFF AND A. M. SHAMS EL DIN, *J. Phys. Chem.*, 60 (1956) 1564.

POTENTIOMETRIC ACID–BASE TITRATIONS IN MOLTEN SALTS
THE NEUTRALIZATION OF SODIUM METAVANADATE AND SODIUM METAPHOSPHATE IN CHLORIDE AND NITRATE MELTS

A. M. SHAMS EL DIN, A. A. EL HOSARY AND A. A. A. GERGES

Laboratory of Electrochemistry and Corrosion, National Research Centre, Dokki, Cairo (U.A.R.)

(Received May 4th, 1963)

INTRODUCTION

In continuation of previous work from this Laboratory[1–4], this paper describes the potentiometric titration of sodium metavanadate and sodium metaphosphate in chloride and nitrate melts. No other similar work on metavanadate has yet been published but the neutralization of sodium metaphosphate in a nitrate melt has recently been reported[3]. VAN NORMAN AND OSTERYOUNG[5] determined both metavanadate and metaphosphate in molten LiCl–KCl eutectic at 400°. Their procedure involved the addition of excess solid sodium carbonate to the melt and measurement of the quantity of CO_2 evolved. From the number of moles of carbonate consumed per mole acid, the neutralization of these oxy-anions was formulated as:

$$VO_3^- + CO_3^{2-} = VO_4^{3-} + CO_2 \tag{1}$$

$$PO_3^- + CO_3^{2-} = PO_4^{3-} + CO_2 \tag{2}$$

or, following the acid–base definition of LUX[6],

$$VO_3^- + O^{2-} = VO_4^{3-} \tag{3}$$

$$PO_3^- + O^{2-} = PO_4^{3-} \tag{4}$$

In the present study we have been able to confirm the formulation of VAN NORMAN AND OSTERYOUNG as far as sodium metavanadate in the chloride melt is concerned, this acid neutralizes in a single step according to eqn. (3). In the nitrate melt, however, metavanadate behaves as a strong acid. It attacks the nitrate base electrolyte and is converted to the corresponding pyrovanadate. Further neutralization with Na_2O_2 brings the pyrovanadate to the ortho-salt.

In both nitrate and chloride melts, sodium metaphosphate neutralizes in two successive steps to the pyro and ortho-salts respectively. Pyrophosphate in a chloride melt is, however, a very weak acid and does not show a distinct potential drop at the equivalence point.

EXPERIMENTAL

The general titration set-up has been previously described[1,2]. Pure KNO_3 and LiCl–KCl eutectic (59 : 41 mol/mol, 1 : 1.22 wt./wt.) were used as base electrolytes. The nitrate melt was used at 350° and was dehydrated by bubbling pure dry oxygen through for 1 h[2]. Experiments using the chloride melt were conducted at 450°; drying was effected by bubbling dry HCl gas through the mixture for 3 h followed by dry oxygen for a further hour. The cold masses of both melts were quickly crushed and kept in a desiccator over CaO until required.

An oxygen (Pt) electrode was used as indicator electrode. The reference half-cell was a 99.9+% silver wire dipping in $AgNO_3$–KNO_3 or AgCl–eutectic melts. In earlier experiments a small G4 sintered glass disc separated the reference electrode from the main melt. Later it was discovered that a solid Pyrex tube enveloping the reference electrode possessed sufficient electrical conductance at these high temperatures to permit definite potentials to be measured, provided that a valve voltmeter was used. Comparison of the potentials measured with both electrodes showed that the solid tube gave values 15–20 mV more negative than the one incorporating the sintered glass disc. The difference is apparently the glass junction potential. The experiments described in this paper were conducted with the Pyrex-glass tube type of electrode because of the evident ease of manufacture. In the nitrate melt the reference electrode, when properly manipulated, had a long service life but in the chloride melt, the electrode as well as other glass parts, suffered seriously from what seemed to be an exchange reaction between the melt and the glass. After long periods of use, the glass could be crushed easily between the fingers. New containers and electrodes were, therefore, used when seen to be advisable.

The titration was conducted by adding weighed quantities of Na_2O_2 to 50.00 g of either melt containing known amounts of the acids. The potentials were established rather quickly (5–8 min after each peroxide addition) and were reproducible to ± 25 mV.

Na_2O_2 was used instead of Na_2O because of its less hygroscopic character. The peroxide is assumed to decompose thermally into oxide and oxygen gas. If the peroxide ion can exist as such in the melts under consideration, it would do so only beyond the equivalence point. There is, therefore, little or no possibility of measuring the O^{2-}/O_2^{2-} redox potential so long as there are acids in the melts. The parts of the potentiometric titration curves beyond the equivalence point are not treated theoretically in the present study.

All salts were A.R. grade chemicals. Na_2O_2 was a product of E. Merck (Germany); titration against standard HCl showed it to be 99.34% pure.

RESULTS

Curves 1–3 of Fig. 1(a) are potentiometric titration curves for $NaVO_3$ in the chloride melt, conducted at 450°. At a molar ratio $VO_3^- : O^{2-}$ of 1 : 1, a potential drop of *ca.* 100 mV is recorded. It is to be noted, however, that the potential of the oxygen electrode remains almost independent of the quantity of the peroxide added until near the equivalence point.

Titration curves for different $NaVO_3$ concentrations in the nitrate melt, are shown in Fig. 2. At the inflection points of these curves, which are characterized by a potential drop of *ca.* 250 mV, the molar ratio $VO_3^- : O^{2-}$ is 2 : 1.

In view of the difference in behaviour of the metavanadate in the two media, we felt it would be of value to compare this behaviour with that for the apparently similar acid $NaPO_3$ under the same conditions.

In the chloride medium, one step is registered, Fig. 3, at a mole ratio, acid : oxide approaching 2 : 1. On the other hand, the titration of $NaPO_3$ in the nitrate melt at

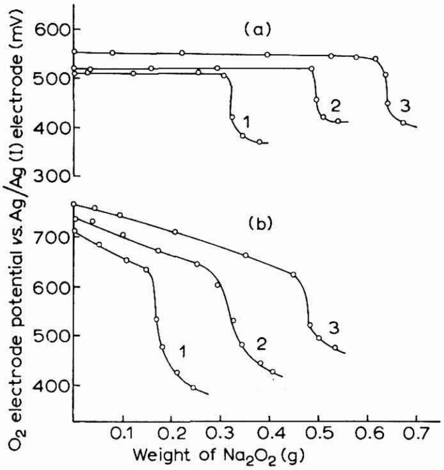

Fig. 1(a). Potentiometric titration of $NaVO_3$ with Na_2O_2 in chloride melt at 450°. (1), 0.500 g; (2), 0.750 g; (3), 1.000 g $NaVO_3$/50.00 g melt. (b). Potentiometric titration of $NaVO_3$ with Na_2O_2 in mixed chloride–nitrate melt at 450°. (1), 0.500 g; (2), 1.000 g; (3), 1.500 g $NaVO_3$/50.00 g melt.

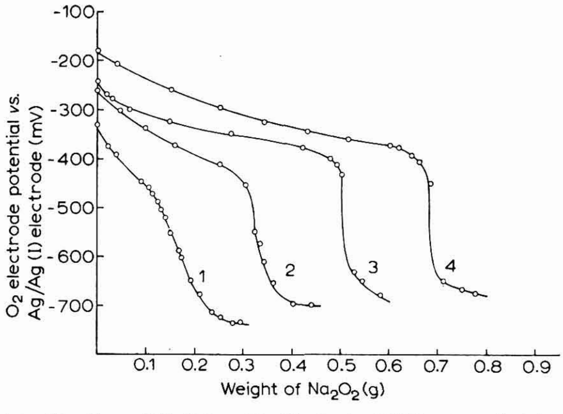

Fig. 2. Potentiometric titration of $NaVO_3$ with Na_2O_2 in KNO_3 at 350°. (1), 0.500 g; (2), 1.00 g; (3), 1.500 g; (4), 2.000 g $NaVO_3$/50.00 g melt.

350° gives rise to curves similar to those in Fig. 4. The neutralization takes place in two equal steps. At the inflection point of the second step the ratio PO_3^- : O^{2-} is 1 : 1.

The curves of Fig. 5 represent the relation between the weights of the acids in the chloride and nitrate melts and the corresponding weights of Na_2O_2 consumed up to the inflection points of the titration curves. The points on Fig. 5 are experimental values while the solid lines are calculated theoretically. As can be seen from the curves, there is a satisfactory agreement between the two sets of figures.

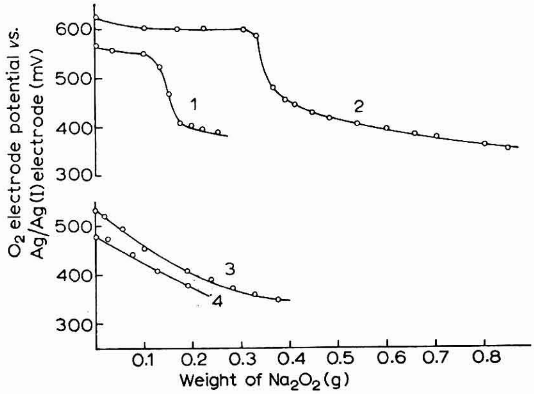

Fig. 3. Potentiometric titration of $NaPO_3$ with Na_2O_2 in chloride melt at 450°. (1) 0.500 g; (2) 1.000 g $NaPO_3$/50.000 melt. (3), 1.000 g $Na_4P_2O_7$; (4) Na_2O_2/50.000 g melt.

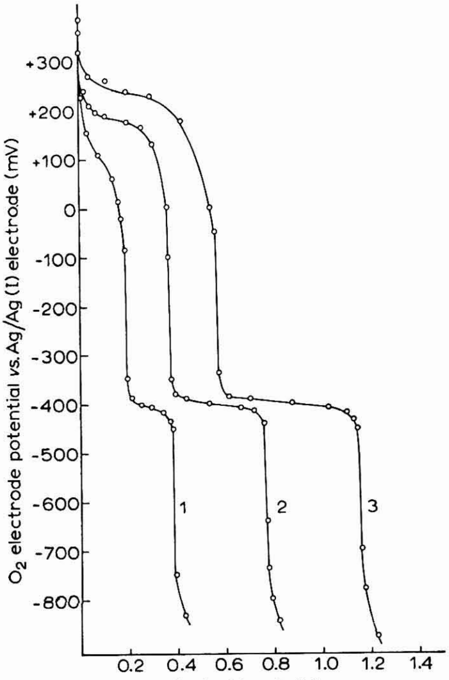

Fig. 4. Potentiometric titration of $NaPO_3$ with Na_2O_2 in KNO_3 at 350°. (1), 0.500 g; (2), 1.000 g; (3), 1.500 g $NaPO_3$/50.000 g melt.

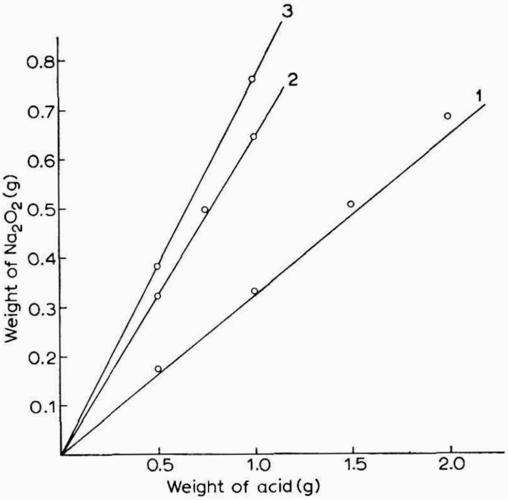

Fig. 5. Relationship between concentration of the acids and quantities of Na_2O_2. (1), $NaVO_3$ in KNO_3; (2), $NaVO_3$ in chloride melt; (3), $NaPO_3$ in KNO_3. Points show experimental values and lines are calculated theoretically.

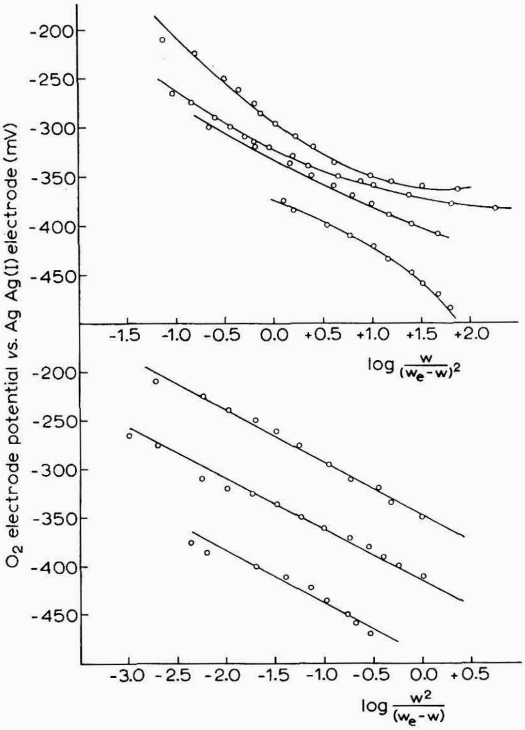

Fig. 6. Theoretical analysis of the titration curves of $NaVO_3$ in KNO_3.

DISCUSSION

The titration curves of sodium metavanadate in the chloride melt are characterized by a distinct potential drop of *ca.* 100 mV at a molar ratio $VO_3^- : O^{2-}$ of 1 : 1. This reveals that the neutralization of the acid in this melt is as follows:

$$VO_3^- + O^{2-} = VO_4^{3-} \tag{3}$$

In this respect our results confirm those of VAN NORMAN AND OSTERYOUNG[5]. The variation of the potential of the oxygen electrode before the equivalence point does not, however, follow the theoretical relation:

$$E = E^\circ + \frac{RT}{2F} \ln K - \frac{RT}{2F} \ln \frac{[VO_4^{3-}]}{[VO_3^-]} \tag{5}$$

where E° refers to the standard O_2/O^{2-} potential relative to our reference electrode and K is the equilibrium constant of reaction (3). This behaviour is not, however, surprising in view of the known fact that the oxygen electrode does not behave reversibly in the chloride melt under consideration[7]. Also, the comparatively small drop in potential at the equivalence point shows that metavanadate in a total chloride melt (see later) is behaving as a weak acid.

The neutralization of $NaVO_3$ in the nitrate melt shows similarly one single step. Here, however, the molar ratio $VO_3^- : O^{2-}$ at the equivalence point is 2 : 1. It was thought at first that this corresponded to the reaction:

$$2\ VO_3^- + O^{2-} = V_2O_7^{4-} \tag{6}$$

However, this view was discarded in view of the following facts:

(i) no second step corresponding to the transformation to orthovanadate, VO_4^{3-}, in comparison with the metaphosphate (see later), was observed;

(ii) the potentials at which neutralization takes place are rather low for a comparatively strong acid like $NaVO_3$.

Two other arguments against reaction (6) will be given later.

The results can be better explained if one assumes that $NaVO_3$, being a strong acid, will attack the nitrate base electrolyte, during the melting period, and become converted to the corresponding pyrovanadate:

$$2\ VO_3^- + 2\ NO_3^- = V_2O_7^{4-} + N_2O_5 \tag{7}$$

Further neutralization using Na_2O_2 as titrant yields the orthovanadate:

$$V_2O_7^{4-} + O^{2-} = 2\ VO_4^{3-} \tag{8}$$

Reaction (8) explains the experimentally determined ratio of 2 : 1 for $VO_3^- : O^{2-}$.

The following experiment was conducted as direct proof for the assumption that nitrate ion acts as a primary oxide donor for metavanadate, during the fusion period:

A weighed quantity of metavanadate (5 g) was fused with 95 g KNO_3 for a period of 3 h, cooled and crushed. Portions of the solid containing known amounts of metavanadate were added to the chloride base electrolyte and titrated potentiometrically with Na_2O_2 (Fig. 1(b)). The curves obtained under these experimental conditions showed that only half the quantity of the peroxide necessary to transfer $NaVO_3$ (if present) to the orthovanadate was consumed. This result cannot be explained except on the assumption that nitrate contributed the other part. It is of interest to note that in the mixed chloride–nitrate melts the oxygen electrode approached reversibility in its behaviour, as indicated by its response to variations in the ratio, acid : salt. Also, judging by the larger potential drop observed at the inflection points, one is bound to conclude that the acid character increases when the melt contains an excess of oxy-anions other than the acid.

Theoretical analysis of the titration curves of $NaVO_3$ in the nitrate melt further supports the assumption that the acid reacts with nitrate ion. For reactions (6) and (8) the variation — during the course of neutralization — of the oxygen electrode potential operated at atmospheric pressure, could be expressed as:

$$E = E^\circ + \frac{RT}{2F} \ln K_{(6)} - \frac{RT}{2F} \ln \frac{[V_2O_7{}^{4-}]}{[VO_3{}^{-}]^2} \qquad (9)$$

and

$$E = E^\circ + \frac{RT}{2F} \ln K_{(8)} - \frac{RT}{2F} \ln \frac{[VO_4{}^{3-}]^2}{[V_2O_7{}^{4-}]} \qquad (10)$$

where $K_{(6)}$ and $K_{(8)}$ are the equilibrium constants for the respective reactions. Equations (9) and (10) could be written in the form:

$$E = \acute{E}^\circ{}_{(6)} - \frac{RT}{2F} \ln \frac{w}{(w_e - w)^2} \qquad (11)$$

and

$$E = \acute{E}^\circ{}_{(8)} - \frac{RT}{2F} \ln \frac{w^2}{(w_e - w)} \qquad (12)$$

where w is the weight of Na_2O_2 added to establish a definite potential, w_e is the total weight of the peroxide required to neutralize completely either acid. The $\acute{E}^\circ$ values incorporate a proportionality constant converting weights to corresponding moles. The plot of the oxygen electrode potential against the logarithmic function should produce straight lines of slopes equal to $2.303\ RT/2F$ if the corresponding reaction is the one actually taking place.

In Fig. 6 the potential, E, of the oxygen electrode is plotted as a function of the logarithmic quantities; the points are taken by interpolation of the corresponding curves of Fig. 2. As is seen from Fig. 6, the $E - \log w/(w_e - w)^2$ curves deviate considerably from straight lines. The $E - \log w^2/(w_e - w)$ plots, on the other hand, fulfil the requirements of eqn. (12) and support the conclusion that we are neutralizing pyrovanadate rather than the meta-salt.

The titration with Na_2O_2 of sodium metaphosphate in the nitrate melt, Fig. 4, has been described recently[3]. The curves show two distinct steps, each corresponding to half the quantity of the peroxide necessary to bring the metaphosphate to the ortho-salt. The stepwise neutralization of $NaPO_3$ in this melt was formulated as[3]:

$$2\ PO_3{}^{-} + O^{2-} = P_2O_7{}^{4-} \qquad (13)$$

$$P_2O_7{}^{4-} + O^{2-} = 2\ PO_4{}^{3-} \qquad (14)$$

The fact that the second step was identical with that for sodium pyrophosphate under the same experimental conditions, supported this conclusion.

One can safely conclude that in the nitrate melt both metavanadate and metaphosphate neutralize in principle in a like manner. The pyro-salts are first formed and upon further neutralization transformation to the ortho-compounds takes place. However, as is clearly demonstrated by the results of the present study, sodium metavanadate is the stronger of the two meta-acids since it siezes its primary oxide ion from the nitrate base electrolyte. The question of the relative strengths of the meta- and pyro-salts will be discussed in a more quantitative manner at the end of this paper.

The titration of $NaPO_3$ in the chloride melt, Fig. 3, gave rise to a single neutralization step but difficulty was experienced, however, in reproducing the titration results. The average error in the determination of known quantities of metaphosphate was in some experiments as high as -20%. This was due — at least in part — to the presence of traces of moisture in the melt. The bubbling of dry HCl gas through the melt directly before the experiment lowered the error but did not eliminate it completely. In no case, however, was the molar ratio $PO_3^- : O^{2-}$ recorded higher than 2 : 1. It is, therefore, safe to conclude that the neutralization step corresponds to the reaction of metaphosphate with oxide ion, in the ratio given above. Because the chloride melt contains no oxide donor ion to react with the metaphosphate, one is bound to ascribe this step to the reaction:

$$2\,PO_3^- + O^{2-} = P_2O_7^{4-} \tag{15}$$

The equilibrium constant of the subsequent reaction, *viz.*,

$$P_2O_7^{4-} + O^{2-} = 2\,PO_4^{3-} \tag{16}$$

in the chloride melt is assumed to be so small that its neutralization is not complete until the final branch of the neutralization curve merges into the Na_2O_2 curve without giving an inflection. As proof for this assumption, we tried to titrate $Na_4P_2O_7$ with Na_2O_2 in a chloride melt. The curve thus obtained (Curve 3, Fig. 3), did not reveal any measurable inflection at the theoretically calculated end-point. The curve was almost identical with that for Na_2O_2 in a pure chloride melt (Curve 4, Fig. 3).

We have recently found that the oxygen electrode in fused KNO_3 assumed definite potentials when the melt was made 10^{-2} *M* with respect to a number of oxy-anions[4]. The potentials depended only upon the type of the oxy-anion and, provided that thermal equilibrium was attained, these potentials were highly reproducible. This enabled us to establish an acidity–basicity scale for oxy-anions in molten KNO_3 at 350°. The establishment of this scale was based upon the idea that with anions giving rise to more positive potentials than that measured in pure KNO_3 there was a decrease in the oxygen ion activity and they were, therefore, acid with respect to the nitrate. On the other hand, oxy-anions which gave more negative potentials than that measured in pure KNO_3 signified an increase in the O^{2-} concentration and were considered basic relative to the nitrate. Assuming a reversible behaviour for the oxygen electrode in these melts (which is true for at least those oxy-anions whose ionization constant is small[8]), the measured potentials were drawn on a straight line. The value of the slope of this line was $2.303\ RT/2F$ at 350°. On this acidity–basicity line we assigned to the nitrate melt an arbitrary value of zero. Oxy-anions whose instability constants were larger than that for pure KNO_3 lay to the right-hand side of the zero and were given a positive sign (bases); anions acid to KNO_3 were on the left-hand side of zero and were assigned a negative sign. Every $2.303\ RT/2F$ V was denoted on the abscissa coordinate as a unit of acidity or basicity. Using this simple arrangement one can directly determine the relative strength of a certain oxy-anion with respect to the nitrate base electrolyte. Thus, for example, an anion of number + 3 is basic relative to pure KNO_3 as indicated by the positive sign, and its 10^{-2} *M* solution in the nitrate melt furnishes 10^3 times as much O^{2-} as that present in pure KNO_3. On this basis we have found that 10^{-2} *M* solutions of Na_2O_2, $Na_4P_2O_7$, $Na_4V_2O_7$ and $NaPO_3$ have the following acidity (basicity) numbers in KNO_3 at 350°:

Substance	*O_2 electrode potential (mV)*	*Acidity (basicity) number*
Na_2O_2	−700	+(4.65)
KNO_3	−420	0.00
$Na_4P_2O_7$	−370	− 0.85
$Na_4V_2O_7$	−260	− 2.63
$NaPO_3$	+265	−11.20
$NaVO_3$		−11.50

For reasons related to the irreversible behaviour of the oxygen electrode in nitrate melts made basic with Na_2O_2, and fully discussed elsewhere[4], the basicity value cited above for 10^{-2} *M* Na_2O_2 is only an approximation. The other three values for pyrophosphate, pyrovanadate and metavanadate are highly reproducible and could be taken as measures for their instability constants.

It can be computed quite simply that a 10^{-2} *M* $Na_4P_2O_7$ melt furnishes 61 times the oxide ion of an equimolar melt of $Na_4V_2O_7$; hence, the pyrophosphate ion is weaker as an acid. If it is assumed that the equilibria for both anions, *viz.*,

$$P_2O_7^{4-} \rightleftharpoons 2\ PO_3^- + O^{2-} \tag{17}$$

$$V_2O_7^{4-} \rightleftharpoons 2\ VO_3^- + O^{2-} \tag{18}$$

lie mainly to the left-hand side, the instability constant of reaction (17) is found to be *ca.* $2.3 \cdot 10^5$ greater than that for reaction (18).

$NaPO_3$ has an acidity number of −11.20, and is thus the strongest acid which could be measured in KNO_3 melts without the latter being attacked. An acidity number could not be determined for metavanadate ion because of its reaction with the nitrate base electrolyte but it is apparently lower than −11.50. Metavanadate is thus a stronger acid than metaphosphate. This is true, at least, in nitrate melts.

SUMMARY AND CONCLUSION

The two acids $NaVO_3$ and $NaPO_3$ were titrated potentiometrically in molten LiCl–KCl eutectic (450°) and in KNO_3 (350°). In the chloride melt $NaVO_3$ neutralizes according to:

$$VO_3^- + O^{2-} = VO_4^{3-}$$

while $NaPO_3$ reacts as:

$$2\ PO_3^{-} + O^{2-} = P_2O_7^{4-}$$

and

$$P_2O_7^{4-} + O^{2-} = 2\ PO_4^{3-}$$

$Na_4P_2O_7$ in the chloride melt is a very weak acid which does not show an inflection at the equivalence point.

In the nitrate melt at 350° both $NaVO_3$ and $NaPO_3$ change to the pyro- and then to the ortho-salts. $NaVO_3$ is the stronger of the two acids; it takes its primary oxide ion from the nitrate base electrolyte and changes to pyrovanadate.

The positions of metaphosphate, pyrovanadate and pyrophosphate on the newly developed acidity–basicity scale in molten KNO_3 have been established. $Na_4V_2O_7$ is stronger than $Na_4P_2O_7$. Relative instability constants for these two anions have been calculated.

REFERENCES

1 A. M. Shams el Din, *Electrochim. Acta*, 7 (1962) 285.
2 A. M. Shams el Din and A. A. A. Gerges, *J. Electroanal. Chem.*, 4 (1962) 309.
3 A. M. Shams el Din and A. A. A. Gerges, *Electrochim. Acta*, in press.
4 A. M. Shams el Din and A. A. A. Gerges, *Paper presented before The First Australian Conference on Electrochemistry, Sydney and Hobart, February, 1963.*
5 J. D. Van Norman and R. A. Osteryoung, *Anal. Chem.*, 32 (1960) 398.
6 H. Lux, *Z. Elektrochem.*, 45 (1939) 303.
7 H. A. Laitinen and B. B. Bhatia, *J. Electrochem. Soc.*, 107 (1960) 705.
8 A. M. Shams el Din and A. A. A. Gerges, unpublished results.

PREFERRED ORIENTATIONS IN NICKEL ELECTRO-DEPOSITS

I. THE MECHANISM OF DEVELOPMENT OF TEXTURES IN NICKEL ELECTRO-DEPOSITS

A. K. N. REDDY

The Electrochemistry Laboratory, University of Pennsylvania, Philadelphia 4 (Pa., U.S.A.)

(Received May 24th, 1963)

I. INTRODUCTION

Electron diffraction studies[1] have clearly demonstrated that there are several stages in the growth of an electro-deposit, each stage being characterized by a definite type of crystal orientation. In the *initial* or *epitaxial stage* of growth, the size, shape and orientation of the deposit-crystals are influenced by the substrate. This substrate-influence on the crystal orientation diminishes during the *transition stage* and is finally eclipsed in the *last stage* of growth which involves the development of a *preferred orientation** of the deposit-crystals**.

In these textured deposits, the orientations of the crystal grains are such that a particular crystal direction (the *preferred orientation axis* or *texture axis*) stands normal to the substrate, and, therefore, parallel to the direction of current flow and to the thickness direction of the deposit. All other atoms rows in the deposit-crystals are randomly oriented; in other words, there is rotational symmetry about the texture axis. It is only in an ideal case, however, that the atom row corresponding to the texture axis stands exactly normal to the cathode surface in *all* the crystallites. In practice, there is a spread about the mean, and only *a degree* of preferred orientation. The texture axis has therefore a *play* about the normal.

Since there is an absence of substrate influence on the orientation observed during the final stage of growth, it is natural that textures are developed irrespective of whether single-crystal, random-polycrystalline or fibre-textured substrates are used[2]. However, the *specific* preferred orientation (*i.e.*, the particular texture axis) that is observed depends on the conditions of electro-deposition. Factors such as temperature, current density, bath composition, pH, etc., are the relevant aspects of the conditions of electro-deposition.

At one stage, attempts were made to correlate these textures with industrially-important characteristics of electro-deposits, especially brightness[3,4], but little success*** seems to have attended these efforts[5,6,7]. Despite this, a study of the origin and

---

* Other terms are also in vogue. Many authors describe preferred orientations as *textures* or *fibre-textures*. FINCH, WILMAN and co-workers have used the term *one-degree orientation*.

** The thickness at which preferred orientation develops depends on several factors, such as bath composition, current density, etc.

*** Recently[8], however, there has been a renewal of interest in the question of whether there is a relationship between preferred orientation and brightness.

development of textures appears to be of great value, because such an investigation cannot but throw light on many fundamental aspects of the growth of electro-deposits.

Bozorth in 1925[9], arguing by analogy with textures developed during cold-working, suggested that preferred orientation results from the compressive stresses generated in growing electro-deposits. Wyllie extended these views and taking into account internal-slip mechanisms, he explained the orientation developed by chromium electro-deposits[10].

In order, however, to establish the validity of internal-slip mechanisms, it is necessary to make quantitative comparisons between the stresses actually developed in electro-deposits and those that occur during cold-working. Further, an approach wherein the orientations are treated as resulting from growth processes appears, on general grounds, to be more plausible.

An important suggestion[11,12,13] was advanced by Wilman in 1955. He based his views on the well-established evidence[1] that electro-deposits develop growth textures only after passing through a random orientation stage in which the crystallites are randomly disposed with respect to each other and with respect to the substrate. Wilman also took into account the experimental fact that the growth of an electro-deposit is associated with the development of facets and plane crystal faces. He suggested therefore that the conditions of electro-deposition favor the preferential growth of those crystals which have two or more main growth-faces simultaneously perpendicular (or nearly perpendicular) to the substrate. The atom row at the common intersection of these faces then becomes the orientation axis.

Gorbunova *et al.* have also independently considered the origin of textures in electrodeposits[14]. Although there is some similarity in the views of Gorbunova and those of Wilman, there is one essential difference. Wilman's view required the development of faces, and the simultaneous orienting of these faces normal (or nearly normal) to the substrate. Gorbunova[14], on the other hand, states that "the deposit surface should not be formed by grain faces."

Sato has recently carried out an elegant study* of the crystal growth of electro-deposited zinc[15]. His work consists of an electron-diffraction study of the preferred orientations of zinc deposits and a presentation of strikingly beautiful electron micrographs of their topography. The micrographs reveal flat, well-developed, plate-like crystals. Sato has interpreted the orientations "from the standpoint of development of crystallographic planes under various degrees of influence of hydrogen and/or organic colloids." Sato made use of observations by Straumanis[16] on the faces developed by zinc vapor deposits in hydrogen atmospheres, and also the idea that a reversal of the growth velocities can result from the adsorption of hydrogen and/or organic colloids. Despite this significant advance in understanding, Sato's discussion of his results leaves unconsidered some essential aspects of the problem. For instance, although Sato has named the agency through which a reversal of growth velocity occurs, the relationship between the deposition conditions and the influence of adsorbed hydrogen has not been established. Further, the question of the inclination which

---

* The author became aware of Sato's work after a preliminary draft of this paper was written. There is one important point which is common to his approach and this. This concerns the attempt to correlate the development of a particular texture with the preferential formation of facets of a particular type.

his plate-like crystals assume relative to the substrate requires deeper examination.

It is seen therefore that there is little detailed work on the *mechanism* of texture development, and hardly any at all on the *causal connection* between the deposition conditions and the specific orientations developed under these conditions.

WILMAN's approach, which appears to be the most fruitful, raises two important questions:

(1) how do the deposition conditions determine the particular type of facets preferentially formed?

(2) what determines the inclination which the preferentially developed facets assume relative to the substrate?

These questions, concerning the process of preferential facet formation and the process of alignment of these facets, have been considered here in detail by taking advantage of previous work on hydrogen overpotential and metallic overpotential, on the adsorption of hydrogen on nickel single-crystal faces, and on crystal growth. It has thereby become possible to propose a theory for the *mechanism* of development of preferred orientation, with special reference to nickel electro-deposits, and to achieve some *correlation* between the textures and the deposition conditions.

2. WHY ARE FACETS FORMED?

A crystal with well-defined faces can be considered to be the product of its growth history. All crystal faces do not advance forward (or grow) at the same rate. The rate of growth of facets determines the probability of their survival. Fast-growing faces grow out of existence, and slow-growing faces survive[17]. This can be proved by simple geometric arguments. In the case of electro-deposits, the surviving faces will be those which have the greatest metallic overpotential and which therefore grow most slowly. Hence, even if growth commences on a sphere, plane crystal faces are soon formed due to differences in growth velocities.

3. WHICH PARTICULAR TYPE OF FACETS ARE FORMED?

(a) *"Free growth"*

Let us first consider the *free growth* of nickel electro-deposits. We define *free growth* in the following way: the deposition is considered to occur on a substrate-surface *free of adsorbed hydrogen atoms*; further, the adsorption of surface-active substances is also explicitly excluded.

The Bravais *law* of crystal growth is adopted as the starting point. This law can be stated thus: the velocity of growth of different crystal faces depends on the atomic population density (*reticular density*) of the faces; the greater the number of atoms per unit area of the face, the lower the rate of growth in a direction normal to the face.

It is now accepted that the Bravais *law* needs to be qualified. The reticular density is not the sole factor determining the growth velocity of a face. Other factors such as rate of deposition, conditions of mass transport and adsorption of impurities must be taken into account. We shall, however, restrict our discussions to current densities (10–50 mA/cm^2) which are low in comparison with the limiting current densities for the concentrated solutions used in nickel electro-deposition. Hence, crystal growth is not likely to be diffusion-controlled. Further, the disturbance of the relative growth velocities due to interference from adsorbed hydrogen is a factor the consequences of which it is our specific intention to follow up in the coming sections. Hence, the use of the Bravais *law* for *free growth* appears to be justified.

Consider the important low-index planes. The velocity (v_{hkl}) of *free growth* of a crystal face {hkl} *decreases* as the population density P_{hkl} increases. Nickel being a face-centered cubic metal, $P_{211} < P_{110} < P_{100} < P_{111}$, and therefore $v_{211} > v_{110} > v_{100} > v_{111}$. But the differences in the velocities of growth are manifestations of differences in the partial current densities on different faces. So, $i_{211} > i_{110} > i_{100} > i_{111}$. We can state the same result in terms of metallic overpotentials*. Designating the *free growth* metallic overpotential for the face {hkl} by the symbol $_{\mathrm{FG}}\eta_{\mathrm{hkl}}$, we have $_{\mathrm{FG}}\eta_{111} > {}_{\mathrm{FG}}\eta_{100} > {}_{\mathrm{FG}}\eta_{110} > {}_{\mathrm{FG}}\eta_{211}$.

Hence, under *free growth* conditions, nickel electro-deposits should tend to preferentially develop {111} octahedral facets.

(*b*) *Adsorbed hydrogen atoms — the cause of "disturbed growth"*

Free growth, however, does not normally obtain in the case of nickel electro-deposits. Hydrogen evolution takes place along with nickel deposition. The formation of adsorbed hydrogen atoms is an essential intermediate step in the evolution of hydrogen gas.

How does the presence of adsorbed atomic hydrogen affect the electro-crystallization of nickel?

It is well-known that the *inert* metals (iron, cobalt, nickel) which require high metallic overpotentials for deposition from simple baths, also have high surface concentrations of adsorbed hydrogen. It has been suggested many times that hydrogen can influence the deposition process. Hence, a correlation between the high metallic overpotential of the *inert* metals and the hydrogen adsorbed on their surfaces, is strongly indicated (see the monograph of ANTROPOV[18]).

It can be assumed, therefore, that adsorbed hydrogen atoms interfere with metal deposition and that the considerable surface concentration of atomic hydrogen is a contributory factor to the high metallic overpotential of the *inert* metals.

The *modus operandi* can be visualized in terms of the work of BOCKRIS[19,20] and GERISCHER[21]. These authors have shown** that the reaction involving the transfer of the metal ion across the double-layer results in the formation of an adsorbed ion (adion) which undergoes surface diffusion before lattice-incorporation at the crystal-building site. The broadcast adsorbed hydrogen atoms must surely impede the surface diffusion process*** which is the rate-determining step at low current densities. At high current densities, the transfer reaction becomes rate-determining. Even in this case, adsorbed hydrogen would increase the energy barrier because the transfer reaction would probably have to take place on to hydrogen which would at least partially screen the electron *cloud* in the nickel.

Hence, whether surface-diffusion or ion transfer is rate-determining, the free energy of activation for nickel deposition on a cathode partially covered with hydrogen atoms, would be greater than the free energy of activation for the deposition process on an adsorbate-free nickel surface. In other words, adsorbed atomic hydrogen increases

---

* The overpotentials are considered to be purely due to activation polarization. Thus, limitations on the deposition reaction due to supply of ions are deemed to be non-existent.

** The deposition of mercury, silver and copper have been studied.

*** A similar suggestion has been made by CONWAY AND BOCKRIS[22].

the metallic overpotential above the *free growth* value (${}_{FG}\eta$). We may term *this* increase as the *hydrogen-contribution to the metallic overpotential* and represent it by ${}_{HC}\eta$.

The total metallic overpotential η_{hkl} for deposition on the face {hkl} can therefore be considered to be the sum of two components; the *free growth* contribution and the contribution due to adsorbed atomic hydrogen, *i.e.*, $\eta_{hkl} = {}_{FG}\eta_{hkl} + {}_{HC}\eta_{hkl}$. The term ${}_{FG}\eta_{hkl}$ has been considered to vary with the reticular density P_{hkl}. Does ${}_{HC}\eta$ vary on different faces of nickel single-crystals, and if so, in what manner?

(c) *The adsorption of hydrogen gas on nickel*

Let us first consider the adsorption of hydrogen *gas* on nickel. Emphasis is given to the following problem: are hydrogen atoms adsorbed to the same extent on different faces of nickel single-crystals?

BEECK and co-workers[23,24,25] have made careful experimental studies of the adsorption of hydrogen gas on nickel catalysts. They prepared two types of nickel films on glass substrates :(1) randomly-oriented films and (2) completely-oriented nickel films with {110} planes lying parallel to the substrate. They observed that the oriented films had five times the catalytic activity of the unoriented films. The results were interpreted in terms of the average lattice-spacings in the two films. BEECK *et al.* argued on the basis of the theoretical work of OKAMOTO *et al.*[26] who carried out quantum-mechanical calculations (modelled on the SHERMAN-EYRING treatment[27]) of the activation energy for adsorption of hydrogen as a function of the distance apart of adjacent nickel atoms. Specifically, their calculations show that the energy of activation for adsorption is less when the adjacent nickel atoms are situated 3.52 Å apart than when they are 2.49 Å apart. Assuming the relation given by HORIUTI-POLANYI[28], it can be said that the standard free energy of hydrogen adsorption (Δg°) is more negative on a pair of sites 3.52 Å apart than on a pair 2.49 Å apart. Now, the distribution of sites with 3.52 Å and 2.49 Å inter-site spacing is not the same on the important low-index planes. When the planes {111}, {100}, {110} and {211} are considered in that order, the fraction of 2.49 Å spacings decreases and that of 3.52 Å spacings increases. This means that hydrogen is adsorbed more easily as we go from $\{111\} \rightarrow \{100\} \rightarrow \{110\} \rightarrow \{211\}$ since the standard free energy of hydrogen adsorption is increasingly negative in that order.

Thus, the greater the average inter-atomic spacing of adjacent nickel atoms on the lattice plane of nickel (*i.e.*, the lower the reticular density), the more negative is the standard free energy of hydrogen adsorption, and hence the greater the surface concentration of adsorbed hydrogen. It is maintained therefore, that under identical conditions of temperature and pressure, etc., the coverages with adsorbed atomic hydrogen on different faces of a nickel single-crystal are different. Representing this concentration on a face {hkl} by the symbol θ_{hkl}, we have $\theta_{211} > \theta_{110} > \theta_{100} > \theta_{111}$.

(d) *The adsorption of hydrogen atoms on nickel cathodes during the electro-deposition of nickel*

There is general agreement on the appreciable surface concentration of adsorbed hydrogen that exists on nickel cathodes in hydrogen overpotential studies. The surface coverage is high, particularly in acid solutions in which nickel deposition is carried out. We may take it, therefore, that there is sufficient hydrogen adsorbed on the various low-index planes of nickel to permit us to discuss the differences in coverage.

The steady-state coverages on various lattice planes is given by a steady-state condition involving the non-equilibrium rates of the various reactions which form and remove adsorbed hydrogen atoms. These non-equilibrium rates depend on the equilibrium rates which in turn depend on the equilibrium coverages — the latter being functions of the standard free energies of hydrogen adsorption. It is suggested, therefore here, that the steady-state coverages at any particular potential are different on different lattice planes of nickel and that they are dependent on the standard free energies of hydrogen adsorption. Further, since for a particular reaction mechanism, the steady-state coverage would be given for *all* the planes by the *same* steady-state condition, the sequence (though not the magnitude) of steady-state coverages would be independent of the reaction mechanism; the sequence at cathodic potentials is the same as the sequence of coverages (as given in Part I. 3(c)).

To sum up — the occurrence at a nickel cathode of several reactions involving atomic hydrogen does not affect the *sequence* of coverages with adsorbed hydrogen atoms, which is given (even on cathodes at which nickel deposition is taking place) by $\theta_{211} > \theta_{110} > \theta_{100} > \theta_{111}$.

(e) The hydrogen-contribution to the metallic overpotential

Corresponding to the conditions of electro-deposition, there is a particular *average* coverage with adsorbed hydrogen atoms ($\theta_{\mathrm{av.}}$) on the cathode surface. This $\theta_{\mathrm{av.}}$ is not distributed uniformly on all the types of facets. It has been argued above that $\theta_{111} < \theta_{100} < \theta_{110} < \theta_{211}$. Hence the hydrogen-contribution to the total metallic overpotential varies thus: $\mathrm{HC}\eta_{111} < \mathrm{HC}\eta_{100} < \mathrm{HC}\eta_{110} < \mathrm{HC}\eta_{211}$.

(f) The role of adsorbed atomic hydrogen in selective facet formation

The coverage $\theta_{\mathrm{av.}}$ is a function of the conditions of electro-deposition. When $\theta_{\mathrm{av.}}$ increases, the θ_{hkl} also increases (until the face is saturated), and hence $\mathrm{HC}\eta_{\mathrm{hkl}}$ also assumes a higher value. And what is more important, it is argued that with an increase in $\theta_{\mathrm{av.}}$, $\mathrm{HC}\eta$ does not increase to the same extent on the different types of crystal faces. The maximum increase occurs on {211}, and the minimum on {111} faces. This can be represented:

$$\Delta(\mathrm{HC}\eta_{211}) > \Delta(<\mathrm{HC}\eta_{110}) > \Delta(\mathrm{HC}\eta_{100}) > \Delta(\mathrm{HC}\eta_{111}).$$

In contrast, since they are determined by crystallographic factors (and current density), the *free growth* metallic overpotentials on all faces are equally affected — or, in certain circumstances not affected at all — by varying the conditions of electro-deposition.

The possibility therefore arises of the relative growth rates varying with the conditions of electro-deposition. Previously fast-growing faces doomed to self-elimination can become the slowest-growing faces and survive by the adsorption of hydrogen. Such arguments are in fact well known in the field of crystal growth where addition agents are deliberately utilized for the purpose of modifying crystal habit[17,29]. It is to be noted that for a reversal of growth velocities, a differential adsorption is not a sufficient condition* though it is a necessary one. The differential adsorption must

---

* SATO has not stressed this point[15].

be such that otherwise fast-growing faces adsorb hydrogen to a greater extent than the slow-growing faces, and thus assume smaller growth velocities. If the adsorption capacities are the other way round, then no reversal of velocities will occur. It is the intention here, to work out the implications of this reversal of the order of growth velocities in the case of nickel electro-deposition.

Consider, for example, two particular types of faces, {111} and {100}. Octahedral {111} facets would be selectively formed to the exclusion of {100} facets, only if $v_{111} < v_{100}$, *i.e.*, if $\eta_{111} > \eta_{100}$, or $({}_{\mathrm{FG}}\eta_{111} + {}_{\mathrm{HC}}\eta_{111}) > ({}_{\mathrm{FG}}\eta_{100} + {}_{\mathrm{HC}}\eta_{100})$. This requires that $({}_{\mathrm{FG}}\eta_{111} - {}_{\mathrm{FG}}\eta_{100}) > ({}_{\mathrm{HC}}\eta_{100} - {}_{\mathrm{HC}}\eta_{111})$. The value of $({}_{\mathrm{HC}}\eta_{100} - {}_{\mathrm{HC}}\eta_{111})$ depends on $(\theta_{100} - \theta_{111})$ which in turn is determined by $\theta_{\mathrm{av.}}$. Hence the condition $\eta_{111} > \eta_{100}$ will be satisfied only when $\theta_{\mathrm{av.}}$ does not exceed a threshold value. Above this value of $\theta_{\mathrm{av.}}$, $(\theta_{100} - \theta_{111})$ will be large enough to make $({}_{\mathrm{FG}}\eta_{111} - {}_{\mathrm{FG}}\eta_{100}) < ({}_{\mathrm{HC}}\eta_{100} - {}_{\mathrm{HC}}\eta_{111})$, and hence, $\eta_{100} < \eta_{111}$. Under these conditions, the growth of {100} facets will be favored.

With increasing values of $\theta_{\mathrm{av.}}$, stages will be successively reached where the growth of {110} or even {211} facets will be preferentially developed. It may be noted however that in certain ranges of values of $\theta_{\mathrm{av.}}$, the growth velocities of two types of facets may be near each other and both types will be formed. We shall term this *mixed-facet formation.*

Hence, with a decrease in $\theta_{\mathrm{av.}}$ there would be a progressive change of the facets chosen for preferential growth in the following sequence: {211} → {110} → {100} → {111}. Since {111} facets would tend to form in the absence of hindrances, we say that, as $\theta_{\mathrm{av.}}$ diminishes, the growth process tends more and more towards *free growth.*

The essential point of the theory therefore is that the average surface concentration of adsorbed hydrogen atoms on the cathode ($\theta_{\mathrm{av.}}$), is a deciding factor in the development of particular facets.

4. WHAT INCLINATION WILL THE PREFERENTIALLY-FORMED FACETS ASSUME RELATIVE TO THE SUBSTRATE PLANE?

In the first instance, it is necessary to consider the two main modes of growth of compact electro-deposits, which were described by FINCH and co-workers[1,30] as well as by FISHER AND HEILING[31].

The outward mode of growth is characterized by deposit-crystals having greater height than width, *i.e.*, by columnar, acicular, needle-like etc., crystals. Such crystals would be obtained when the outward velocity of growth in a direction normal to the substrate is greater than the lateral velocity in a direction parallel to the substrate.

The lateral mode of growth is characterized by deposit-crystals with greater width than height. These lamellar, tabular, plate-like crystals would result from the lateral crystal growth velocity being greater than the velocity in a direction normal to the substrate.

The conditions of electro-deposition are largely responsible for determining which particular mode of growth is adopted by electro-deposits. This relationship has been discussed recently[23]. In our view, two factors are mainly responsible for affecting the mode of growth in *unadulterated* baths:

(1) The metallic overpotential influences the nucleation rate. Nickel, with a high metallic overpotential, has a high nucleation rate. The girth of the crystals is therefore effectively reduced.

(2) When the transference number of the nickel ions is high, they move mainly by migration. The nickel ions are therefore very sensitive to differences in the field near the cathode, and there will be differences in the concentrations of nickel ions near regions of the cathode where the field strength is different. On a nonuniform cathode surface, nonhomogeneity of the field also exists. The field will be more intense near peaks than near the recesses. Hence, peaks will receive a greater supply of nickel ions than recesses, giving rise to preferential deposition on peaks. This further accentuates the nonhomogeneity of the field. Thus there is a cumulative tendency for deposition on to peaks and an outward growth is obtained.

Let us consider nickel electro-deposits obtained from baths (a) containing molar concentrations of nickel and (b) without addition agents. Under these circumstances, the nickel ions move (near the cathode) mainly under the influence of the electrical field. Therefore, it may be expected that nickel deposits from such baths adopt an outward mode of growth.

In many cases however such an inferential argument need not be made. The optical microscopy evidence clearly shows an outward growth in nickel deposits whose preferred orientations have also been determined[33].

Hence the conditions of electro-deposition demand that the growth process satisfies two requirements:

(1) Depending on the magnitude of $\theta_{av.}$, facets of a certain crystallographic type $\{hkl\}$ should be the slowest-growing facets and hence they should be selectively formed;

(2) The deposit-crystals should adopt an outward mode of growth. This means that the velocity of growth in a direction parallel to the substrate surface is least. The slowest-growing facets should be therefore developed normal to the substrate.

The distinction between these two necessary conditions is as follows. Condition (1) refers only to the *indices* $\{hkl\}$ of the facets preferentially developed; it does not state anything about whether these $\{hkl\}$ facets are parallel or normal or inclined to the substrate. Condition (2), on the other hand, is only concerned with the *inclination* or *orientation* (with respect to the substrate) of the slowest-growing, selectively-developed facets; it does not, however, tell us anything about the indices of the particular facets chosen for development.

These two stipulations for the growth process are simultaneously fulfilled only when facets of $\{hkl\}$ type are developed *normal* to the substrate. In other words, the lattice row at the common intersection of the selectively-developed facets — the zone axis — grows normal to the substrate.

5. THE RELATIONSHIP BETWEEN THE PROCESSES OF SELECTIVE-FORMATION AND PREFERENTIAL-INCLINATION OF FACETS AND THE DEVELOPMENT OF TEXTURES

We have considered so far the conditions responsible for influencing the growth of facets on one deposit-crystal and orienting them with respect to the substrate. Since similar growth factors obtain in all the deposit-crystals, a similar orientation of the preferentially-developed facets (so that they are normal to the substrate) would take place in all the crystals. This is equivalent to stating that there is a *preferred orientation* of the deposit-crystals. The orientation is such that the zone-axis of the selectively-formed facets is the *preferred orientation axis*. The above arguments have therefore resulted naturally in WILMAN's hypothesis.

For obvious reasons, the term *Wilman facets* is proposed to describe facets which grow preferentially normal to the substrate.

Thus we have established a correlation between the facets selected for growth and the orientations developed*. Corresponding to the *Wilman facets*: {211}, {110}, {100} and {111} the preferred orientations are ⟨210⟩, ⟨100⟩, ⟨100⟩ and ⟨110⟩ respectively.

WILMAN's hypothesis, it may be noted, would be valid only in the case of electro-deposits which adopt the outward mode of growth. A brief consideration of the textures of lateral growths is presented in Part III, 2.

6. THE MECHANISM OF GRADUAL DEVELOPMENT OF PREFERRED ORIENTATION

The development of a texture out of a random orientation is not, however, a sudden and discontinuous transition. The preferred orientation gradually develops as the thickness of the electro-deposit increases.

To explain this phenomenon, let us consider the random stage of growth with crystals oriented in all possible ways. Facets are slowly forming and increasing in size. The mode of growth, if outward, is making the velocity of crystal growth in a direction normal to the substrate, preponderate increasingly over the lateral growth velocity. A random orientation stage should therefore suddenly give way to a prefered orientation.

If this is not the case, it is because there is a factor opposing the development of texture. Each crystal grain of the random orientation stage acts as a substrate for the growth of the deposit-grain lying above it along the growth axis and it impresses its own orientation on the deposit-grain. Thus the random orientation stage exerts a *substrate* influence on the further deposit. It promotes randomness — not orientation — and by doing so delays the development of preferred orientation. The preference for a texture therefore increases with the thickness of electro-deposit and the preferentially-developed facets are only gradually aligned normal to the substrate. In other words, the degree of preferred orientation increases with thickness.

7. THE INFLUENCE OF ADSORBED HYDROGEN ON THE SPECIFIC TEXTURES THAT ARE DEVELOPED

It has been shown (see I, 3(f) and 5), that as $\theta_{\text{av.}}$ decreases, there is a successive development of *Wilman facets* in the following sequence: {211} → {110} → {100} → {111}. Hence the following preferred orientations would be successively observed with decreasing values of $\theta_{\text{av.}}$:

$$\langle 210\rangle \rightarrow \langle 100\rangle \rightarrow \langle 110\rangle .$$

On the other hand, if $\theta_{\text{av.}}$ is increased, the orientations would change in the opposite manner.

---

* Our picture is over-simplified on one point. In actual crystal growth, considerations of symmetry, the need for one crystal to conglomerate and compact with other crystals and the necessity for crystals to be bounded by faces — all these factors generally require that faces of other types also develop along with the *Wilman facets*. These other faces, we suggest, have nearly equal growth-velocities or they are faster-growing. Our main contention is that only the *Wilman facets* are responsible for determining the preferred orientation.

8. THE RELATIONSHIP BETWEEN THE HYDROGEN CONTENT OF ORIENTED NICKEL ELECTRO-DEPOSITS AND THEIR TEXTURES

The hydrogen within a deposit depends on the amount of hydrogen adsorbed on the surface[34]. Hence, the higher the $\theta_{av.}$, the higher would be the hydrogen content of the electro-deposit.

We have argued, however, that differing values of $\theta_{av.}$ are necessary to lead to the development of different *Wilman facets*, and hence different textures.

Thus the hydrogen content of a deposit should vary with the texture that it reveals. Further, the hydrogen contents should increase with the following sequence of preferred orientations:

$$\langle 110\rangle \rightarrow \langle 100\rangle \rightarrow \langle 210\rangle \rightarrow \langle 211\rangle^{*}.$$

Further, as a first approximation, let us argue that the ratio of the surface concentrations on two faces is the inverse of the ratio of their population densities. On this basis the hydrogen contents of deposits with $\langle 110\rangle$, $\langle 210\rangle$ and $\langle 211\rangle$ orientations should be 1, 2.75 and 5.8 respectively. YANG[35] measured the hydrogen contents of deposits showing $\langle 110\rangle$, $\langle 210\rangle$ and $\langle 211\rangle$ preferred orientations and found that their relative hydrogen contents were about 1, 2 and 4 respectively. Considering that our argument assumes (1) that the deposit has faces of only one type and (2) that there is complete preferred orientation, *it can be seen that the expected values of hydrogen content are in the same sequence and of the right order as the observed values.*

The above correlation between the texture developed by an electro-deposit and its hydrogen content does not appear to have been achieved hitherto. The correlation strongly suggests the basic correctness of the mechanism of texture development proposed in this paper. Further support for the theory can be derived from a consideration of the dependence of textures on deposition conditions. This dependence will be discussed in Part II of this paper.

ACKNOWLEDGEMENT

The author wishes to record his deep gratitude to Professor L. I. ANTROPOV, formerly UNESCO Technical Assistance Mission Expert at the Indian Institute of Technology, Bombay, to Dr. S. RAMASESHAN, Professor of Physics, Indian Institute of Technology, Madras, and Dr. S. PANCHARATNAM, Reader in Physics, University of Mysore, for their useful discussion of the preliminary draft of this paper, prepared in 1959.

SUMMARY

This paper presents a mechanism for (a) the preferential formation of electro-deposit facets of a particular type and (b) the alignment of these facets normal to the substrate, and then shows that the result of these two growth processes is the development of a preferred orientation in thick electro-deposits. The discussion is confined to the growth of nickel electro-deposits from *unadulterated baths*.

---

* For a treatment of this point the $\langle 211\rangle$ orientation is also considered. This texture corresponds (see the discussion in Section 5) to the development of $\{210\}$. *Wilman facets*, the formation of which requires a $\theta_{av.}$ still higher than that necessary for the development of $\{211\}$ facets. We assume here that $\theta_{210} > \theta_{211}$ and ${}_{FG}\eta_{210} < {}_{FG}\eta_{211}$ — the type of dependence of θ_{hkl} and ${}_{FG}\eta_{hkl}$ on P_{hkl} being the same as for the other facets.

Facets are formed because of differences in growth velocities. Both *crystallographic* and *electrochemical* factors produce these differences. The crystallographic factors are considered in terms of the Bravais *law* of crystal growth. It is suggested that different lattice planes have different *free growth* metallic overpotentials. The electrochemical disturbance to *free growth*, stems from the hydrogen evolution reaction. BEECK's experimental studies on hydrogen adsorption on nickel are used to argue that the intermediately-produced hydrogen atoms are adsorbed more easily on lattice planes which during *free growth* have faster growth velocities. If hydrogen atom adsorption increases metallic overpotential, then facets of different types are formed with different surface coverages.

The {hkl} facets so formed are aligned normal to the substrate because the deposits tend to adopt an outward mode of growth which requires that the slowest-growing {hkl} facets (and therefore the zone-axis ⟨uvw⟩ of the {hkl} *Wilman facets*) stand perpendicular to the substrate surface.

All deposit-crystals being subject to similar growth influences, they get identically oriented, *i.e.*, a preferred orientation develops with the texture-axis ⟨uvw⟩ being the zone-axis of the *Wilman facets*. The random orientation stage — which precedes the texture stage — exercises a *substrate* influence and therefore permits only a gradual development of texture.

Two important consequences follow from the theory proposed in this paper:
(1) texture changes are induced by changes in surface coverage with hydrogen atoms, and by factors such as temperature which affect this coverage;
(2) deposits having different textures should have different hydrogen contents. The experimental data of YANG supports the latter conclusion.

REFERENCES

1 G. I. FINCH, N. WILMAN AND L. YANG, *Discussions Faraday Soc.*, 1 (1947) 144.
2 G. I. FINCH AND C. H. SUN, *Trans. Faraday Soc.*, 32 (1936) 852.
3 W. A. WOOD, *ibid.*, 31 (1935) 1248.
4 W. HUME-ROTHERY AND M. R. J. WYLLIE, *Proc. Roy. Soc. (London)*, A 181 (1943) 331.
5 C. L. CLARK AND S. H. SIMONSON, *J. Electrochem. Soc.*, 98 (1951) 110.
6 W. SMITH, J. H. KEELER AND H. J. READ, *Plating*, 36 (1949) 355.
7 K. M. GORBUNOVA AND A. A. SUTYAGINA, *Zh. Fiz. Khim.*, 32 (1958) 785.
8 R. WEIL AND R. RAQUIN, *J. Electrochem. Soc.*, 107 (1960) 87.
9 R. M. BOZORTH, *Phys. Rev.*, 26 (1925) 390.
10 M. R. J. WYLLIE, *J. Chem. Phys.*, 16 (1948) 52.
11 H. WILMAN, *Trans. Inst. Metal. Finishing*, 32 (1955) 281.
12 H. WILMAN, *J. Chem. Eng. Soc.*, Imperial College, London (1956).
13 A. K. N. REDDY AND H. WILMAN, *Trans. Inst. Metal Finishing*, 36 (1958–59) 97.
14 K. M. GORBUNOVA, O. S. POPOVA, A. A. SUTYAGINA AND M. YU. POLUKAROV, *Growth of crystals, Reports at the First Congress of Crystal Growth*, 5–10th March 1956. Eng. trans., Consultants Bureau Inc., 1958, p. 46.
15 R. SATO, *J. Electrochem. Soc.*, 106 (1959) 206.
16 M. STRAUMANIS, *Z. Phys. Chem.*, B13 (1931) 316; B19 (1932) 63.
17 H. E. BUCKLEY, *Crystal Growth*, John Wiley and Sons, Inc., New York, 1951.
18 L. I. ANTROPOV, *Kinetics of Electrode Process and Null Points of Metals*, Council of Scientific and Industrial Research, New Dehli, India, 1960 20–21.
19 B. E. CONWAY AND J. O'M. BOCKRIS, *Proc. Roy. Soc., (London)*, A248 (1958) 394.
20 W. MEHL AND J. O'M. BOCKRIS, *Can. J. Chem.*, 37 (1959) 190.
21 H. GERISCHER, *Anal. Chem.*, 31 (1959) 33.
22 B. E. CONWAY AND J. O'M. BOCKRIS, *Plating*, 46 (1959) 371.
23 O. BEECK, A. E. SMITH AND A. WHEELER, *Proc. Roy. Soc. (London)*, A177 (1940) 62.
24 O. BEECK, *Rev. Mod. Phys.*, 17 (1945) 61.

25 O. Beeck and A. W. Ritchie, *Discussions Faraday Soc.*, 8 (1950) 159.
26 G. Okamoto, J. Horiuti and K. Hirota, *Sci. Papers Inst. Phys. Chem. Res., (Tokyo)*, 29 (1936) 223.
27 A. Sherman and H. Eyring, *J. Am. Chem. Soc.*, 54 (1932) 2661.
28 S. Glasstone, K. J. Laidler and H. Eyring, *The Theory of Rate Processes*, McGraw Hill Book Co., New York, 1941, p. 144.
29 O. Knache and I. N. Stranski, *Z. Elektrochem.*, 60 (1956) 816.
30 G. I. Finch and D. N. Layton, *J. Electrodepositors' Techn. Soc.*, 27 (1951) 215.
31 H. Fischer and H. F. Heiling, *Trans. Inst. Metal Finishing*, 31 (1954) 90.
32 S. R. Rajagopalan and A. K. N. Reddy, *paper presented at the First Seminar in Electrochemistry, Central Electrochemical Research Institute, Karaikude, India*, 20th April, 1960.
33 V. Zenter, A. Brenner and C. W. Jennings, *Physical properties of Electrodeposited Metals*, A.E.S. Research Report, serial No. 20, 1952.
34 F. W. Thompson and A. R. Ubbelhode, *J. Appl. Chem. (London)*, 3 (1953) 27.
35 L. Yang, *J. Electrochem. Soc.*, 97 (1950) 241.

PREFERRED ORIENTATIONS IN NICKEL ELECTRO-DEPOSITS

II. A CONSIDERATION OF THE EFFECT OF DEPOSITION CONDITIONS ON THE TEXTURES DEVELOPED

A. K. N. REDDY* AND S. R. RAJAGOPALAN

Central Electrochemical Research Institute, Karaikudi-3 (India)

(Received May 24th, 1963)

1. INTRODUCTION

In Part I of this paper[1], a mechanism has been proposed for the development of preferred orientation with special reference to nickel electro-deposits.

We shall here discuss the causal connection between deposition conditions and the textures developed.

2. SCOPE AND METHOD OF ANALYSIS

The discussion here is confined to the textures: ⟨210⟩, ⟨100⟩ and ⟨110⟩ because these are the most commonly-reported orientations and also because certain unusual textures (for example ⟨111⟩)have sometimes been reported[2] but not reproduced by other workers[3].

The preferred orientation corresponding to a c.p.h. form of nickel (which generally occurs along with a f.c.c. nickel ⟨211⟩ texture) has been omitted from our discussion even though many authors have reported[4,5,6,7] this orientation. We do not doubt the occurrence of a substance with a c.p.h. structure and with the observed lattice parameters, but it is felt that there are firm grounds for exercising a certain caution in identifying the substance as hexagonal nickel and that, therefore, a consideration of a c.p.h. nickel should await its unequivocal identification. The basis for this caution is being presented elsewhere.

In discussions on the dependence of growth textures on deposition conditions, the general mode of approach is to concentrate on $\theta_{\mathrm{av.}}$, the average surface coverage with adsorbed atomic hydrogen. We then consider what changes, if any, in $\theta_{\mathrm{av.}}$ are brought about by altering the conditions of electro-deposition. The *trend* of change of texture can be predicted when it is known whether $\theta_{\mathrm{av.}}$ increases, decreases or remains constant (see Part I, Section 7). A change of preferred orientation ⟨210⟩ → ⟨100⟩ → ⟨110⟩ will be termed a change towards *free growth*. The expectations will then be compared with the experimental results. Several authors have studied the textures of nickel electro-deposits[1-4,6-8,10,11].

At this stage of theory and experiment, it appears advisable to distinguish the main patterns amidst the welter of data and to explore the *systematic* texture varia-

---

* Present address: *Post-doctoral Research Associate, The Electrochemistry Laboratory, University of Pennsylvania, Philadelphia 4, Pa., (U.S.A.)*

tions that result from changes in deposition conditions. By a systematic variation we mean a regular increase in the atomic population density of the atom row constituting the preferred orientation axis. Thus the variation in textures: ⟨210⟩ → ⟨100⟩ → ⟨110⟩ (which has been termed a change towards *free growth*) corresponds to a regular increase in the close-packed character of the texture axis. *Such systematic trends, though contained in the experimental results, appear to have escaped the attention of previous workers.*

From the data available we have isolated the following systematic changes in textures:

Change in deposition conditions	*Trend of change of preferred orientations*
Increase of temperature	Change towards *free growth*
Increase of current density	Slight change towards *free growth*
Addition of oxidizing agents	Change towards *free growth*

The variations in texture quoted above refer to those observed when a Watts type bath has been used. It should be pointed out that similar trends also obtain in the case of a pure chloride bath.

3. THE INFLUENCE OF TEMPERATURE ON PREFERRED ORIENTATION

The relationship between the steady-state coverage (θ) with adsorbed hydrogen atoms and temperature (T) can be simply written in the following manner:

$$\frac{\mathrm{d}\theta}{\mathrm{d}T} = \frac{\mathrm{d}\theta}{\mathrm{d}\theta^*}\,\frac{\mathrm{d}\theta^*}{\mathrm{d}T}$$

where θ^* is the coverage under equilibrium conditions. In this section we are only interested in whether a temperature increase causes an increase or a decrease of θ. The exact dependence of θ on T will depend on the mechanism of the hydrogen evolution reaction, but this need not concern us here.

From a consideration of the expressions for θ for various rate-determining steps[12], it can easily be shown that $(\delta\theta/\delta\theta^*)_T$ is positive, θ decreasing when θ^* decreases. With regard to $\mathrm{d}\theta^*/\mathrm{d}T$, it can be seen from the Langmuir adsorption isotherm that θ^* decreases when T increases.

We conclude therefore that θ depends upon the temperature of the nickel cathode in thermal equilibrium with the electrolyte.

An increase in bath temperature brings about a decrease in $\theta_{\mathrm{av.}}$ and consequently the following trend of change of preferred orientation is possible:

$$\langle 210\rangle \rightarrow \langle 100\rangle \rightarrow \langle 110\rangle$$

(Our theory permits the simultaneous formation of two types of *Wilman facets* — mixed facet formation — and hence the development of *mixed orientations* (see Part I, 3(f)). Thus, it is quite likely that at a particular temperature, only mixed — and not pure — orientations are observed).

A rise in bath temperature, therefore, scavenges the cathode of its adsorbed hydrogen and the orientation change is towards *free growth*. At sufficiently high temperatures, therefore, nickel electro-deposits would show the *free growth* orientation ⟨110⟩. GOSWAMI'S *results show that, below a pH of 5, the trend of change of observed preferred orientations is precisely predicted by the theory.*

Thus at a pH 2, BANERJEE AND GOSWAMI[6] observed at 15° a ⟨210⟩ texture; at 25°, ⟨210⟩ + ⟨100⟩; at 45°, ⟨100⟩ + ⟨110⟩; and 55°–75°, ⟨110⟩. At pH 4, the results showed a ⟨210⟩ + ⟨100⟩ texture at 15°, ⟨100⟩ at 30°, ⟨100⟩ + ⟨110⟩ at 45° and ⟨110⟩ at 50°–75°. *Above pH 5, however, there are deviations from the "free growth" trend.* A hexagonal nickel orientation appears along with f.c.c. nickel ⟨211⟩, and at higher temperatures a ⟨100⟩ orientation is observed.

4. THE EFFECT OF CURRENT DENSITY ON PREFERRED ORIENTATION

The main result of an increase of current density is a small change of textures towards *free growth* (as stated in the table in Section 2). From a sulphate–chloride bath (pH 4) a change from 10–20 mA/cm^2 causes an orientation change ⟨100⟩ → ⟨110⟩. At pH 2, the variation is unsystematic. Despite this, the same trend appears to be there — thus at 2 mA/cm^2, we have ⟨210⟩; 5 mA/cm^2, ⟨100⟩ and 20 mA/cm^2, ⟨110⟩. At 10 and 100 mA/cm^2, however, the (⟨210⟩ + ⟨100⟩) and (⟨210⟩ + ⟨110⟩) orientations occur.

When the current density used for deposition is increased, a change towards *free growth* orientations can arise in two possible ways: (1) through changes in $\theta_{\mathrm{av.}}$, and/ or (2) through changes in the *free growth* metallic overpotential.

(1) *Effect of current density on* $\theta_{\mathrm{av.}}$

An increase in current density brings about an increase in current efficiency, *i.e.*, in $i_{\mathrm{Ni}}/i_{\mathrm{H}}$. The increase in the ratio is mainly due to the increase of i_{Ni} with cathode potential (which depends on the total current density) — the increase in i_{H} is negligible. This conclusion has been arrived at from a study of the partial curves for nickel deposition and hydrogen evolution, which are obtained by the resolution of the total *i–E* curves[13]. It may be concluded therefore that an increase in total current density leads most probably only to a very small increase in $\theta_{\mathrm{av.}}$.

$\theta_{\mathrm{av.}}$ can also change by another mechanism. Whereas with a current density increase, i_{H} does not increase significantly, the same cannot be said for i_{Ni}. Since $i_{\mathrm{Ni}} \gg i_{\mathrm{H}}$, it is quite likely that nickel ions are deposited on to the adsorbed hydrogen atoms, which thus get locked up in the nickel lattice,particularly because the rate of nickel deposition is probably much greater than the slow diffusion of hydrogen into the metal. The net effect of this enveloping of adsorbed atomic hydrogen within the lattice, is a small decrease of $\theta_{\mathrm{av.}}$. The particular mechanism discussed here, although operative at all current densities, probably merits consideration only at high current efficiencies where $i_{\mathrm{Ni}} \gg i_{\mathrm{H}}$. Even then it cannot be unequivocally stated that $\theta_{\mathrm{av.}}$ is considerably reduced. However, if the effect is significant at all, then it would tend to offset (at least partially) the small increase in $\theta_{\mathrm{av.}}$ resulting from a small increase in i_{H} (discussed in the previous paragraph).

It seems therefore that changes in $\theta_{\mathrm{av.}}$ due to the above two opposite effects cannot be major in character, and that the coverage can be considered more or less constant. Hence, a current density increase should not have much effect on the preferred orientation through changes in $\theta_{\mathrm{av.}}$.

(2) *Effect of current density on "free growth" metallic overpotential*

In a study of the electro-deposition of lead, PIONTELLI AND POLI[14] have experimentally demonstrated that $b_{111} > b_{100}$, where b_{hkl} is the slope of the $_{FG}\eta_{hkl}$ *vs.* i curve. The case of lead is of significance because the growth of lead approximates to what we have termed *free growth*. This is because lead has a high hydrogen overvoltage and a positive free energy of hydrogen adsorption. Hence hardly any hydrogen evolution occurs and θ is almost zero.

If PIONTELLI's result is interpreted by saying that b depends on the population density of the plane such that $b_{111} > b_{100} > b_{110} > b_{211}$, then it can be seen that a current density increase can lead to changes in texture towards *free growth* because it leads to different increases in the *free growth* overpotentials on different lattice planes.

The ideas advanced in the above discussion must be regarded as tentative. One important handicap has been the lack of data on surface coverage as a function of the partial current for hydrogen. It must also be emphasized that several deviations from the *free growth* trend have been observed especially at low current densities (below 10 mA/cm^2) where current efficiency is low.

5. THE EFFECT OF ADDITION OF OXIDIZING AGENTS ON PREFERRED ORIENTATION

The effect of the addition of hydrogen peroxide or nitrate ions can be explained by assuming that they compete with hydrogen ions to get reduced at the cathode. Thus the yield of hydrogen is diminished — which is the reason why hydrogen peroxide is used as an *anti-pitting* agent. Hence, if nickel is deposited in the presence of a sufficient concentration of these agents, we can expect a decrease in $\theta_{av.}$. The result of this diminution of $\theta_{av.}$ is that the preferred orientation changes in the direction of *free growth*.

The published data on the influence of the addition of oxidizing agents on the preferred orientations of nickel electro-deposits largely bears out these expectations. BANERJEE AND GOSWAMI have observed that in a sulphate–chloride bath, the addition of hydrogen peroxide (1 g/l) brings about a change of orientation $\langle 210\rangle \rightarrow \langle 210\rangle + \langle 100\rangle$; and nitrate ions (0.426 g/l nickel nitrate) the change $\langle 210\rangle \rightarrow \langle 110\rangle$. The change, it may be noticed, is more marked with nitrate ions which are perhaps more easily reduced and/or which remove (through the reduction reaction) a larger quantity of atomic hydrogen per gm ion of nitrate ions reduced.

6. LIMITATIONS OF THE PRESENT WORK

In the treatment presented above little reference has been made to the influence of bath composition on texture. Such an influence is certainly indicated in the data. For example, under the same conditions of temperature, pH and current density, a Watts bath yields deposits with textures different from those of deposits from an approximately molar chloride bath. This is another aspect of the well-known difference in metal deposits obtained from sulphate and chloride baths. The cause of the differences appears to lie not only in the extents to which sulphate and chloride ions are adsorbed on the cathode, but also in the differences in metal ion activities in the sulphate and chloride baths. Further experimentation is necessary before this aspect of texture dependence is discussed.

A very important point that has been ignored is the possible influence of the formation of nickel hydroxide at high pH (> 5) where the theory is not as successful as at low pH.

Finally, it cannot be emphasized too strongly that several deviations do occur from the texture sequences expected by the theory. In the absence of explicit statements on the reproducibility of the observed orientations, no assessment of this problem could be made. While it is tempting to attribute the deviations to the well-known capricious nature of crystal growth, it is nevertheless better to ascribe them to weaknesses in theory too. It is not likely that a simple theoretical view-point can encompass the varied factors involved in the growth history of electro-deposits. The growth of crystalline electro-deposits cannot be viewed as the sum of the growths of individual crystals. The necessity to compact together is itself a disturbing factor on the growth of the individual crystals. Further, mass transfer factors also deserve recognition under certain circumstances.

Nevertheless, it is worth emphasizing that even the limited correlation between textures and deposition conditions achieved in this work has not been hitherto accomplished. The theory is therefore presented in the hope that a careful consideration of the deviations will refine, and if necessary, radically alter, both the theoretical approaches and experimental techniques. In a further communication an attempt is made to generalize the theory to lateral growths, to the adsorption of addition agents and to the textures of the electro-deposits of other metals.

ACKNOWLEDGEMENT

We thank Professor L. I. Antropov, formerly UNESCO Technical Assistance Mission Expert at the Indian Institute of Technology, Bombay, for his valuable comments and helpful discussions.

SUMMARY

The theory of texture development in nickel electro-deposits, proposed in Part I of this paper, is used here to explain the trends of texture changes which result from variations in nickel deposition conditions.

Only the commonly-reported $\langle 210 \rangle$, $\langle 100 \rangle$ and $\langle 110 \rangle$ orientations are considered. The occurrence of systematic texture changes (with increase of temperature and current density and with addition of oxidizing agents) is indicated in the experimental data of previous workers.

It is suggested that an increase in bath temperature leads to a decrease in the average surface concentration of adsorbed hydrogen atoms, and thus to changes of textures towards *free growth, i.e.*, $\langle 210 \rangle \rightarrow \langle 100 \rangle \rightarrow \langle 110 \rangle$. This conclusion is completely in agreement with experiments conducted at a pH less then 5.

The slight *free growth* trend observed with an increase of current density is tentatively ascribed to differences in the slopes of the *free growth* η–i curve for different single-crystal faces of nickel.

The addition of oxidizing agents — it is argued — reduces surface coverage and hence produces texture changes towards *free growth.*

Some limitations of the present work are indicated.

REFERENCES

1 A. K. N. Reddy, Part I, *J. Electroanal. Chem.*, 6 (1963) 141.
2 V. Sentner, A. Brenner and C. W. Jennings, *Physical properties of electrodeposited metals*, A.E.S. Research Peport, serial No. 20, 1952, p. 34.
3 D. J. Evans, *Trans. Faraday Soc.*, 54 (1958) 1086.
4 L. Yang, *J. Electrochem. Soc.*, 97 (1950) 241.
5 D. J. Evans and M. R. Hopkins, *J. Electrodepositors' Tech. Soc.*, 28 (1952) 229.
6 B. C. Banerjee and A. Goswami, *J. Electrochem. Soc.*, 106 (1959) 590.
7 B. C. Banerjee and A. Goswami, *ibid.*, 106 (1959) 23.
8 R. M. Bozorth, *Phys. Rev.*, 26 (1925) 390.
9 G. I. Finch, H. Wilman and L. Yang, *Discussions Faraday Soc.*, 1 (1947) 144.
10 K. M. Gorbunova, O. S. Popova, A. A. Sutyagina and Yu. M. Polukarov, *Growth of Crystals, Reports at the First Conference on Crystal Growth*, 5–10th March, 1956, Eng. trans. Consultants Bureau Inc., 1958, p. 46.
11 H. Fisher, *Z. Elektrochem.*, 54 (1950) 459.
12 J. O'M. Bockris and E. C. Potter, *J. Electrochem. Soc.*, 99 (1952) 169.
13 H. T. S. Britton, *Hydrogen Ions*, Chapman and Hall, New York, 4th edn., 1956, vol. 2, p. 224.
14 R. Piontelli and G. Poli, *Z. Elektrochem.*, 62 (1958) 320.

PREFERRED ORIENTATION OF NICKEL ELECTRO-DEPOSITS

III. GENERALIZATION OF THE THEORY

A. K. N. REDDY* AND S. R. RAJAGOPALAN

Central Electrochemical Research Institute, Karaikudi-3 (India)

(Received 24th May, 1963)

1. INTRODUCTION

The theory proposed in Part I of this paper[1], is limited in three ways: (a) it is concerned only with deposits which adopt the *outward* mode of growth; (b) it has been restricted to a discussion of electro-deposits of only one metal, *viz.*, *nickel*; and (c) it has considered only *unadulterated* baths, *i.e.*, baths without addition agents. Let us now consider the lines on which the theory may be generalized.

It may be recalled that the mechanism of texture development that we have proposed (following WILMAN) focusses attention on two processes:

(1) the preferential formation of facets;

(2) the aligning of these facets so that in all the crystals they are identically-oriented with respect to the substrate.

2. MODIFICATION OF THE THEORY FOR LATERAL GROWTHS

A preferred orientation, by definition, assumes rotational symmetry about the orientation axis. Hence if one of the most densely-populated atom-rows constitutes the texture axis, then the identical alignment of facets can be achieved only when the favored facets stand either normal to the substrate surface (in which case they are called *Wilman facets*) or parallel to it.

The inclination of the facets depends mainly on the mode of growth adopted by the electro-deposit; *i.e.* on the relative velocities of growth of the crystal in the outward (normal to the substrate) and lateral (parallel to the substrate surface) directions. If one of the growth velocities is predominant, then alignment of the facets can occur easily.

We have only considered the outward mode of growth, because this is the main mode of growth adopted by nickel electro-deposits (obtained from *unadulterated baths*) whose textures we have considered. In this case, the {hkl} *Wilman facets* are aligned normal to the substrate and the orientation axis ⟨uvw⟩ is the zone axis of the {hkl} faces.

It is quite likely that, in the case of other metals and/or under other conditions, the lateral mode of growth (with lamellar or plate-like deposits) would be favored. In the case of *ideal* lateral growths, the preferentially-developed {hkl} facets will be parallel to the substrate, and the preferred orientation axis will be the atom-row normal to the {hkl} planes.

---

* See note on p. 153.

In *actual* lateral growth, however, *errors* can arise in the alignment of the preferentially-formed facets. In this case, the plate-like crystals will not be perfectly parallel to the substrate plane, neighboring crystals being tilted out of registry. The net effect will be a *lifting-up* of the plate-like crystals from the deposit plane parallel to the substrate surface. Under these circumstances, the deviations from the ideal orientation may take the form of a scatter of the orientation axis from the ideal position.

One source of alignment error arises if the deposit-crystals are not sufficiently far removed from the *substrate influence* of the random orientation stage. The mis-alignment of the underlying random stage will then be inherited by the crystals at or near the surface. This type of error is progressively corrected with increasing thickness of deposit.

A second source of error is due to the inevitable growth roughening (in unadulterated baths) which brings in its wake non-uniformity of field distribution and hence an increasing outward-growth tendency. In this case, until the lateral-growth tendency is overwhelmed, the favored facets assume positions of varying compromise — neither exactly parallel nor normal to the substrate. The texture in these compromise stages can either be described in terms of the lattice plane exactly parallel to the substrate surface* (in which case it will be a very sparsely-populated plane) or in terms of the normal to the physically-real *predominantly-formed* facets, giving the spread from the ideal position of the facet-normal. This ideal position corresponds to the facet-normal being exactly perpendicular to the substrate.

Whenever the outward and lateral growth velocities become comparable, the process of *orienting* the facets with respect to the substrate becomes a more difficult affair. It would be expected that in this case the development of preferred orientation only occurs at much greater thicknesses than when one of the growth velocities preponderates. The difficulty in developing a texture which results from rotation of the cathode at high rev./min[3] — a hitherto unexplained observation — is probably due to the point under discussion. Rotation of the cathode changes the mode of transport of nickel ions to convective diffusion and hence probably evens out to some extent the supply of ions to the peaks and recesses. Thus the outward and lateral growth velocities tend to have comparable values.

3. EXTENSION OF THE THEORY TO THE TEXTURES OF OTHER METALS

The theory of the preferential growth of facets of a particular type has been developed in two steps:

(i) a consideration of the *free growth* of deposits;

(ii) a treatment of *disturbed growth, i.e.*, growth taking place under the active hindrance of adsorbed hydrogen atoms.

Whereas the *free growth* treatment is probably valid for the electro-deposits of all metals (duly taking into account the crystallographic differences between f.c.c., b.c.c. and c.p.h. metals), the applicability of arguments based on *disturbed growth* depends on the coverage of the surface with adsorbed hydrogen atoms**. This coverage ($\theta_{\text{av.}}$)

---

* SATO[2] has adopted this alternative.

** The discussion in the rest of this section is influenced mainly by a suggestion made by ANTROPOV[4] to whom we are very grateful.

is different on different metals, and is mainly determined by the heat of hydrogen adsorption.

We shall consider (following ANTROPOV[5]) the metals which are usually electro-deposited, as falling into two broad groups: Group A metals (Pb, Ag, Cu) having a low heat of hydrogen adsorption and therefore a low $\theta_{\mathrm{av.}}$; and Group B metals (Fe, Co, Ni) having a high heat of hydrogen adsorption and hence a high $\theta_{\mathrm{av.}}$.

In the electrolytic crystal growth of Group A metals, the interference from adsorbed atomic hydrogen can largely be neglected. The growth here can be considered as largely *free*. If the electro-deposits of these metals adopt the outward mode of growth, then they would mainly reveal *free growth* orientations — $\langle 110 \rangle$ for f.c.c. metals and $\langle 111 \rangle$ for b.c.c. metals. On the other hand if they adopt the lateral mode of growth, then the *free growth* orientations that would normally be obtained are $\langle 111 \rangle$ for f.c.c. and $\langle 110 \rangle$ for b.c.c. metals.

The experimental data largely bears out these arguments. Thus silver shows[6] either $\langle 110 \rangle$ or $\langle 111 \rangle$. The theory can make a precise distinction between these two textures only if the mode of growth is revealed by photomicrography. There are however lacunae in the experimental data. Where textures have been studied, the morphology has often not been determined. Hence, a more rigorous testing of the theory must await further experimentation. Nevertheless, the theory appears to be sufficiently *fine-grained* to accommodate both outward and lateral growths.

Further, we have shown[1] that it is mainly due to a varying coverage (with temperature, for example) that a number of textures are obtained in the case of nickel electro-deposits. In the case of Group A metals, hydrogen interference can be largely ignored. Hence the number of texture-types would also be relatively few in number. The meagre experimental evidence available[6] indicates the basic correctness of this conclusion.

In the case of Group B metals which have a high heat of hydrogen adsorption (*e.g.* cobalt, chromium, iron), the hindrance from adsorbed hydrogen would have to be dealt with in the same manner as for nickel. Two factors impeded the work of extending the theory to these metals: (1) data on the adsorption of hydrogen on different single-crystal faces of these metals is not available and (2) detailed work on the dependence of the textures of these metals on the deposition conditions is also lacking.

4. EXTENSION OF THE THEORY TO THE INFLUENCE OF ADDITION AGENTS ON TEXTURES

Once *adulterated* baths are considered we must perforce consider the influence of addition agents. Addition agents are adsorbed and they can influence the electro-crystallization via the total metallic over-potential. The latter has been considered to consist of two components — a free growth component (${}_{\mathrm{FG}}\eta$) and another component due to the adsorption of species other than nickel ions. We have hitherto considered only the adsorption of intermediately-produced hydrogen atoms, in which case the second component is ${}_{\mathrm{HC}}\eta$. By being adsorbed, the addition agent can assume the role of adsorbed atomic hydrogen either partially or completely. In general, therefore, we must write $\eta_{\mathrm{hkl}} = {}_{\mathrm{FG}}\eta_{\mathrm{hkl}} + {}_{\mathrm{HC}}\eta_{\mathrm{hkl}} + {}_{\mathrm{AAC}}\eta_{\mathrm{hkl}}$, where the last term is the addition-agent-contribution to the total metallic overpotential.

The addition agent can affect the process of facet formation and/or the mode of growth of the electro-deposit. There are many aspects of this problem and we shall merly mention some possible ways in which addition agents act:

(1) The kinetics of the hydrogen evolution reaction can be affected quite profoundly by some addition agents[7,8,9]. The latter can modify the heat of hydrogen adsorption or introduce a spatial hindrance to hydrogen evolution through the sheer bulk of the adsorbed addition-agent molecules. In either case, ${}_{H}\theta_{av.}$ and therefore ${}_{HC}\eta$ is altered, which in turn may cause texture changes.

(2) It is of great import that, even when huge macro-molecules are adsorbed on the cathode, preferential facet formation and the development of growth textures has been unambiguously observed[2]. It can be concluded therefore, that the adsorption does not necessarily obliterate the differences in the growth velocities of different facets. Further, the textures change as the bulk concentration of the addition agent is altered[2]. This implies that there is an anisotropy in the adsorption of addition-agent molecules — there being a differential adsorption on the different facets. Thus ${}_{AAC}\eta$ would be different on different single-crystal faces because of the variation in ${}_{AAC}\theta_{hkl}$, the surface concentration of adsorbed addition agent on the face $\{hkl\}$. Further ${}_{AAC}\theta_{hkl}$ and ${}_{AAC}\eta_{hkl}$ would change with ${}_{AAC}\theta_{av.}$, the average surface concentration of addition agent. ${}_{AAC}\theta_{av.}$ is related to the bulk concentration (${}_{AAC}C$) through an adsorption isotherm in which the statistical free-energy of adsorption is used. Hence ${}_{AAC}C$ affects ${}_{AAC}\eta_{hkl}$ and can therefore modify the texture. It may be noted here that habit modification — a common phenomenon in crystallization from solution[10] — clearly indicates that the habit-modifier is not adsorbed to the same extent on different crystal faces. Obviously there is a *fine structure* to the adsorption process.

(3) Further evidence of the complexity involved in the influence of addition agents is the fact that all addition agents do not have the same effect. Differences in the surface activity of different classes of organic compounds and of different compounds within a class will have to be reckoned with. One indirect method of doing this would be to carry out electro-capillary measurements with mercury and to extrapolate the results on the basis of a scale of potentials which is a direct measure of the charge on the electrode, for instance, the ϕ-scale[5]. When the added organic compounds give rise in solution to charged ions, the charge on the cathode during electro-deposition is an important factor. A nickel cathode, for instance, is charged negatively during deposition and hence it is likely that cationic compounds are more easily adsorbed and initiate changes in crystal growth and/or texture. This has been observed by Denise and Leidheiser[11].

(4) When the total metallic overpotential increases considerably due to ${}_{AAC}\eta$, the nucleation rate is also increased. Greater nucleation leads to a decrease in the girth of the crystals, and the mode of growth can thereby be affected. Under certain circumstances, this can result in a change in preferred orientation.

(5) Finally, addition agents can modify the nature of growth in two further ways (a) by complexing metal ions in solution, thus modifying the initial state in the deposition process and (b) by getting reduced, the reduction product changing the chemical composition of the cathode surface and thereby affecting the energetics.

It is clear therefore that a definitive treatment of the problem is impossible at this stage. What is obvious, however, is that preferred orientations can only be determined with the aid of micrographs (optical and/or electron) of the deposit section *and* surface, with surface activity measurements and lastly with studies on electrochemical factors, such as cathode potential, cathode film, pH, current density etc.

SUMMARY

This paper discusses the lines along which the proposed theory of texture development (for nickel electro-deposits) can be extended to include (a) lateral growths, (b) deposits of other metals and (c) deposits from ***adulterated*** baths.

It suggested that when deposits adopt the lateral mode of growth, the slowest-growing {hkl} facets are formed — in the ideal case — parallel to the substrate. The normal to these facets becomes the texture-axis. In practice, the {hkl} facets may deviate from parallelism and the texture-axis then develops a scatter from its ideal position.

The theory can be generalized to cover other metals by using the fact that surface coverage with hydrogen atoms depends on the heat of hydrogen adsorption which varies from metal to metal. Hence, the textures of Pb, Ag and Cu should correspond more to *free growth* orientations, whereas those of Fe and Co should be coverage-dependent like Ni.

The many ways in which addition agents can influence textures are indicated. Addition agents can influence, for instance, the hydrogen evolution reaction, the nucleation rate and the mode of growth. Their differential adsorption on different facets and their surface activity are also discussed.

REFERENCES

1 A. K. N. Reddy and A. K. N. Reddy and S. R. Rajagopalan, Parts I and II, *J. Electroanal. Chem.*, 6 (1963) 141, 153.
2 R. Sato, *J. Electrochem. Soc.*, 106 (1959) 206.
3 L. Yang, *ibid.*, 101 (1954) 456.
4 L. I. Antropov, personal communication.
5 L. I. Antropov, *Kinetics of Electrode Processes and Null Points of Metals*, Council of Scientific and Industrial Research, New Delhi, India, 1960.
6 C. S. Barrett, *Structure of Metals* 2nd edn., McGraw-Hill Book Company, New York, 1952, p. 515.
7 H. I. Kobozev and N. I. Nekrasov, *Z. Elektrochem.*, 36 (1930) 529. quoted in reference[5].
8 J. O'M. Bockris and B. E. Conway, *J. Phys. Coll. Chem.*, 53 (1949) 527.
9 L. I. Antropov, *Kinetics of Electrode Processes and Null Points of Metals*, Council of Scientific and Industrial Research, New Delhi, India, 1960, p. 65.
10 H. E. Buckley, *Crystal Growth*, John Wiley and Sons Inc., New York, 1952.
11 F. Denise and H. Leidheister, *J. Electrochem. Soc.*, 100 (1953) 490.

Short Communication

Electro-oxidation followed by light emmission

Luminol (5-amino-2,3-dihydrophthalazine-1,4-dione) is an example of a compound which is sufficiently chemi-luminescencent to give a visible luminescence in alkaline solutions which contain an oxidant and hydrogen peroxide or oxygen. An interesting observation was made by HARVEY[1] in 1929, that luminescence could be initiated at an anode when a solution of luminol containing oxygen was made alkaline. Luminescence also appeared at a mercury cathode in alkaline luminol solutions[1,2] apparently due to the reaction of luminol with the hydrogen peroxide which was produced electrolytically. Solution chemi-luminescence which has been generated purely by chemical means, has been intensively studied but the investigation of the luminescence of luminol, produced electrochemically, has not received much attention except for some anodic work at carbon electrodes[3]. The status of luminol chemi-luminescence has been reviewed recently by WHITE[4].

The purpose of the present paper is the following: (1) to indicate some of the interesting aspects and reaction steps which occur in the electrolytic production of luminescence from luminol in the presence and absence of oxygen and (2) suggest a means for distinguishing the anodic potentials at which oxygen electro-generation begins, during a concurrent process of platinum oxide formation and luminol oxidation in alkaline solutions.

A quartz cell with 2-in. diameter windows was used in this study. The working electrode was *ca.* 3 cm^2 bright platinum foil. The general cell configuration and other necessary electrodes and circuitry used have been described previously[5,6,7]. An Electro-Instruments Model 101TB X-Y recorder was employed.

An anodic chronopotentiogram is shown in trace A of the figure, for the oxidation of $10^{-3}F$ luminol in 0.1 F Na_2CO_3. The platinum electrode with platinum oxide on the surface was precathodized to platinized platinum[8] prior to the run. There are three regions of interest on the chronopotentiogram. The first is region F which corresponds to the potential range at which the initial oxidation of platinized platinum to platinum oxide commenced. As the oxidation continued, the potential increased until luminol was oxidized (region G). If oxygen was present in the solution, luminescence appeared as soon as this region G was reached. Clearly, luminol must be oxidized prior to reacting with oxygen to produce luminescence. In solutions which were vigorously stirred, the intensity of luminescence was found to be proportional to the rate of luminol electro-oxidation[9].

Immediately following the anodic scan of trace A, the solution was stirred and allowed to quiet. A cathodic chronopotentiogram of trace A′ was then obtained. This cathodic wave is welldefined, and could not have arisen from the reduction of a soluble product produced during the anodic scan of trace A as it would have been swept into the solution from the electrode surface by the stirring process. The cathodic chronopotentiogram could only be obtained, if the anodic scan was made first. Similar cathodic chronopotentiograms were also found if the electrode was anodized in solutions of 0.1 *F* Na_2SO_4 or 0.1 *F* Na_2CO_3. These cathodic chronopotentiograms are undoubtedly due to the reduction of platinum oxide. Traces B′, C′ and D′ are also cathodic chronopotentiograms which were obtained after varying periods of anodic oxidation corresponding to traces, B, C, and D, respectively. Platinum oxide formation appears to begin initially in the potential range of region F, and continues with the concurrent oxidation of luminol in region G. The latter region is where luminescence was first detected when the solution contained dissolved oxygen.

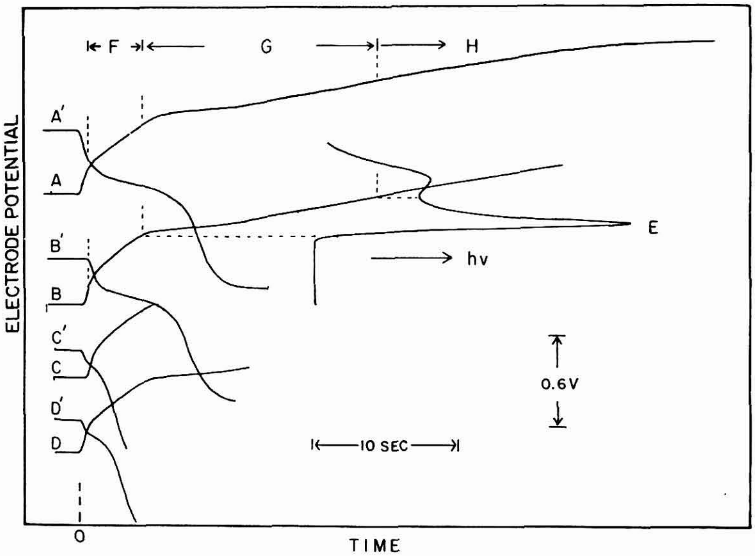

Chronopotentiograms for the oxidation of 10^{-3} *F* luminol in 0.1 *F* Na_2CO_3. Current, 400 μA. A to D are anodic potential–time traces. Traces A′ to D′ are cathodic chronopotentiograms run after the corresponding A to D anodic scans. Solution was stirred between the anodic and cathodic runs. Trace E is light emission *vs.* potential, for chronopotentiogram B.

The relative intensity of luminescence is recorded as a function of the potential for chronopotentiogram B and shown in trace E of the figure. As may be seen from this trace, an immediate rise in luminescent intensity began as soon as region G was reached. In this region, luminol was being oxidized and it is evident that the oxidized luminol reacted rapidly with the oxygen present to produce luminescence. The reaction probably takes place through a free radical chain process[10,11]. The emission intensity continued to increase until a maximum was reached, and then decreased. Another increase soon followed, however. This increase occurred in the same potential region (region H) where luminescence first appeared, if oxygen was *totally absent* from the solution. If an anodic scan was made after the potential in region H was maintained on the electrode for a period of time in well-degassed, stirred solutions of luminol, luminescence then appeared in the potential range of region G. Oxygen was apparently being generated into the solution during the electrolysis, at the potential of region H, in sufficient quantities that luminescence appeared on the next scan as soon as luminol was oxidized.

It is usually difficult, and sometimes impossible, to distinguish the exact potentials at which platinum oxide or oxygen formation begins or ends during a concurrent oxidation process of an electro-active species. The regions of potential breaks found for the anodic scan of the platinum electrode, in the presence of the background electrolyte, have been conventionally taken as the places at which oxide formation occurs. The potential range at which oxygen is being formed from either the oxidation of water or hydroxyl ion (basic solutions), is usually taken as the region in which the potential tends to level out and remain constant with time. These regions of oxide and oxygen formation on platinum electrodes are seldom clearly defined. In the oxidation process under discussion the potential at which oxygen formation began, could be distinguished.

In Na_2CO_3 solutions of luminol, the amount of oxide formed, as ascertained from the cathodic strip-out times, seemed to be proportional only to the total time of the anodic electrolysis. The strip-out times approached a constant value at longer anodic electrolysis times. Since instrumental sensitivity to the light emitted is high, a very low concentration of luminol can be used for the study of oxide and oxygen formation on platinum electrodes.

Cyclic voltammetry of 10^{-3} F luminol in 0.1 F Na_2CO_3 or K_2CO_3 solutions, showed well-defined anodic peak-type waves for the oxidation of luminol. The solutions were not degassed. The anodic scan limit used was +0.8 V. *vs.* S.C.E. The value of the anodic halfpeak potential, $E_{p/2}$ varied between +0.40 and 0.53 V. *vs.* S.C.E., and was dependent on the amount of platinum oxide removed from the electrode surface during the previous scan in the cathodic direction. A similar dependence of potential for oxidation of a substance, on the oxide formed, has been observed by others[12,13]. No evidence of a reduction wave due to the oxidized luminol was found on the cathodic scan.

If the signal from the photomultiplier tube, which monitored the light emission, was recorded in place of the current on the Y-axis of the recorder during voltage scan, identical peak-type traces were obtained. These traces were truly *photo-voltage* curves and as such, may be appropriately called, photo-polarograms. The anodic half-peak potentials showed the same dependence on the surface oxide (determined by the potential limit in the cathodic direction) as the conventional current–voltage curves. They differed, however, in the following respects:

(1) The cathodic wave due to platinum oxide reduction was no longer present, since it was not a light-emitting reaction.

(2) If the potential limit of the cathodic scan was made less than −0.1 V *vs.* S.C.E., the peak height of the light emission decreased on the anodic cycle. This decrease was caused by the depletion of oxygen near the electrode surface from the oxygen reduction at potentials less than −0.1 V during the cathodic scan. There was then less oxygen at the electrode to react with the oxidized luminol during the anodic scan, and consequently, a lower peak height of emission was found. The conventional current–voltage curves did not show such a peak-height decrease. It appears therefore, that the luminol reaction may be used to delineate the potentials of oxygen from platinum oxide reductions at the platinum electrode in basic carbonate solutions.

The photo-polarograms were obtained in the present case, from a luminescent reaction which was initiated by the electron-transfer process. It is expected that there are processes where luminescence may be produced directly from the electron-transfer process itself. These may involve formation of excited molecules or ions in the higher singlet or triplet states by the electron-transfer process. No such phenomenon has so far been observed, however, for a heterogeneous electron-transfer system.

A more detailed report of this work will appear shortly.

ACKNOWLEDGEMENT

This work was sponsored in part by the Air Force Cambridge Research Laboratories, Office of Aerospace Research, under contract AF19 (604) 8069.

Department of Chemistry,
University of California,
Riverside, California (U.S.A.)

THEODORE KUWANA

1 N. HARVEY, *J. Phys. Chem.*, 33 (1929) 1456.
2 V. VOJIIR, *Collection Czech. Chem. Commun.*, 19 (1954) 862.
3 A. BERNANOSE, TH. BREMER, AND P. GOLDFINGER, *Bull. Soc. Chim. Belg.*, 56 (1947) 269.
4 E. H. WHITE, *Life and Light*, edited by W. D. McElroy and B. Glass, John Hopkins Press, Baltimore, 1961, p. 183.
5 J. N. PITTS, JR., H. JOHNSON AND T. KUWANA, *J. Phys. Chem.*, 66 (1962) 2456.
6 P. DELAHAY, *New Instrumental Methods in Electrochemistry*, Interscience Publishers, Inc., New York, 1954, ch. 16.
7 J. R. ALDEN, J. Q. CHAMBERS AND R. N. ADAMS, *J. Electronal. Chem.*, 5 (1963) 152.
8 F. ANSON, *Anal. Chem.*, 33 (1961) 934; *ibid.*, 33 (1961) 935, 939. (See discussions on reduction of platinum oxide to form platinized platinum.)
9 T. KUWANA, B. EPSTEIN AND E. SEO, to be published.
10 K. WEBER, *Chem. Ber.*, 75 (1942) 565.
11 A. SPRUIT-VAN DER BURG, *Rec. Trav. Chim.*. 69 (1950) 1536.
12 F. C. ANSON AND J. J. LINGANE, *J. Am. Chem. Soc.* 79 (1957) 1015.
13 D. G. DAVIS, *Talanta*, 3 (1960) 335.

(Received May 14th, 1963)

REPORT

AUSTRALIAN ELECTROCHEMISTRY CONFERENCE

The first Australian Conference on Electrochemistry was held at the University of New South Wales, Sydney, from 13th–15th February and at the University of Tasmania, Hobart, from 18th–20th February, 1963. It was sponsored by the Royal Australian Chemical Institute, The University of Tasmania, the University of New South Wales, and 39 industrial companies based in Australia. With about 180 active participants, it was by no means a large chemistry meeting. Nevertheless, the field covered was extremely wide and a number of important contributions were made to our knowledge of both reversible and irreversible processes. Some 18 countries were represented by 26 overseas conferees.

The proceedings were divided into 12 sessions, 6 at each of the centres, and each session began with the chariman's address which was followed by 5 or 6 contributed papers. Mr. J. M. BUTLER, the chairman of the first session at Sydney on *Applications (Electroplating, Anodizing)*, delivered a lecture on *Electrochemistry in Industry* in which he surveyed the whole field. Then followed six papers dealing with the practical side of electroplating; *Electrolytic Tin Plating* (J. LE BAS), *Practical Applications of Anodic Coating in Nameplate Manufacture* (A. RAYMOND), *Some Problems Associated with Industrial Anodizing* (R. D. ISAACS), *Electrochemistry of Corrosion of Decorative Ni–Cr Coatings* (G. N. FLINT and S. H. MELBOURNE), *Electroplating of Die-Cast Parts* (W. H. BURTON) and *Electrodeposition from a Sulphamate Bath* (T. L. RAMA CHAR).

The next session, *Solid State Chemistry*, was chaired by Dr. A. L. G. REES who addressed the Meeting on the subject *Elementary Processes in Solid State Reactions*. In this he gave a most interesting account of the present state of the theory and in the 6 contributed papers that followed, a number of techniques such as electron diffraction, surface potential, nuclear quadrupole resonance, and microscopic investigations were applied to the problem of semiconductor surface structure and some other reactions occurring at solid surfaces. D. HANEMAN (University of N.S.W.) discussed the effect of solute ions at a semiconductor–electrolyte interface in disturbing surface bond orbitals. In two contributions from Melbourne University, J. R. ANDERSON and N. J. CLARK discussed the mechanism of the interaction of chlorine and of oxygen with evaporated sodium films, whilst P. J. THISTLETHWAITE, K. R. TURNBULL and P. J. FENSHAM considered the electrical properties of poly-crystalline oxide semiconductors. Professor J. A. ALLEN (Newcastle University College) followed with an interesting paper on the electrochemistry of the silver oxides with special reference to thermal properties.

It was most unfortunate that Professor DELAHAY, the chairman of the session on Electroanalytical Methods, was unable to attend the conference owing to a serious illness. At short notice however, Professor W. H. REINMUTH deputised and gave an engaging account of the advantages of using analogue amplifiers for tackling problems associated with electrode–solution interfaces. The talk was of particular interest to the less electronically minded electrochemists. In three contributions from the University of Sydney new developments in the use of a.c. polarography were described. The session concluded with a number of papers concerned with analytical aspects of polarographic, potentiometric, coulometric and spectrophotometric methods of investigation.

The next series of papers was concerned with corrosion. The chairman, Professor A. E. JENKINS, addressed the meeting on the subject of *Corrosion at High Temperatures*. The importance of equilibrium potential–pH diagrams in explaining some of the experimental results of corrosion experiments and the use of potentiostats in such studies, was discussed in two papers by M. POURBAIX and co-authors (Centre Belge de L'Étude de la Corrosion, Brussels). Potentiostatic methods also formed the basis of papers by W. T. DENHOLM (potentiostatic study of Fe–Cr alloys) and A. E. SUSSEX (two applications of potentiostats in corrosion research). K. F. LORKING showed that in neutral solutions of containing anions less polarisable than OH^-, initiation and inhibition of the corrosion iron could be explained in terms of anodic formation and chemical solution of the oxide.

Reversible processes were represented by a section dealing with the thermodynamics of electrolytes, under the chairmanship of Professor R. O. STOKES. The chairman gave a most stimulating account of multi-component systems with special reference to his own extensive studies in the field. D. D. PERRIN and C. J. HAWKINS (Australian National University, Canberra) discussed the oxidation–reduction potentials of some copper complex ions especially in relation to their stereochemistry, and A. F. M. BARTON and G. A. WRIGHT (Auckland University) described experiments using the bismuth amalgam electrode designed to gain some insight into the thermodynamics of Bi^{3+} ion. The enthalpies and entropies of ion association involving bivalent transition metal ions were discussed by G. H. NANCOLLAS (Univeristy of Glasgow). L. LEIFER and E. HOGFELDT (M.I.T. and Royal Institute of Stockholm) suggested a most interesting approach to the interpretation of the properties of concentrated electrolyte solutions. Combining Hammett acidity functions with activity data, they were able to show that the water activity at very high electrolyte concentrations is of prime importance. An important contribution to the problem of hydration, salting-out and dielectric saturation was made by Profesor B. E. CONWAY and J. E. DESNOYERS (University of Ottawa). These authors developed a theory of salting-out for poly-ions taking into account dielectric saturation in the vicinity of the ions.

The chairman, Dr. J. R. MACDONALD, of the following session on the *Theory of Double-Layers* spoke about equilibrium double-layer theories, and Professor CONWAY discussed equilibrium and non-equilibrium theory of adsorption pseudo-capacitance (B. E. CONWAY and E. GILEADI). In the latter paper it was shown that the study of pseudo-capicitance can lead to important information about the adsorption isotherm for the intermediates and to relations involving the kinetics of the steps in the electrode reaction.

On Saturday, 16th February, the conference moved by various means of transport down to Hobart where the weather was a good deal cooler and more pleasant, at least for the British participants. The opening session on the Monday, *Non-aqueous Electrolytes*, was presided over by Professor H. N. PARTON. He gave a most interesting account of the subject in his lecture on ions in non-aqueous solutions. Contributed papers included: *Voltage Current Characteristics of Benzene* (E. O. FORSTER), *The Behaviour of Silver and Halide Ion Responsive Electrodes in Mixed Solvents* (E. BISHOP and R. G. DHANESWHAR) and *Triple Ion Equilibria in Acetic Acid* (R. J. L. MARTIN). In the last paper *Investigation of the Kinetic of Electrode Reactions of Organic Compounds.* (M. FLEISCHMANN, I. N. PETROV and W. F. WYNNE-JONES), Professor Wynne-Jones gave an elegant account of the possibilities of using controlled potential pulse electrolysis to examine the detailed electrode processes.

A session dealing with molten salts indicated the range of interests covered by the conference. Dr. G. W. MELLORS, the chairman, discussed the solvation of ions in molten salts. Contributed papers dealt with standard electrode potentials and the electromotive force series in molten $MgCl_2$–NaCl–KCl (H. C. GAURAND and W. K. BEHL), polarised electrode methods for the study of diffusion coefficients in fused salts (J. W. TOMLINSON and C. A. ANGELL), potentiometric acid-base titrations in fused salts (A. M. SHAMS EL DIN and A. A. A. GERGES), the surface tension of molten fluorides (K. J. WILMHURST, S. SENDEROFF and G. W. MELLORS) and transport number measurements (H. BLOOM and A. J. EASTEAL).

In a special session on electrochemical processes, the chairman, Professor B. E. CONWAY, spoke about the position of electrochemistry in up-to-date chemical physics and physical chemistry. The contributed papers in this session covered a wide field ranging from differential electrolytic potentiometry (E. BISHOP, R. G. DHANESWAR and G. D. SHORT), to some biochemical aspects (M. J. ALLEN and M. NICHOLSON). Professor J. O'M BOCKRIS in his paper on the structure of charged interfaces, put forward a model of the electrical double-layer which involved a fixed layer of solvent between solvated ions and the electrode surface. He also proposed a formulation of the double-layer in terms of electrostatic forces only. Although this model explains some of the observed phenomena, it obviously has a number of shortcomings which were debated during a lively discussion.

Fuel cell electrochemists were catered for in an interesting session under the chairmainship of Dr. R. A. WYNVEEN and contributed papers dealt mainly with the practical problems of cell construction and possible electrode reactions. The work at the C.S.I.R.O. Laboratories at Melbourne was described in two papers by H. R. SKEWES and D. F. A. KOCH, and P. L. SPEDDING discussed fuel cell electrolytes. A session on electrode processes began with a lecture by the chairman, Professor J. O'M. BOCKRIS, on *Basic Problems in Electrode Processes.* The papers which followed dealt mainly with kinetic aspects of the subject including a quantum mechanical treatment (S. G. CHRISTOV of Bulgaria) and a discussion of the hydrogen evolution reaction (J. HORIUTI, A. MATSUDA, N. ENYO and H. KITA of Hokkaido University).

A final session of the conference on electro-winning and electro-refining was presided over by Dr. N. E. RICHARDS who spoke about some recent developments in the electrolytic extraction of light metals. The papers which followed covered a variety of aspects of the subject including surface properties of molten mixtures (H. BLOOM and B. W. BURROWS) and the electrodeposition of zinc (two papers; one by I. W. WARK and the other by G. C. BRATT and W. N. SMITH).

A visitor to Australia is immediately impressed by the tremendous potentialities of the country. The meetings were held in the delightful new buildings of the Universities of New South Wales and of Tasmania, and since the number of participants was relatively small, there was ample opportunity for discussions outside the conference hall. Indeed it was this which made the conference as a whole so successful. The proceedings of the conference will be published shortly by Pergamon Press Limited, and will contain, in full, the chairmen's addresses and all the contributed papers.

(Received May 14th, 1963) G. H. NANCOLLAS

Book Review

The Analysis of Titanium, Zirconium and their Alloys, par W. T. ELWELL et D. F. WOODS, John Wiley and Sons Ltd., London 1961, 198 pp., 54 s.

Ce livre présente les derniers procédés utilisés régulièrement au laboratoire par les auteurs dans le domaine de l'analyse du titane, du zirconium et de leurs alliages.

La première partie de l'ouvrage est consacrée à l'échantillonnage et l'on y insiste spécialement sur les précautions à apporter aux opérations de machinage qui doivent s'effectuer sans échauffement excessif, le titane finement divisé et surtout le zirconium s'oxydant très rapidement et étant, de plus, pyrophorique.

Quelques renseignements généraux sur les réactifs, la mise en solution etc. suivent cette première partie.

Il serait fastidieux d'énumérer ensuite tous les éléments déterminés aussi bien dans le titane que dans le zirconium, une trentaine dans chaque cas, par des méthodes chimiques, ainsi que ceux déterminés par spectrographie. Dans la plupart des cas, les méthodes utilisées pour le titane et pour le zirconium sont identiques, seuls quelques détails qui sont d'ailleurs parfaitement décrits. Nous croyons utile de signaler les méthodes plus spéciales appliquées au dosage dur carbone, de l'hydrogène, de l'azote et de l'oxygène. On sait en effet combien il est important de pouvoir contrôler exactement la teneur en ces éléments, les propriétés mécaniques des métaux purs étant fortement influencées par leur variation.

Pour le carbone, trois procédés sont décrits; ils permettent de doser jusqu'à 0.01% de carbone dans le métal avec une précision de 10%.

Pour l'hydrogène, on utilise une méthode basée soit sur l'extraction du gaz par chauffage du métal sous vide, soit sur la fusion réductrice du métal et la mesure succéquante de l'hydrogène (dans ce dernier cas l'oxygène est dosé en plus sous forme de CO). La première de ces méthodes permet de doser jusqu'à 0.005% d'hydrogène avec une précision de 6%.

L'azote est déterminé par le procédé Kjeldahl (réduction des nitrures en ammoniac et distillation). La mesure se fait, soit par titration, soit par spectrophotométrie.

L'oxygène est dosé avec l'hydrogène, par la méthode de fusion réductrice sous vide. On atteint une teneur de 0.1% avec une précision de 10%. Si l'on veut déterminer uniquement l'oxygène, une méthode chimique simple peut être utilisée.

La dernière partie de l'ouvrage est consacrée au dosage du hafnium et des autres impuretés par la méthode spectrographique d'émission.

Quoique le livre contienne 58 références, les procédés analytiques sont extrêmement bien décrits. Il s'agit, en fait, d'un véritable manuel de laboratoire, très utile aux analystes et presque indispensable à ceux que préoccupe l'analyse de matériaux utilisés en énergie nucléaire.

P. MECHELYNK

Announcement

COURSE IN ELECTROCHEMICAL ANALYSIS

A weeks course of post-graduate lectures will be held from Monday September 9th to Saturday September 14th. 1963, inclusive, in the *Chemistry Department of the Sir John Cass College, Aldgate, London. EC3.*

Two lectures, followed by discussion, will be held between 9.30 and 12.30. p.m. each morning. The lectures will be given by Dr. K. E. JOHNSON., Ph.D., (Lond), B.Sc., A.R.C.S., D.I.C., and Mr. J. V. WESTWOOD., M.Sc. (Lond)., F.R.I.C.

LECTURE SYLLABUS

Basic principles of electrode potentials, pH and Buffers. Potentiometric titrations, direct, differential and automatic. Coulometric titrations. Conductometry and high frequency titrations. Electrolysis—mass transfer processes. Charlots approach. Polarography-theory and applications to aqueous, organic and molten salt systems. Cathode ray and A.C. polarography, Amperometric titrations. Electrolysis at controlled current and controlled potential. Internal electrolysis. Chronopotentiometry. Kinetics of electrode processes.

COLLOQUIUM

The afternoon of September 13th will be devoted to a colloquium at which the following distinguished visitors will give short talks to be followed by discussions.

Professor G. J. HILLS, on *Electrochemistry of Molten Salts.*

Dr. G. C. BARKER, on *Radiofrequency Polarography.*

Mr. E. BISHOP, on *Differential Electrolytic Potentiometry.*

This will be followed by an Informal Gathering of all members of the course and later a Dinner. Invited members of the Press will also attend. A small exhibition of apparatus and literature will be held during the course.

The Fee for the lecture course will be £7/–/–, which includes morning coffee, lunch and admission to the colloquium, Informal Gathering and Dinner.

Applications for enrolment forms, or further enquiries, should be made to Mr. J. V. WESTWOOD, Senior Lecturer in Physical Chemistry, as soon as possible, and before September 1st. 1963.

VOL. 6 NO. 2 JOURNAL OF ELECTROANALYTICAL CHEMISTRY AUGUST 1963

CONTENTS

Original papers

Short communication

Report

ELSEVIER PUBLISHING COMPANY, AMSTERDAM
Printed in The Netherlands by
NEDERLANDSE BOEKDRUK INRICHTING N.V., 'S-HERTOGENBOSCH